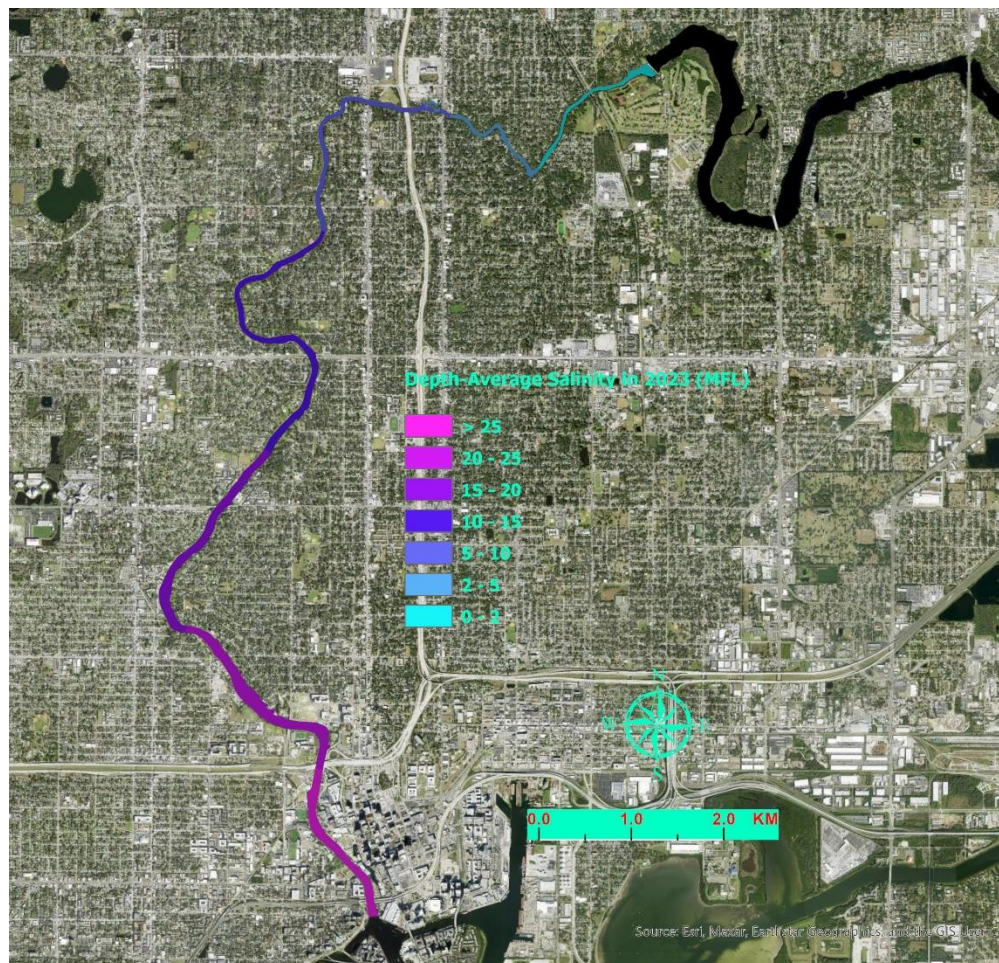# Appendix J

Use of the Updated LAMFE Model for the Third 5-Year Assessment of the Lower Hillsborough River MFL (Chen 2024)

Use of the Updated LAMFE Model for the Third 5-Year Assessment of the Lower Hillsborough River MFLs

XinJian Chen, Ph.D., P.E.

Southwest Florida
Water Management District

August 2024

Summary

This technical report summarizes the development of the updated Laterally Averaged Model for Estuaries (LAMFE) for the lower Hillsborough River (LHR), a tributary of Tampa Bay located on the west coast of the Florida peninsula. Recently surveyed bathymetry data and LiDAR data were used to generate model grids for the simulation domain, which stretches from the mouth of the river to the base of the Tampa dam. The update of the LAMFE model for the LHR also included the Sulphur Springs (SS) run in the simulation domain, which was discretized with 144 and 7 longitudinal grids for the LHR and SS run, respectively.

The updated LAMFE model for the LHR was calibrated and verified with real-time field data of water level, salinity, and temperature measured at several fixed locations in the LHR and SS run during a 5-year period, from October 2017 to October 2021. The calibrated LAMFE model was used to conduct scenario runs for the third 5-year assessment of the LHR minimum flows and levels (MFL) implementation. Three scenarios were simulated: existing flow condition, no MFL condition, and fully implemented MFL condition. Low salinity habitats such as ≤2 psu and ≤5 psu water volumes, bottom areas, and shoreline lengths for the upstream river segment between the dam and the confluence of the SS run were calculated based on model outputs of salinity at all the grid cells in the simulation domain. Thermal habitats for manatees such as water volumes and surface areas for temperature $\geq 20\ ^oC$ and for temperature between $15\ ^oC$ and $20\ ^oC$ were calculated based on simulated temperature results for the refuge for manatees of the system, which was defined as the entire SS run plus a 50-m segment in the LHR at the confluence of the spring run.

Comparisons of simulated low salinity habitats in the upstream segment of the LHR for various flow conditions demonstrate a substantial improvement of low salinity habitats in the upstream portion of the river for the existing flow condition over the no MFL flow condition. At the same time, the analysis also shows the discrepancy of the existing flow condition in comparison with the fully implemented MFL flow condition in terms of the low salinity habitats. For the thermal habitats, $\geq 20\ ^oC$ water volume and surface area could experience small gains in the refuge for manatees with the implementation of the MFL for the LHR during manatee seasons between October 2007 and December 2023 but water volume and surface area for temperature between $15\ ^oC$ and $20\ ^oC$ could have a loss. However, such a comparison of gain or loss of thermal habitats for manatees could be problematic and misleading, because the computation of the thermal habitats for manatees was done for the refuge for manatees, which could be significantly different from the actual plume of the SS flow. In any case, average $\geq 20\ ^oC$ volumes and surface areas for the three flow scenarios do not vary too much and there are always enough thermal habitats available in the estuary for manatees to use on the coldest days of the year.

Table of Contents

List of Figures

1. Introduction

The lower Hillsborough River (LHR) is the most downstream part of the Hillsborough River, which is about 60 miles long and originates from the Green Swamp, a region between Orlando and Tampa that is east of I-75, west of Highway 27, and south of SR-50. The lower Hillsborough River is a narrow and meandering estuary, which starts at the City of Tampa dam and ends at its mouth in downtown Tampa, Florida (Fig. 1.) From the base of the dam, which releases fresh water to the river, to its mouth at Platt Street in downtown Tampa, the lower Hillsborough River is about 10 miles (16 km) long and flows first southwestward and then southward to Hillsborough Bay, an estuarine embayment of Tampa Bay. About 1.1 miles (3.5 km) downstream from the dam, there is an artesian spring (Sulphur Springs, or SS for short) which in recent years has discharged an average of 0.88 m^3/sec (31 cfs) laterally to the river via a short channel (the SS run.) The average depth of the LHR is about 3 m and the average width is about 64.8 m at 0 m, North American Vertical Datum of 1988 (NAVD88.) The deepest area of the river is about -6.25 m, NAVD88.

The river has been impounded by a succession of structures near the site of the present dam for over 100 years. Daily streamflow records at the present reservoir spillway extend back to 1945 (Coffin and Fletcher 1997). Stoker et al. (1996) reported a declining trend for streamflow at this location and suggested that rainfall deficits, drainage alterations, decreased baseflow, and increased water use from the reservoir were contributing factors. Prior to 1970 there was nearly always flow over the reservoir spillway. Since 1970 there have been prolonged periods in the dry season when flows from the reservoir have ceased except for small amounts of leakage through the dam. Both freshwater and estuarine biota occur below the dam, with the zonation of these organisms shifting when there is no flow from the reservoir (Water and Air Research and SDI Environmental Services, Inc. 1995).

The river experiences density stratification most of the time due to relatively weak tides, as the maximum variation of surface elevation at the river mouth is about 1.2 m during spring tides. The stratification is further enhanced by the lateral spring water input to the top layer of the river. Near the inflow point of the spring flow, salinity can increase from 4 – 5 psu near the water surface to about 15 psu within a depth of 2 m. This enhanced salinity stratification at the confluence of the SS run allows saltier water to be transported further upstream at the bottom layer of the river. As a result, salinity values immediately below the dam become elevated (8 to 12 psu) during times of no flow from the reservoir. This caused ecological conditions in freshwater and oligohaline zones to be degraded even more (Southwest Florida Water Management District 1999).

In order to improve the salinity characteristics of the lower river, a minimum flow of 10 cfs for the LHR was established in 2000. It was allowed to use flow from the SS for the MFL of the LHR. For this purpose, a flume was built on the north bank of the LHR just below the Tampa dam and an existing pumping mechanism of the City of Tampa was modified to pump SS water to the newly built flume, so that SS flow would be aerated before entering the LHR. The 2000 MFL rules were evaluated and updated in 2007, along with the establishment of the MFL rules for the Sulphur Springs run (SWFWMD, 2004). Updated MFL rules for the LHR (SWFWMD, 2006) increased the required flow rate set in 2000 (10 cfs) to 24 cfs during April – June and 20 cfs during

July – March, with some adjustments according to the discharge gaged at the USGS Hillsborough River at State Park near Zephyrhills station. Because the SS water has a salinity of up to 3.5 psu, additional 3 cfs freshwater was added to the MFLs as fresh equivalent to compensate for the loss of freshwater flow entering the LHR, which is caused by the use of the SS flow to meet the MFL requirement.
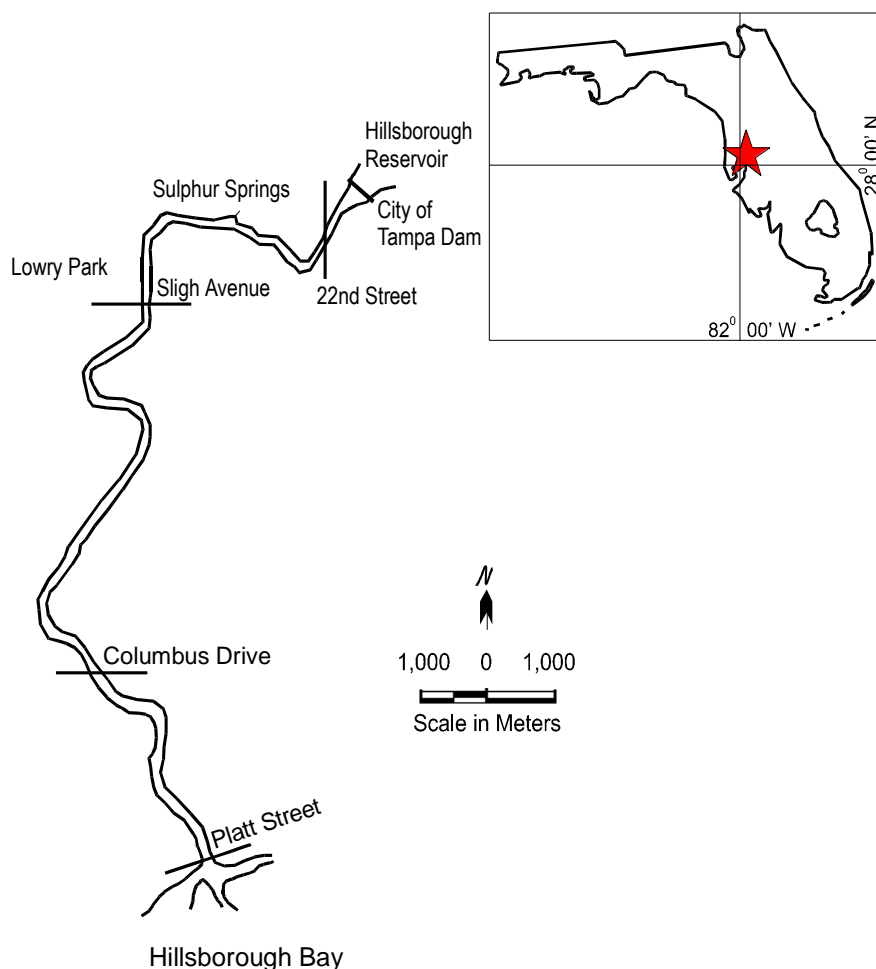
Figure 1. A sketch of the lower Hillsborough River and its location in Florida.

The new MFL rules for the LHR require the MFL implementation to be assessed every 5 years after the adoption of the MFL rules in 2007. The first 5-year assessment was completed in 2015 (SWFWMD & Atkins North America, Inc., 2015), while the second 5-year assessment was done in 2020 (Water & Air Research, Inc., 2020). This study is to support the third 5-year assessment.

In the previous two 5-year assessments, the same version of LAMFE model as the one used during the MFL re-evaluation process (Chen, 1999) was used to simulate hydrodynamics and salinity transport processes in the LHR. Although that version of the LHR LAMFE model was well calibrated and verified against real-time data of water level and salinity measured about 20

years ago, it used some old survey data that were obtained by digitizing blueprints of the cross sections which were generated in the 1980s. The morphological change over the last few decades and the outdated method used in obtaining the cross-sectional data points inevitably caused some errors associated with the model grids, which are important for an accurate simulation of hydrodynamics and salinity transport processes in the LHR. Therefore, it is necessary to update the LAMFE model for the LHR by using new bathymetric and topographic data collected with current surveying technology.

This technical report presents the development and use of the updated LAMFE model in the third 5-year assessment of the MFL implementation for the LHR. The updated LAMFE model for the LHR used the newly surveyed bathymetric data and LiDAR data to generate the model grids. It was calibrated and verified against real-time data at several stations during the last few years, before it was used to conduct the assessment runs for a 195-month period, from October 2007 to December 2023. The assessment runs included the existing, MFL, and no MFL flow conditions.

Section 2 of this report describes available data used in the development of the LAMFE model for the LHR. Section 3 presents the model development of the LAMFE model for the LHR, followed by model calibration and verification in Section 4. Section 5 provides details about scenario simulations for the 5-year MFL assessment for the LHR. Conclusions of this modeling study are summarized in Section 6.

2. Data for Model Calibration and Verification

2.1   Bathymetry Data

Previous LAMFE models involved usage of some outdated bathymetry data in the LHR, which were surveyed more than 40 years ago. To improve the model, a new bathymetry survey was conducted in 2021 (George F. Young, Inc., 2021) using a state-of-the-art water depth detecting method. In the new LHR LAMFE model, newly surveyed bathymetry data and available LiDAR data were used to generate model grids. Fig. 2 shows data points of the 2021 survey for the most upstream segment of the LHR, while Fig. 3 shows data points for the most downstream segment of the river. As can be seen from the figures, the new survey for the LHR had a very high resolution. Other segments of the LHR had a similar survey resolution as these shown in Figs. 2 and 3, which is suitable for the grid generation of the LAMFE model for the estuary.
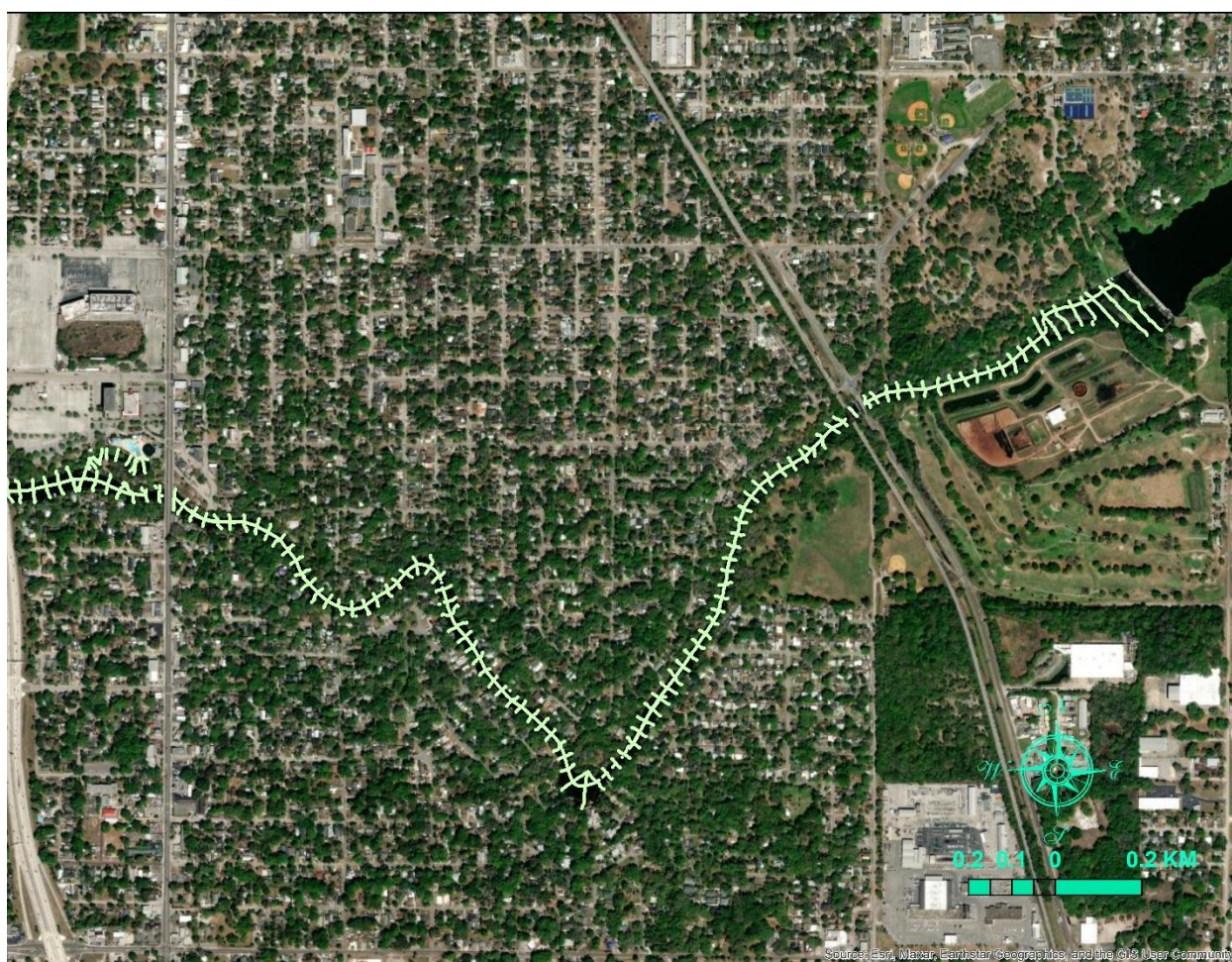
Figure 2. Survey points of the 2021 survey in the most upstream segment of the lower Hillsborough River.
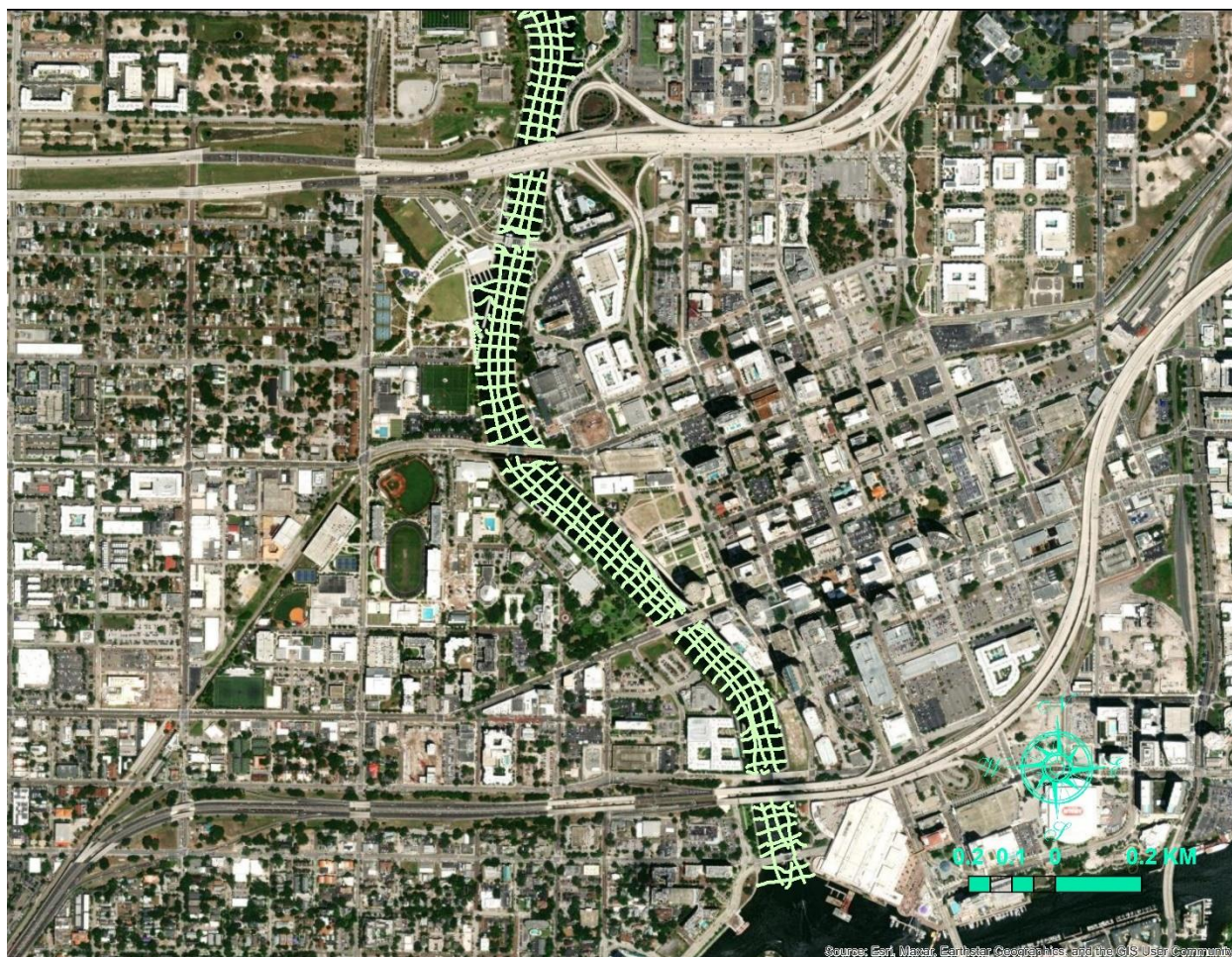
Figure 3. Survey points of the 2021 survey in the most downstream segment of the lower Hillsborough River.

2.2   CTD Data

Real-time data for conductivity, temperature, and depth (CTD) were collected by the USGS and the District at several stations along the LHR, including the USGS Hillsborough River at Platt Street at Tampa FL station (#02306028), the USGS Hillsborough River at I-275 Bridge at Sulphur Springs FL station (#023060013), the USGS Hillsborough River below Hannah's Whirl near Sulphur Springs FL station(#02304517), the USGS Hillsborough River at Rowlett Park near Tampa FL station (#02304510), and the District Hillsborough River at SS station (#19206). The USGS also has a real-time station in both the SS run and the SS pool, namely the USGS Sulphur Springs Run at Sulphur Springs FL station (#023060003) and the USGS Sulphur Springs at Sulphur Springs FL station (#02306000). Triangles marked in Fig. 5 indicate locations of the CTD data stations.

Table 1 below lists locations and periods of the record of the real-time data of water level, specific conductance, and temperature at these stations. The ending dates of the period of record were the ending dates of the approved data at the time when the LHR LAMFE model was developed. Provisional USGS data were excluded in the model calibration and verification but

used in the 5-year assessment runs. Table 2 shows sensor elevations (in feet, NAVD88) for specific conductance and temperature measurements at these real-time stations.

At the USGS stations, CTDs were recorded with a 15-minute interval, while they were recorded every 60 minutes at the District station. Salinity was calculated from conductivity data, which was recorded as specific conductance at 25 ºC. The Cox formula (Cox et al., 1970) was used for the conversion from specific conductance at 25 ºC to salinity. Water depths were converted to water surface elevation relative to the NAVD 88 datum. Conductivities and temperatures were measured at all the seven stations listed in Table 1, while water levels were measured at six of them. The only station at which the water level was not recorded was the USGS Hillsborough River below Hannah's Whirl near Sulphur Springs FL station.

Table 1. Locations and periods of record of real-time CTD data stations in the lower Hillsborough River and Sulphur Springs run.

Station	Station ID No.	Location		Period of Record	
		Longitude	Latitude	Staring Date	Ending Date
Platt Street	02306028	-82.45871	27.94197	≤ 1/1/2010	10/20/2021
I-275	023060013	-82.45482	28.02030	10/19/2012	10/13/2021
Hannah's Whirl	02304517	-82.44241	28.01516	10/25/2017	10/15/2021
Rowlett Park	02304510	-82.43454	28.02113	<1/1/2010	10/12/2021
District	19206	-82.45040	28.01978	4/15/2020	4/11/2022
Sulphur Springs Run	023060003	-82.45232	28.02113	< 1/1/2015	4/8/2022
Sulphur Springs Pool	02306000	-82.45176	28.02113	<12/1/2006	4/8/2022

While conductivity and temperature data were recorded at the top, middle, and bottom layers at the Platt Street station, they were recorded at the top and bottom layers at the I-275, Hannah's Whirl, and Rowlett Park stations. At the District station in the LHR and the USGS station in the SS run, conductivities and temperatures were only measured at the bottom layer. Table 2 shows elevations at which the conductivity and temperature sensors were located.

Table 2. Elevations where specific conductance and temperature were measured at the real-time stations in the lower Hillsborough River (units are feet, NAVD88).

Station	Top Layer	Middle Layer	Bottom Layer
Platt Street	-2.00	-4.00	-5.90
I-275	-4.00		-6.50
Hannah's Whirl	-2.70		-6.70
Rowlett Park	-2.84		-5.64
District			-2.00'
Sulphur Springs Run			-1.44'

2.3   Flow Data

Hydrological loadings to the LHR estuary consist of gaged and ungagged flows, and both are important factors affecting salinity transport processes in the estuary. Gaged flows enter the model domain through the upstream boundaries, including the base of the dam and the starting cross section of the SS run. Because of the complexity of the updated MFL rules and the requirement for the Hillsborough River reservoir to maintain a certain minimum level to ensure the water supply for the City of Tampa, several components of gaged flows are involved at the upstream end of the LHR, including (1) reservoir flow over the Tampa dam, (2) flow pumped from the reservoir over the dam, (3) flow through a sluice gage at the dam, (4) flow from Blue Sink, and (5) SS flow pumped to the base of the dam. At the starting cross section of the SS run, gaged flows are SS flow from the pool to the spring run over a weir and pumped flow from the SS pool to the SS run.

Data of reservoir flow over the Tampa dam and SS flow over the pool weir were measured and provided by the USGS, while pumped flows, including SS flow routed to the base of the dam and pumped over the dam, were recorded by City of Tampa and the District. These flow data have different periods of record, which are listed in Table 3. The ending dates of the USGS flows were the last days when the data were approved.

Table 3. Periods of record of various gaged flow sources for the lower Hillsborough River.

Gaged Flow	Starting Date	Ending Date
Reservoir flow over the Tampa dam (USGS)	≤ 1/1/2010	12/7/2021
Reservoir flow pumped over the dam	12/31/2007	7/20/2018
Blue Sink flow	9/15/2017	6/20/2022
Sluice gate flow	7/20/2018	6/20/2022
Sulphur Springs flow pumped to the base of the dam	≤ 1/1/2010	2/20/2022
Sulphur Springs flow over the pool weir (USGS)	10/9/1986	10/11/2022
Sulphur Springs flow pumped to the run	≤ 6/1/2015	2/20/2022

Ungaged flows from the LHR watershed were estimated based on rainfall data measured at the District Hillsborough River at Sulphur Springs station. When rainfall information was not available on days at the District station, rainfall data measured by the USGS at their Sulphur Springs Pool station was used to fill the data gap. For days when rainfall data was not available at both the District station and the USGS Sulphur Springs Pool station, rainfall data measured at the UF IFAS Dover station was used. It is assumed that rain was uniformly distributed over the entire drainage basin of the LHR. By incorporating a previous study conducted by HSW Engineering, Inc. (1992), the drainage basin was divided into 17 sub-basins to consider variations in runoff characteristics among different sub-basins (Fig. 4). Hourly runoff from each individual sub-basin was calculated based on a method described in Chen and Flannery (1997).

2.4   Other Data

In addition to the bathymetry data, CTD data, and flow data, meteorological data such as air temperature, rainfall, air humidity, solar radiation, and wind speed and wind direction were also needed for a successful development of the LAMFE model that can be used to simulate circulations, salinity transport processes, and thermal dynamics in the LHR. As mentioned above, rainfall data was recorded at the Hillsborough River at Sulphur Springs station by the district. Other meteorological data such as air temperature, rainfall, air humidity, solar radiation, and wind speed and wind direction were obtained from the Dover station of the Florida Automated Weather Network (FAWN), which is located at an extension station of the Institute of Food and Agricultural Sciences (IFAS) of the University of Florida (UF).

The District rainfall data at the Hillsborough River at Sulphur Springs were available since 1/1/2010 or earlier, while some of the meteorological data at the Dover station of the UF IFAS were available since 5/5/1998. NEXRAD data for the area were reviewed but not used, because the precipitation estimate based on radar images was calibrated with measured rainfall data, including those measured in the LHR basin. As such, there is no reason to use any model-generated rainfall data when the actual data are available. Skinner et al. (2009) compared NEXRAD data with rainfall data measured in south Florida during 2002 – 2005 and found that NEXRAD data had considerable localized bias and exhibited the tendency to overestimate low rain events but underestimate high rain events. In one of the four years, the annual NEXRAD rain total was about 11% lower than measured data (Table 6 in Skinner et al., 2009).
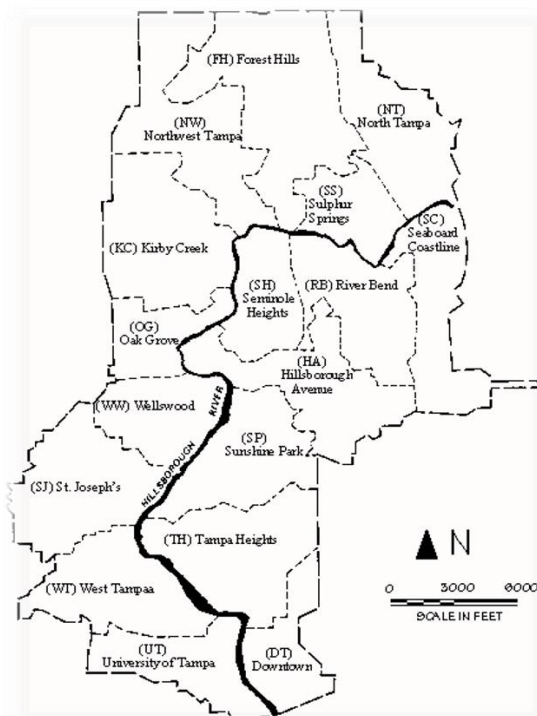
Figure 4. The lower Hillsborough River watershed and its sub-basins.

Because of the establishment of the MFL for the SS run, a weir structure was built in the SS run in 2012. As the SS run is included in the simulation domain, detailed information about the weir structure in the spring run should be given to the model. One feature of the weir structure is the use of stoplogs to alter the elevation of the weir. Operational data about the use of stoplogs were provided by the City of Tampa.

3. Model Development

In the updated LHR LAMFE model for the LHR, the simulation domain is from the dam to the USGS Platt Street station in downtown Tampa (Fig. 5). One of the improvements of the new LAMFE model for the LHR is the inclusion of the SS run in the simulation domain. The SS run is the only tributary for the LHR river and including it in the new LAMFE model for the LHR allows simulations of salinity and temperature distributions in the SS run, making the model a useful tool for the assessment of the spring run.

Figure 5. LAMFE model grids for the entire simulation domain, including the lower Hillsborough River and the Sulphur Springs run. Triangles are locations of the CTD data stations.

The simulation domain was discretized with 154 cross sections, resulting in 144 and 7 longitudinal grids in the longitudinal direction for the LHR main stem and the SS run, respectively. The longitudinal spacing of the grids varies between 23 m and 349 m. In the vertical direction, the water column was discretized with 17 layers, with the layer thickness varying between 0.3 m and 1.4 m. Fig. 5 shows the plane view of the new LAMFE model grids for the entire simulation domain, including the LHR and the SS run. A zoom-in view of the area near the SS run is given in Fig. 6. Green triangles in Figs. 5 and 6 represent locations of the CTD data stations described in the last section.

Figure 6. A zoom-in view of the model grids for the Sulphur Springs run and the segment of the LHR near the confluence of the run.

A side (*x-z*) view of the discretization used the LHR LAMFE model is shown in Fig. 7. In the figure, the *x*-axis is reversed River KM, which is the longitudinal distance measured in kilometers from the mouth (Platt Street) of the lower Hillsborough River. As can be seen from the figure, relatively thin layers were used within the depth where the tidal variation occurs. Fig. 7 only shows *z*-layers below 0 m, NAVD88, and there are six additional layers above 0 m, NAVD88, which are not shown in the figure but included in the LAMFE model for the LHR. The vertical discretization of the LHR covers an elevation range from -6.25 m, NAVD88 to 3.2 m, NAVD88. Compared with the side view of the discretization used in the previous LHR LAMFE model (Chen, et al., 2000), the new LHR LAMFE model is greatly improved in terms of the discretization of the simulation domain.
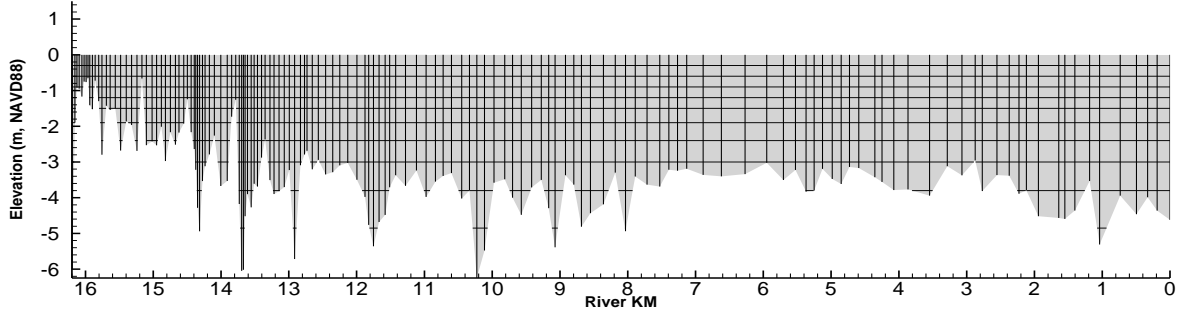
Figure 7. A side (*x-z*) view of the discretization used in the lower Hillsborough River LAMFE model. The left end is at the dam, while the right end is the river mouth at Platt Street.

The downstream boundary is set at Platt Street in downtown Tampa, where the USGS collects real-time data of water elevation, specific conductance, and temperature every 15 minutes. The upstream boundaries included the base of the dam and the upstream end of the SS run, where slightly saline water in a range of 1.85 - 4.0 psu and a mean of 2.68 psu enters the run from the SS pool either through a weir or a pump operation by the City of Tampa. Sulphur Springs flow routed to the base of the dam was treated as a tributary, because the flow enters the river through a flume at the north bank of the river. The use of the flume allows aeration for the SS flow routed to the base of the dam and thus improves the oxygen level in the upstream reach of the LHR.

As mentioned above, a weir structure was built in the SS run as a part of the MFL implementation for the spring run. To deal with this structure inside the simulation domain, the LAMFE code was modified to incorporate a scheme for the calculation of fluxes of water, salt, and heat over a rectangular crested weir. In the LAMFE model, the cross sections where rectangular sharp-crested weirs are located are chosen as the cross sections for LAMFE grids. The actual bottom elevations immediately upstream and downstream of the cross section of the weir are used in the volume calculation in the model, while the weir elevation is used in the calculation of the cross-sectional area. The calculation of the flow over the weir depends on the water levels on the upstream and downstream sides of the weir. When the water levels on both sides of the weir are below the weir elevation, the flow over the weir is zero. When the water levels on both sides of the weir are above the weir elevation (the top panel of Fig. 8), the flow is calculated from the velocity, which is solved from the continuity and momentum equations. When one side of the water level is above the weir elevation and the other side is below the weir elevation (the bottom panel of Fig. 8), discharge is calculated from the weir equation (Brater and King, 1982):

$$Q = \frac{2}{3} C_{wr} L \Delta H \sqrt{2g\Delta H} \tag{1}$$

where Q is the flow over the weir, C_{wr} is a weir coefficient, L is the length of the weir, g is the gravity, ΔH is the head above the weir.

Velocity is obtained by solving the continuity and momentum equations using the FSC method

Discharge is calculated as

$$Q = \frac{2}{3}C_{wr}L\sqrt{2g}\,\Delta H^{3/2}$$

ΔH
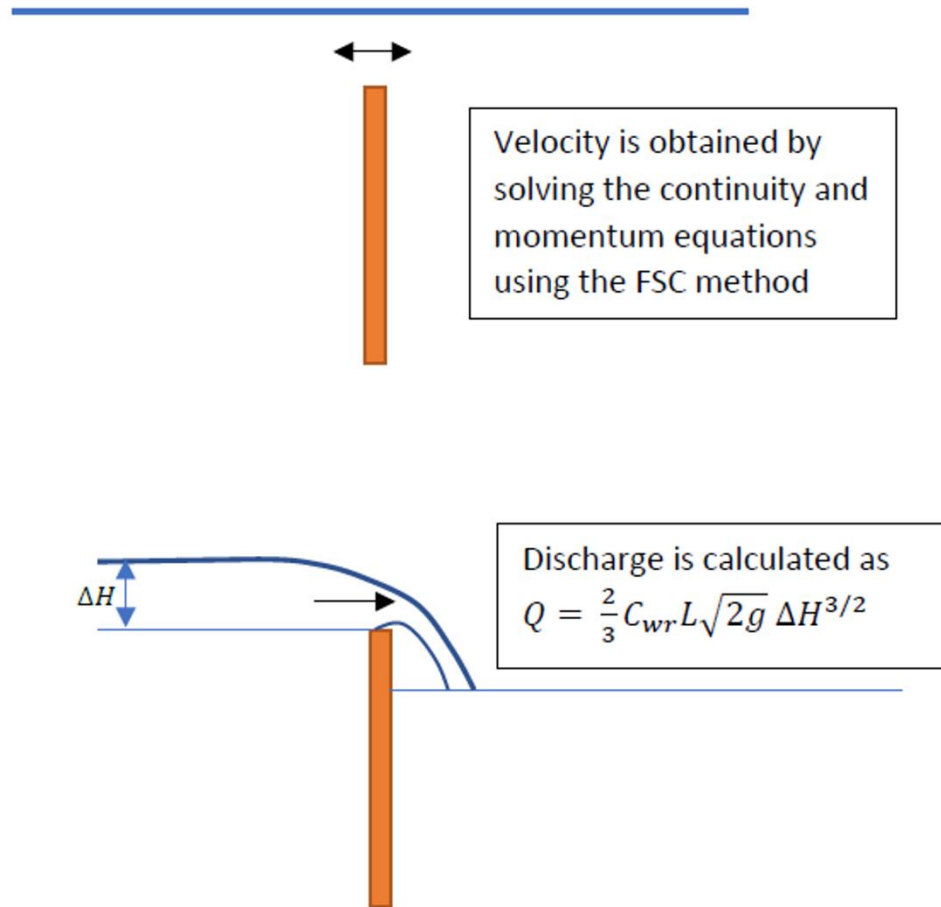
Figure 8. Methods used to calculate the flow over the weir in Sulphur Springs run depending on the water levels at both sides of the weir.

4. Model Calibration and Verification

Based on the available CTD data, gaged flow data, as well as meteorological data, a five-year period between 10/25/2017 and 10/12/2021 was chosen for model calibration and verification. As the CTD data at the District station was only available from 4/15/2020 on, the second half of the 5-year period, during 4/15/2020 – 10/12/2021, was chosen for model calibration. As such, the model was calibrated against real-time water levels, salinities, and temperatures at the District station and three USGS stations within the simulation domain, including the I-275, Hannah's Whirl, and Rowlett Park stations in the LHR and the Sulphur Sprung Run station. After the model was calibrated, it was verified using real-time CTD data collected at the USGS stations at I-275, Hannah's Whirl, Rowlett Park, and Sulphur Springs run during 10/25/2017 – 4/14/2020.

Fig. 9 shows comparisons of simulated water levels with measured field data at the USGS Rowlett Park, I-275, and Sulphur Springs run stations and the District station during a 40-day period from 4/29/2021 to 6/8/2021. As can be seen from the figure, simulated water levels matched very well with measured data at the four stations. The diurnal and semidiurnal tidal variations of the water surface elevation in the LHR and in the SS run were correctly simulated by the LAMFE model. The water level cutoff at roughly 0 cm, NAVD88 was caused by the weir operation in the spring run, resulting in a damming effect between the spring pool and the weir.

Fig. 10 shows comparisons of simulated and measured salinities at the top and bottom layers of the USGS Rowlett Park station in a 60-day period during 5/31/2021 – 7/30/2021. The first 25 days were in the dry season, while the remaining 35 days were in the wet season of the year for the LHR. From the figure, it can be seen that salinity at Rowlett Park station was well-mixed and generally low. During the first 25 days of the 60-day period, salinity is about 2 psu, while in the remaining 35 days, salinity is close to 0 psu. The variation of salinity at this station represents the mixture of flows from different sources entering the river below the dam. As the first 25 days were during the dry season, the MFL implementation called for pumping SS water to the flume near the base of the dam. From data provided by the City of Tampa, SS flow routed to the flume was between 10.9 and 18.2 cfs during the first 25 days. Salinity in the SS pool during this period was between 2.58 and 3.48 psu. At the same time, freshwater flows from other sources were provided to the LHR, including about 2.78 cfs pumped from Blue Sink and about 5.70 cfs released through the sluice gate. Reservoir flow over the spillway was zero during the 25 days. The flow weighted average salinity of all these flows was about 1.97 psu, which matched the average salinity simulated at the Rowlett Park station during the 25 days. After the wet period started around Jun 24, 2021, regular summer thunderstorms caused the water level in the reservoir to increase and the spillway flow from the reservoir started to occur in the afternoon on 6/25/2021. Almost at the same time in that afternoon, pumpage from Blue Sink was turned off, before the sluice gate was closed 12 hours later in the early morning of 6/26/2021, because the reservoir flow over the spillway became much higher than the MFL requirement for the LHR.

Fig. 11 shows comparisons of simulated and measured salinities at the USGS Hannah's Whirl station. While salinity at the USGS Rowlett Park station is dominated by the flows received at the base of the dam with a very small tidal influence, noticeable tidal signals can be seen in both the simulated and measured salinities at the Hannah's Whirl station, indicating the tidal influence

20

on salinity at the site. Although the LAMFE model slightly over-predicts the tidal influence on some days and under-predicts it on some other days during the 25 days of the dry season, long-term salinity variations at the USGS Hannah's Whirl station were correctly simulated. After the wet season started, the freshwater flow became so strong that any saline water previously existed in that segment of the river was pushed downstream of the station. As a result, both the simulated and measured salinities at the USGS Hannah's Whirl station were reduced to almost 0 psu, with the bottom layer being a little saltier than the top layer.
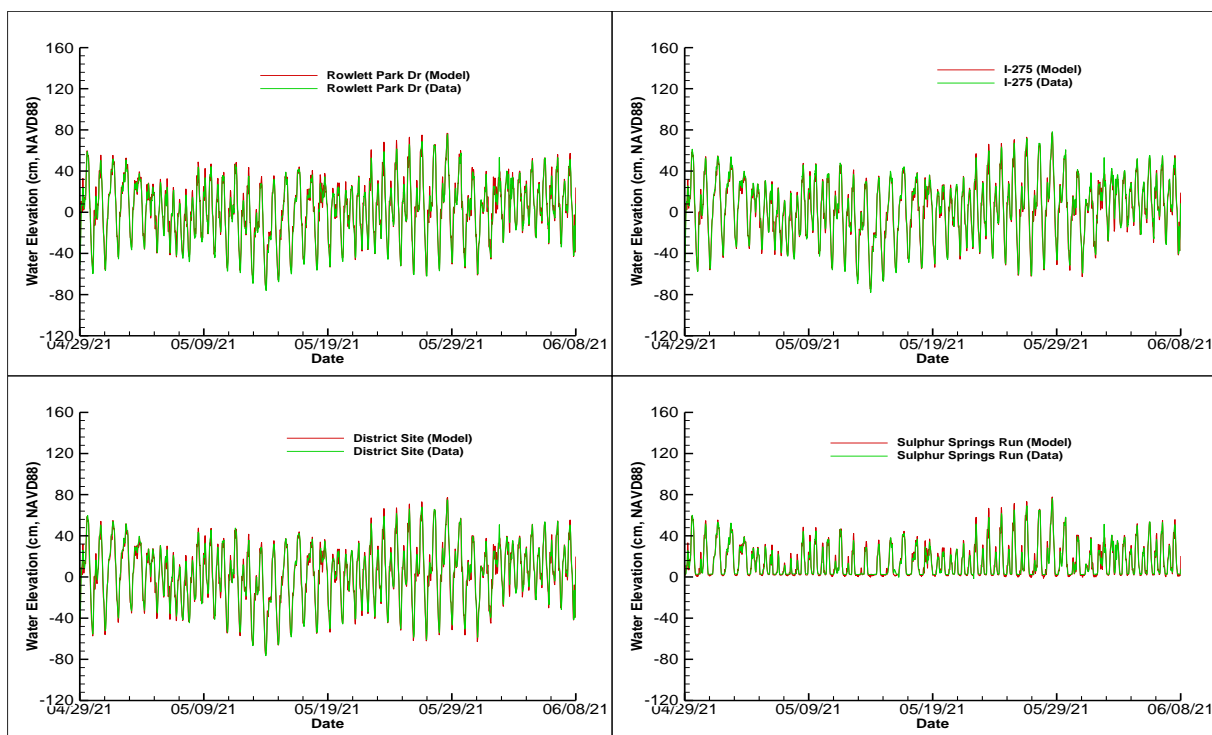
Figure 9. Comparisons of simulated and measured water elevations at the USGS Rowlett Park, I-275, and Sulphur Springs run stations and the District station during 4/29/2021 – 6/8/2021.

Simulated salinities at the bottom layers of the District station and the USGS Sulphur Springs run station are compared with those collected at the field and shown in the top and bottom panels, respectively in Fig. 12. Because the District station is further downstream from Hannah's Whirl, tidal signals in the simulated and measured salinities at this station are more discernible than those at the USGS Hannah's Whirl and Rowlett Park stations. Overall, although the tidal variability in the simulated salinity is a little bigger than that of measured salinity, long-term trends in simulated and measured salinities matched well at the District station. Both the simulated and measured salinities varied between less than 1 psu to over 5 psu during the first 25 days, while they were reduced to almost zero after 6/25/2021, except on 7/26/2021 when a small peak (about 1 psu) occurred. This small increase of salinity at the District station was caused by a sudden decrease of total freshwater inflow at the base of the dam, which decreased from about 435 cfs on 7/25/2021 to about 22 cfs on 7/26/2021.
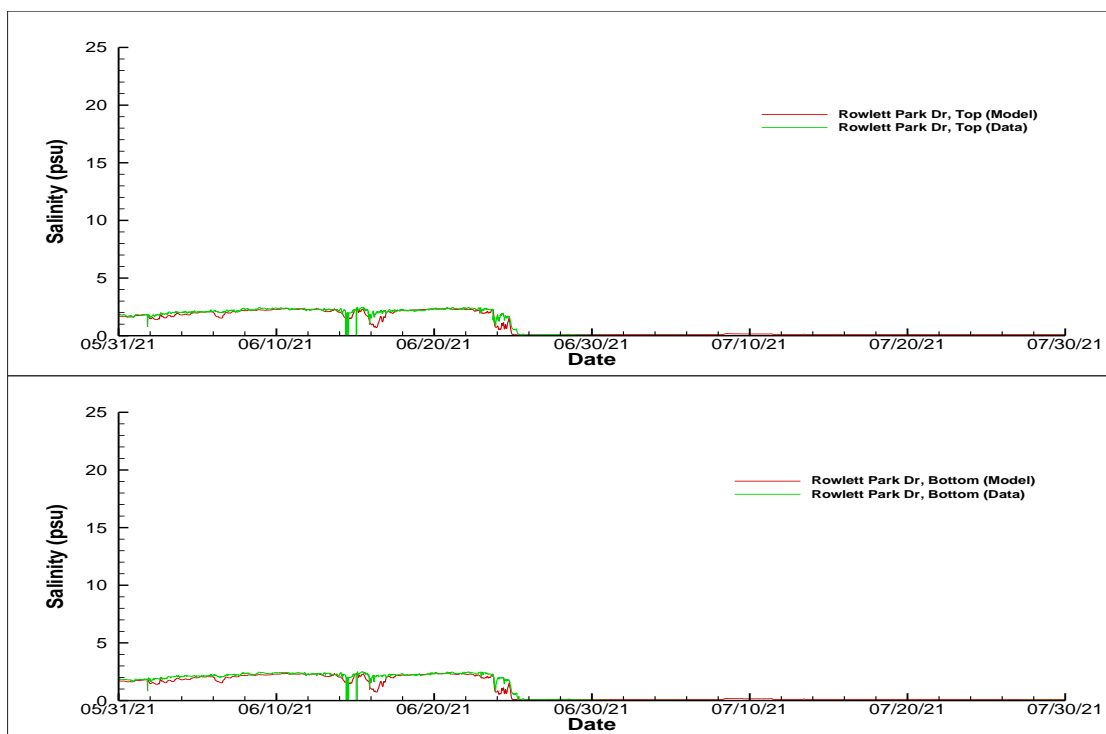
Figure 10. Comparisons of simulated and measured salinities at the top and bottom layers at the USGS Rowlett Park station during 5/31/2021 – 7/30/2021.
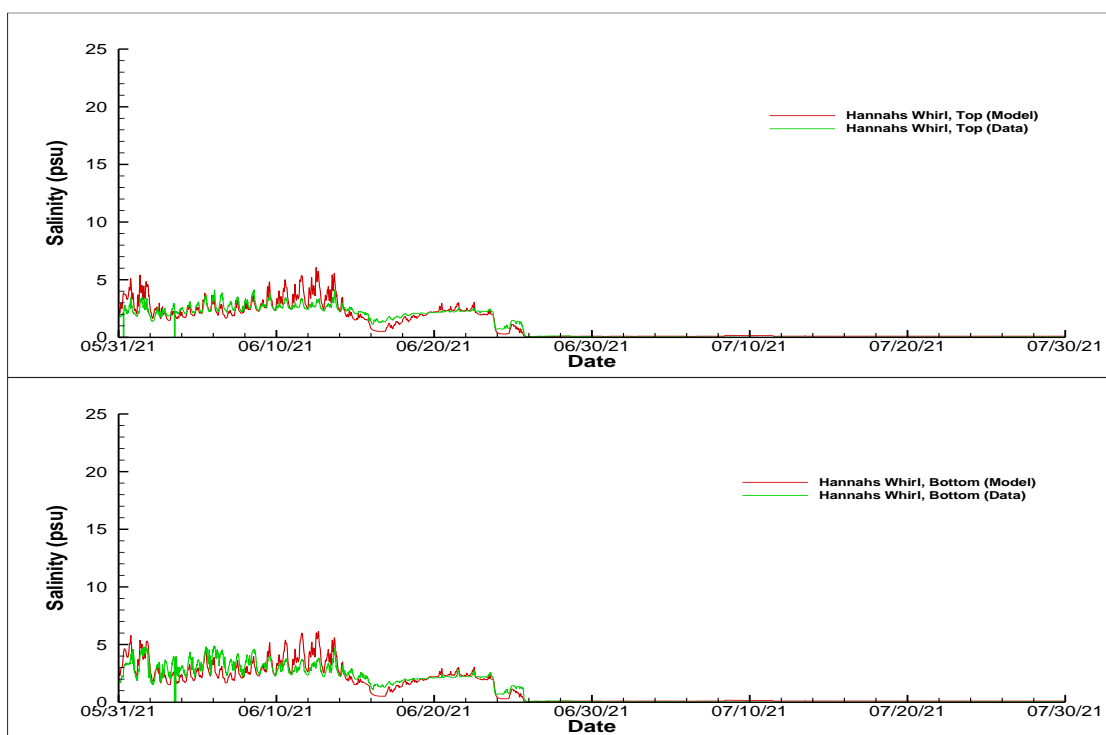
Figure 11. Comparisons of simulated and measured salinities at the top and bottom layers of the USGS Hannah's Whirl station during 5/31/2021 – 7/30/2021.

During the 60 days from 5/31/2021 to 7/30/2021, salinity at the USGS Sulphur Springs run was basically determined by salinity in the SS pool. Both simulated and measured salinities exhibited relatively stable value that is very close to that in the pool, except for two bad data points in measured data and a small peak in simulated salinity, which may be caused by some bad input data.
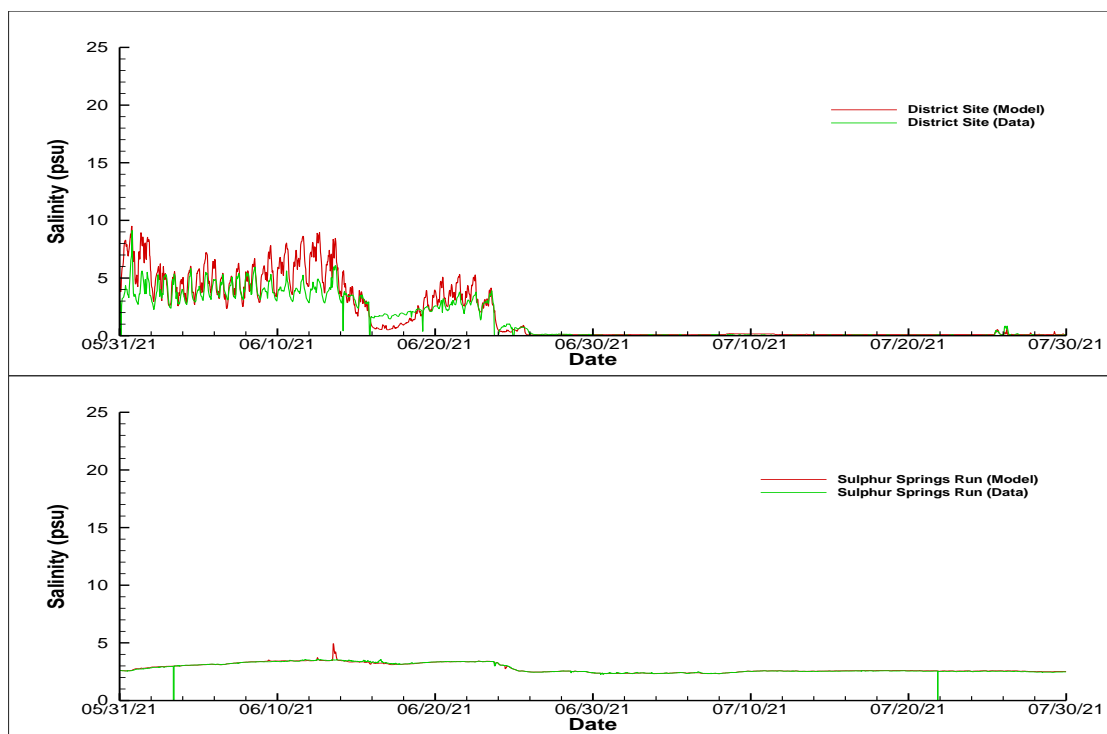
Figure 12. Comparisons of simulated and measured salinities at the bottom layers at the District station (top panel) and the USGS Sulphur Springs run station (bottom panel) during 5/31/2021 – 7/30/2021.

Fig. 13 are comparisons of simulated salinities at the top and bottom layers to measured real-time data at the USGS I-275 station during 5/31/2021 – 7/30/2021. As the site is further downstream, tidal influence on salinity at the USGS I-275 is most visible among the five data stations used for model calibration. Similar to the District station, the tidal variability in simulated salinity is little larger than that in measured salinity at this station. Like other more upstream stations, long-term variabilities in simulated and measured salinities matched well, though there was a mismatch between simulated and measured salinities at the bottom layer during a 3-day period in early June 2021. The salinity variation at the bottom layer during the 3 days did not match that at the top layer at the same station. It also did not match those at other upstream stations such as the District station and the USGS Hannah's Whirl station. Therefore, the mismatch of simulated and measured salinities at the bottom layer of the USGS I-275 station is most likely due to bad data of the field measurement.

Figure 13. Comparisons of simulated and measured salinities at the top and bottom layers of the USGS I-275 station during 5/31/2021 – 7/30/2021.

Simulated temperatures were compared with real-time measurements and are presented in Figs. 14 – 17 at the USGS Rowlett Park, Hannah's Whirl, Sulphur Springs Run, and I-275 stations. No real-time temperature data was available for the District station. Like the specific conductance data, temperature data were collected at both the top and bottom layers at these USGS stations, except for the USGS Sulphur Springs Run station, where only the bottom layer temperature was measured.

Comparisons shown in Figs. 14 -17 are for a 60-day period during 12/30/2020 – 2/28/2021. January and February are generally the coldest time of the year in the Tampa Bay region, when the water temperature in the LHR drops to the yearly minimum. From the figures, one can see that the water temperature in January and February is generally higher than 15°C at all real-time stations in the LHR, even during days of cold fronts which could bring near frozen air to the region. For example, the air temperature at the UF IFAS Dover station reached 0.91°C at 5:15 AM on February 4, 2021, simulated and measured water temperatures at the time were still above 15 °C at the four USGS stations in the LHR. This would be good news for manatees, as they would have a hard time surviving water temperature below 15 °C for more than four hours.

Figs. 14 and 15 show good matches between simulated and measured temperatures at both the top and bottom layers at the USGS Rowlett Park and Hannah's Whirl stations. Both the diurnal variations and long-term variations were correctly simulated, except for a few days around the end

of January 2021, which appears to be related to some bad weather data collected at the UF IFAS Dover station.

Figure 14. Comparisons of simulated and measured temperatures at the top and bottom layers of the USGS Rowlett Park station during 12/30/2020 – 2/28/2021.

As expected, water temperature in the SS run is dominated by that in the SS pool. As a result, simulated and measured temperatures at the USGS Sulphur Springs station were relatively stable at about 25.5 °C, with a very small diurnal variation. The cold front at the end of January caused the water temperature to have a decline of about 1 °C in the spring run.

For the USGS I-275 station, there are some high frequency noises in the real-time data, which must be false signals. Neglecting these unreal noises in the field data, the match between simulated and measured data is good, because the general trend as well as the diurnal variations were well simulated.

To quantify the performance of the LHR LAMFE model, a set of statistics were calculated, including the mean error, mean absolute error, coefficient of determination, and Willmott (1981) skill parameter defined as follows.

$$S_k = 1 - \frac{\Sigma(y^M - y^D)^2}{\Sigma(|y^M - \overline{y^D}| + |y^D - \overline{y^D}|)^2} \qquad (2)$$

where y^M and y^D are simulated and measured variables (surface elevation or salinity) and $\overline{y^D}$ and $\overline{y^M}$ are means of y_i^D and y_i^M, respectively. Skill in Equation (2) varies between 0 and 1: a

perfect agreement between simulated results and measured data yields a skill of one and a complete disagreement yields a skill of zero.

The skill assessment metrics are shown in Tables 4, 5, and 6 for model predictions of the water level, salinity, and temperature, respectively. The mean error for the water level prediction was -0.71 cm for the model calibration period, 0.53 for model verification period, and 0.11 for the entire simulation period. The mean absolute errors of the water level prediction were respectively 5.76, 6.19, and 6.03 cm for the three periods. The coefficients of determination for the water level prediction were all above 0.90 for the calibration and verification periods as well as the entire simulation period, while the Willmott skill parameters were all above 0.97 for the three periods. All these statistics have suggested that the LAMFE model can predict water levels in the LHR and SS run very well.
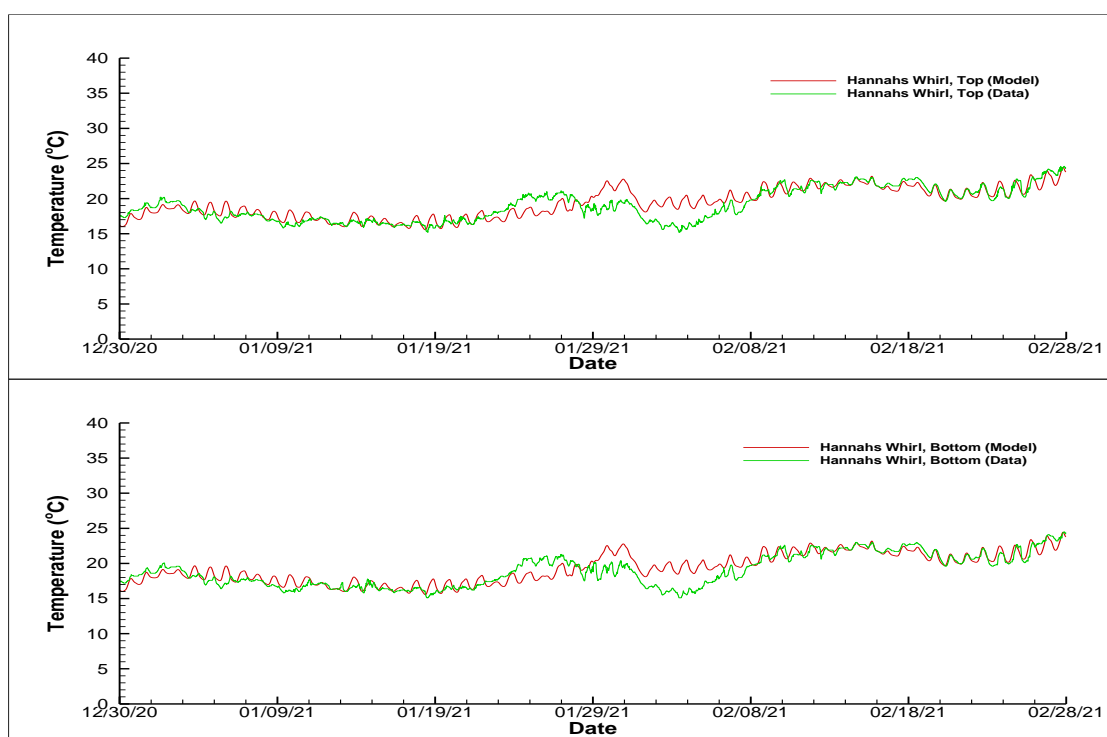
Figure 15 Comparisons of simulated and measured temperatures at the top and bottom layers of the USGS Hannah's Whirl station during 12/30/2020 – 2/28/2021.

For the salinity prediction, the LAMFE model prediction has a mean error of -0.02 psu for the calibration period, -0.08 psu for the verification period, and 0.06 psu for the entire simulation period. The mean absolute errors for these three periods were 0.46, 0.47, and 0.47 psu, respectively. The coefficients of determination for the calibration, verification, and entire simulation periods were all about 0.77, while the Willmott skill parameters were 0.93 or higher. These statistics show that the LAMFE model can simulate salinity transport process in both the LHR and SS run, with satisfactory prediction of salinity transport processes in the estuarine system.

26
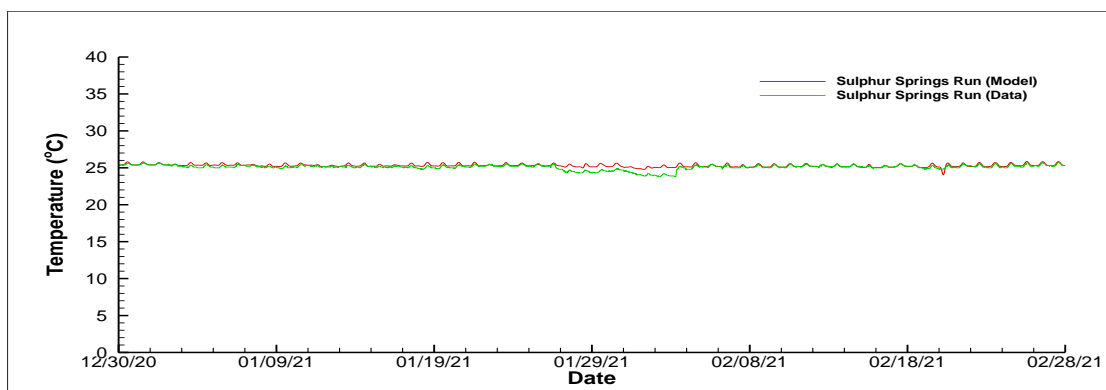
Figure 16. Comparisons of simulated and measured temperatures at the bottom layer of the USGS Sulphur Springs run station during 12/30/2020 – 2/28/2021.
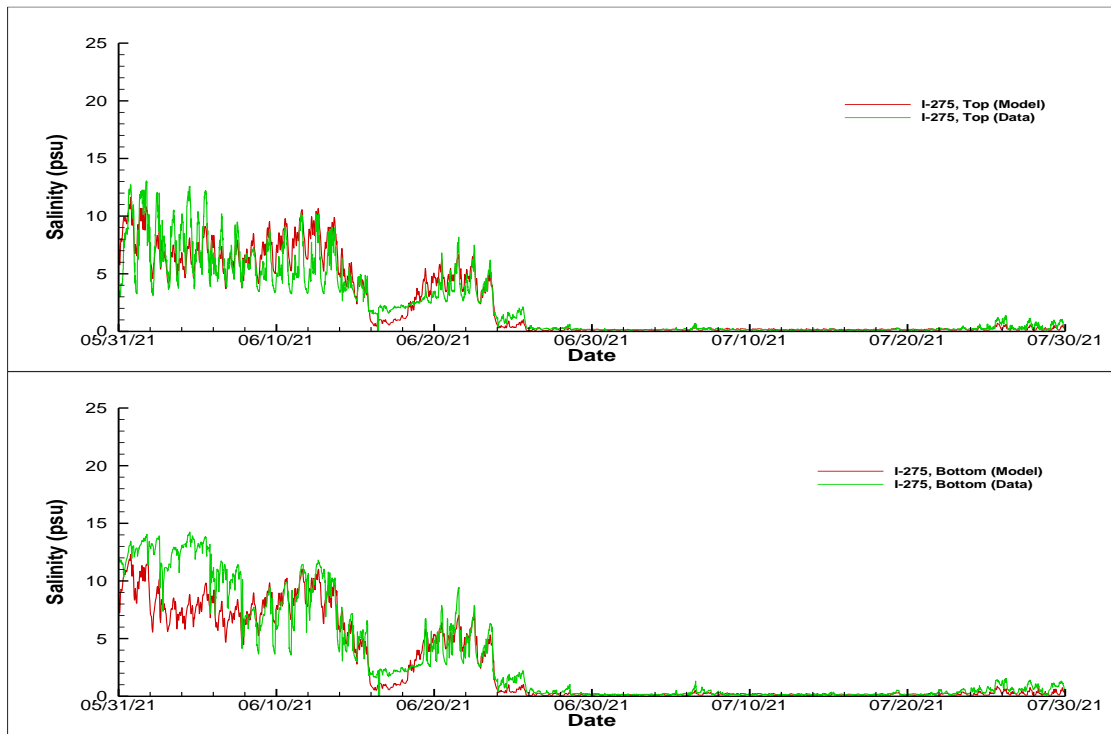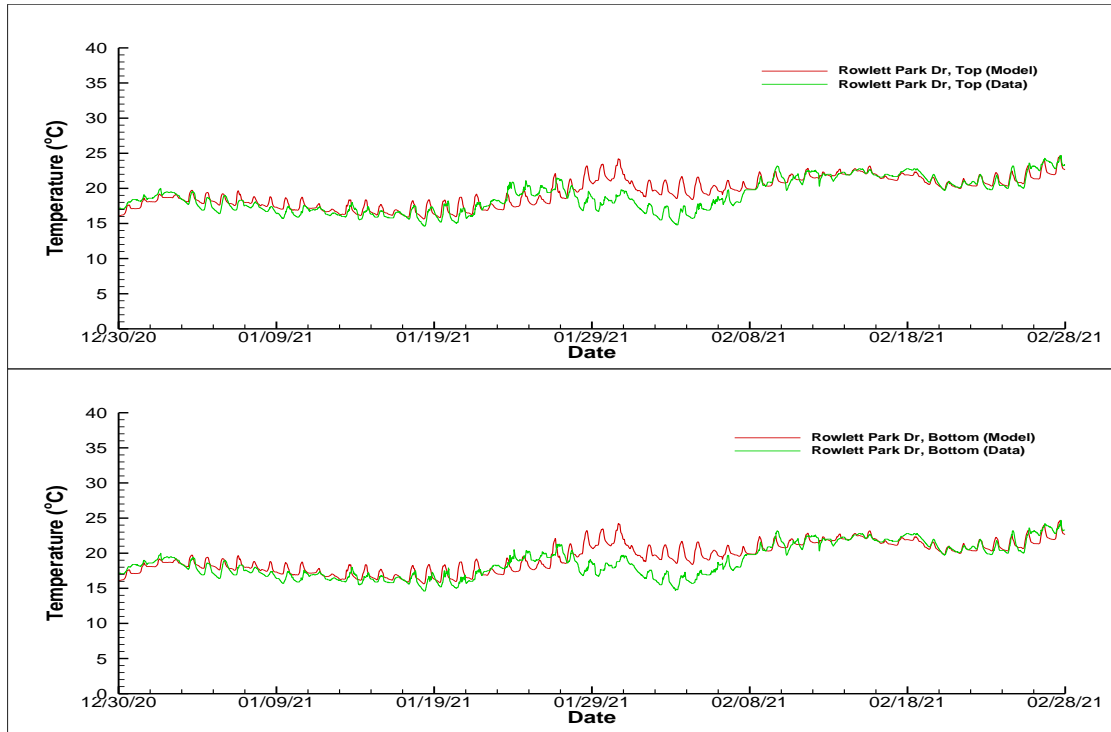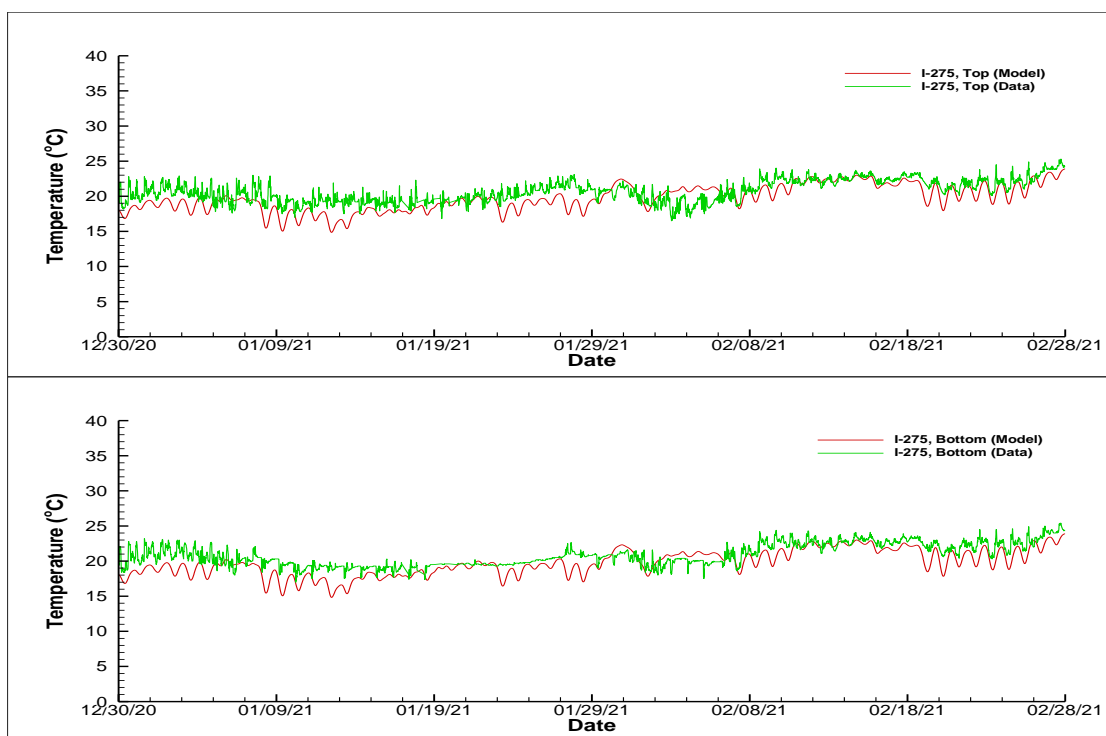

Figure 17. Comparisons of simulated and measured temperatures at the top and bottom layers of the USGS I-275 station during 12/30/2020 – 2/28/2021.

The skill assessment metrics also show a good performance of the LAMFE model for the temperature prediction in the LHR and the SS run. As can be seen in Table 6, the mean errors for the temperature prediction were 0.09, 0.16, and 0.14 °C during the calibration, verification, and entire simulation periods, respectively. The mean absolute errors were respectively 1.10, 1.05, and 1.07 °C for the three periods. The coefficients of determination for the temperature simulation in the LHR and SS run were about 0.83 for the calibration, verification, and entire simulation periods, while the Willmott skill parameters were all above 0.95.

Table 4. Skill assessment metrics for the water level simulation in the LHR and the Sulphur Springs run during the calibration period (4/15/2020 – 10/12/2021), the verification period (10/25/2017 – 4/14/2020), and the entire simulation period (10/25/2017 - 10/12/2021.)

Water Level	Mean Error (cm)	Mean Absolute Error (cm)	R^2	Willmott Skill
Calibration	-0.708	5.762	0.909	0.976
Verification	0.532	6.189	0.902	0.974
Entire Period	0.105	6.035	0.904	0.975

Table 5. Skill assessment metrics for the salinity simulation in the LHR and the Sulphur Springs run during the calibration period (4/15/2020 – 10/12/2021), the verification period (10/25/2017 – 4/14/2020), and the entire simulation period (10/25/2017 - 10/12/2021.)

Salinity	Mean Error (psu)	Mean Absolute Error (psu)	R^2	Willmott Skill
Calibration	-0.017	0.460	0.772	0.935
Verification	-0.083	0.472	0.766	0.930
Entire Period	-0.060	0.469	0.765	0.931

Table 6. Skill assessment metrics for the temperature simulation in the LHR and the Sulphur Springs run during the calibration period (4/15/2020 – 10/12/2021), the verification period (10/25/2017 – 4/14/2020), and the entire simulation period (10/25/2017 - 10/12/2021.)

Temperature	Mean Error (ºC)	Mean Absolute Error (ºC)	R^2	Willmott Skill
Calibration	0.091	1.102	0.828	0.951
Verification	0.163	1.049	0.830	0.953
All	0.137	1.066	0.831	0.953

5. MFL Assessment Simulations

With the LAMFE model being calibrated and verified for the water level, salinity, and temperature simulations, it was used to assess the MFL implementation in the LHR. Three flow scenarios were determined to be run for the third 5-year MFL assessment, including the existing flow condition, the full MFL implementation condition, and the no MFL implementation condition. It was decided to run the LHR LAMFE model for a period from October 2007 to December 2023, a total of 195 months (more than 16 years.)

Like the model simulation during model calibration and verification, time series of CTD at Platt Street and flows entering the river at the base of the dam and at the upstream cross section of the SS run are obtained from various data sources for the entire period of the scenario run. Meteorological data for the 195-month period were retrieved from the FAWN website at the UF IFAS station at Dover, except for the rainfall data, which mainly came from the District station in the LHR, with data gaps being filled with those recorded at the USGS Sulphur Springs Pool station or the UF IFAS station at Dover. These rainfall data were used to estimate ungagged flows to the LHR using the method described in Section 2.3.

The scenario runs used the same downstream boundary conditions, ungagged flows, and meteorological forcing, and the only difference among the scenarios is the gaged flows entering the LHR at the base of the dam and at the upstream section of the SS run. The flow input to the LAMFE model for the existing flow condition was prepared based mainly on the operational data provided by the City of Tampa, which included daily or hourly information for flows pumped from the SS pool to the base of the dam, from the SS pool to the spring run, from Blue Sink to the flume, from reservoir over the dam, and/or released through the sluice gate. For the MFL fully implemented scenario, the flow input file was prepared based on the current and previous MFL rules for the LHR. Currently, the LHR MFL rules consider several factors related to the LHR, including inflow entering the reservoir (flow measured at the USGS Hillsborough River at State Park near Zephyrhills station), the dry and wet seasons, and the use of SS water, which has an average salinity of about 2.68 psu. Details about the current LHR MFL rules are explained below.

Let Q_{dam} be the discharge reported by the USGS through the Hillsborough River dam (cfs), Q_{zh} the discharge reported by the USGS at its Zephyrhills station (cfs), and Q_{MFL} the MFL for the lower Hillsborough River (cfs), which was determined to be

$$Q_{MFL} = \begin{cases} 20, & Jul - Mar \\ 24, & Apr - Jun \end{cases} \tag{3}$$

Q_{MFL} needs to be adjusted based on the discharge measured at the USGS station near Zephyrhills, with the consideration of a low flow threshold of 58 cfs, as follows.

$$\Delta Q_{zh} = max\,(58 - Q_{zh}, 0) \tag{4}$$

$$Q_{MFL\_a} = \begin{cases} 20 - 0.35\Delta Q_{zh}, & Jul - Mar \\ 24 - 0.40\Delta Q_{zh}, & Apr - Jun \end{cases} \tag{5}$$

where ΔQ_{zh} is the flow deficit relative to the low flow threshold of 58 cfs at the USGS station near Zephyrhills and Q_{MFL_a} is the adjusted minimum flow for the LHR.

Considering the use of the Sulphur Springs flow for the MFL, 3 cfs freshwater should be added:

$$Q_{MFL\_a3} = 3 + \begin{cases} 20 - 0.35\Delta Q_{zh}, & Jul - Mar \\ 24 - 0.40\Delta Q_{zh}, & Apr - Jun \end{cases} \tag{6}$$

Freshwater flow received by the LHR at the base of the dam, without using the SS flow, is:

$$Q_{LHR} = max\,(Q_{dam}, Q_{MFL\_a}) \tag{7}$$

The final total flow entering the LHR at the dam, with the use of the SS flow, is:

$$Q_{LHR} = Q_{dam}S + (1 - S)Q_{MFL\_a3} \tag{8}$$

where S represents the Heaviside step function

$$S = H(Q_{dam} - Q_{MFL_a}) = \begin{cases} 1, & Q_{dam} > Q_{MFL\_a} \\ 0, & Q_{dam} \leq Q_{MFL\_a} \end{cases} \tag{9}$$

For the no MFL scenario, all the flow movements by the City of Tampa are assumed to be stopped. For example, reservoir flow pumped by the city over the dam is assumed to be zero, no Blue Sink flow is pumped to the flume, and no flow is released through the sluice gate. The SS flow that is supposed to routed to the base of the dam now enters the spring run. In other words, there exists no flume flow and the SS run receives flows over the weir at the pool and the total flow pumped by the city from the SS pool. It is further assumed that all these changes from the existing flow conditions do not affect the flow of SS pool and the spillway flow from the Tampa reservoir.

Simulated salinity and temperature results at all grid cells of the LHR LAMFE model were saved to an output file every 30 minutes. The model results were post-processed to calculate various salinity habitats and thermal habitats for manatees. Salinity habitats obtained include salinity volumes, bottom areas, and shoreline lengths for various salinity ranges. Thermal habitats for manatees include water volume and surface areas for temperature $\geq$ 20 ºC and for temperature between 15ºC and 20 ºC.

5.1 Simulated Low Salinity Habitats

As low salinity habitats such as those of $\leq$ 2 and 5 psu in the upstream segment of the LHR between the dam and the confluence with the SS run are the primary focus of the third 5-year MFL assessment, only $\leq$ 2 and $\leq$ 5 psu water volumes, bottom areas, and shoreline lengths are presented and discussed below. Figs. 18, 20, and 22 are time series plots of simulated water volumes (top panel), bottom areas (middle panel), and shoreline lengths (bottom panel) of $\leq$ 2 psu (blue) and $\leq$ 5 psu (orange) between the dam and the confluence with the SS run in the LHR during October 2007 – December 2023 for the existing, MFL, and no MFL flow conditions respectively. Because MFL rules for the LHR were strictly implemented since January 2023, the same time series plots for January – December 2023 were generated and presented in Figs. 19, 21, and 23, respectively for the existing, MFL, and no MFL flow conditions. From a visual comparison of the figures, one

can see that low salinity habitats in the most upstream segment of the LHR for the existing flow condition had a significant improvement over the no MFL flow condition. One obvious fact is that there existed no occurrences where ≤ 5 psu water volume, bottom area, or shoreline length was reduced to zero in the LHR since October 2007. Nevertheless, if no MFL rules were implemented, there would be numerous times when ≤ 5 psu salinity habitats became zero during the 16-year period. For most part of the simulation period between October 2007 and December 2023, simulated low salinity habitats for the existing flow condition were very close to those of the MFL flow condition. However, some improvements could be achieved when the MFL rules were fully implemented. One can see such an improvement by a detailed comparison of Figs. 18 and 20. For example, near the end of the dry season in 2012, there were several days when the ≤ 2 psu water volume, bottom area, and shoreline length were zero in the LHR for the existing flow condition (see the blue lines in Fig. 18 during the dry season of 2012). These zero ≤ 2 psu days would be eliminated if the MFL were fully implemented (see blue lines in Fig. 20 during the same dry season of 2012.)

Because the MFL rules for the LHR were fully implemented, the existing flow condition was the same as the MFL flow condition for the LHR. As a result, plots shown in Fig. 19 are identical to those shown in Fig. 21. Compared with the plots shown in Fig. 23, the improvement of the MFL is significant and obvious, with the period of no ≤ 5 psu habitats that lasted for about 4.5 months before the wet season and 2 months after the wet season being eliminated.

Figure 18. Simulated water volumes (top), bottom areas (middle), and shoreline lengths (bottom) of ≤ 2 psu (blue) and ≤ 5 psu (orange) between the dam and the confluence of the Sulphur Springs run in the LHR during October 2007 – December 2023 for the existing flow condition.

Figure 19. Simulated water volumes (top), bottom areas (middle), and shoreline lengths (bottom) of ≤ 2 psu (blue) and ≤ 5 psu (orange) between the dam and the confluence of the Sulphur Springs run in the LHR during January – December 2023 for the existing flow condition.

Figure 20. Simulated water volumes (top), bottom areas (middle), and shoreline lengths (bottom) of ≤ 2 psu (blue) and ≤ 5 psu (orange) between the dam and the confluence of Sulphur Springs run in the LHR during October 2007 – December 2023 for the MFL flow condition.

Figure 21. Simulated water volumes (top), bottom areas (middle), and shoreline lengths (bottom) of ≤ 2 psu (blue) and ≤ 5 psu (orange) between the dam and the confluence of Sulphur Springs run in the LHR during January – December 2023 for the MFL flow condition.

Figure 22. Simulated water volumes (top), bottom areas (middle), and shoreline lengths (bottom) of ≤ 2 psu (blue) and ≤ 5 psu (orange) between the dam and the confluence of Sulphur Springs run in the LHR during October 2007 – December 2023 for the no MFL flow condition.
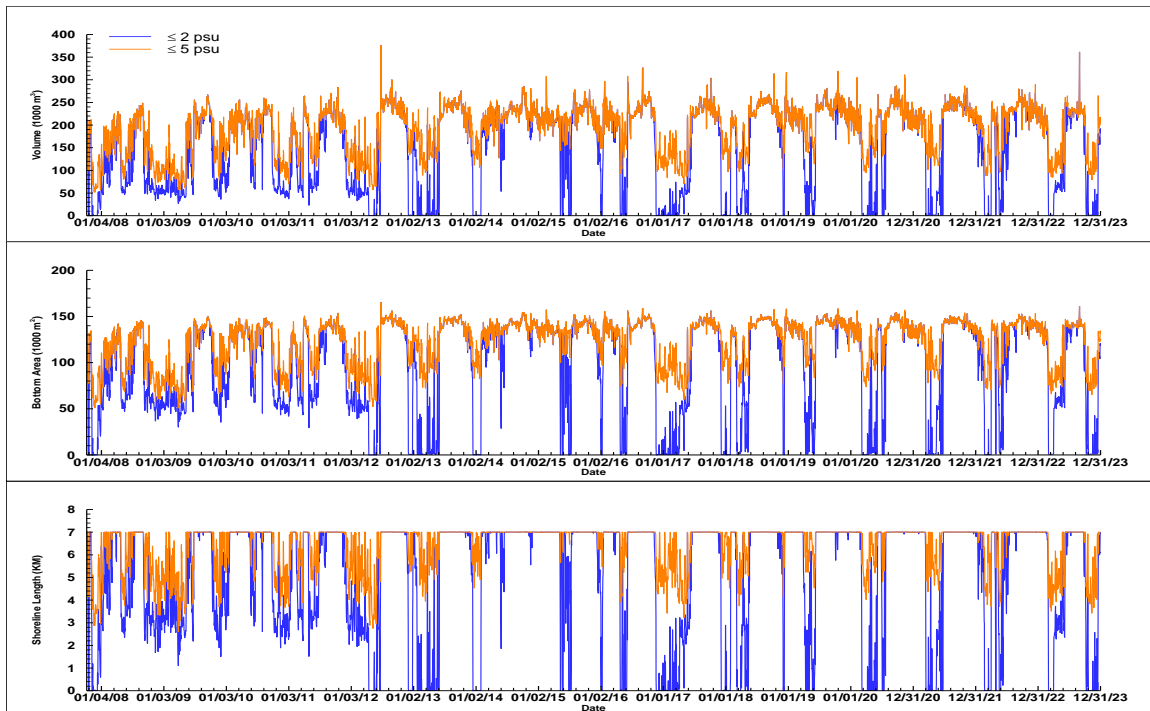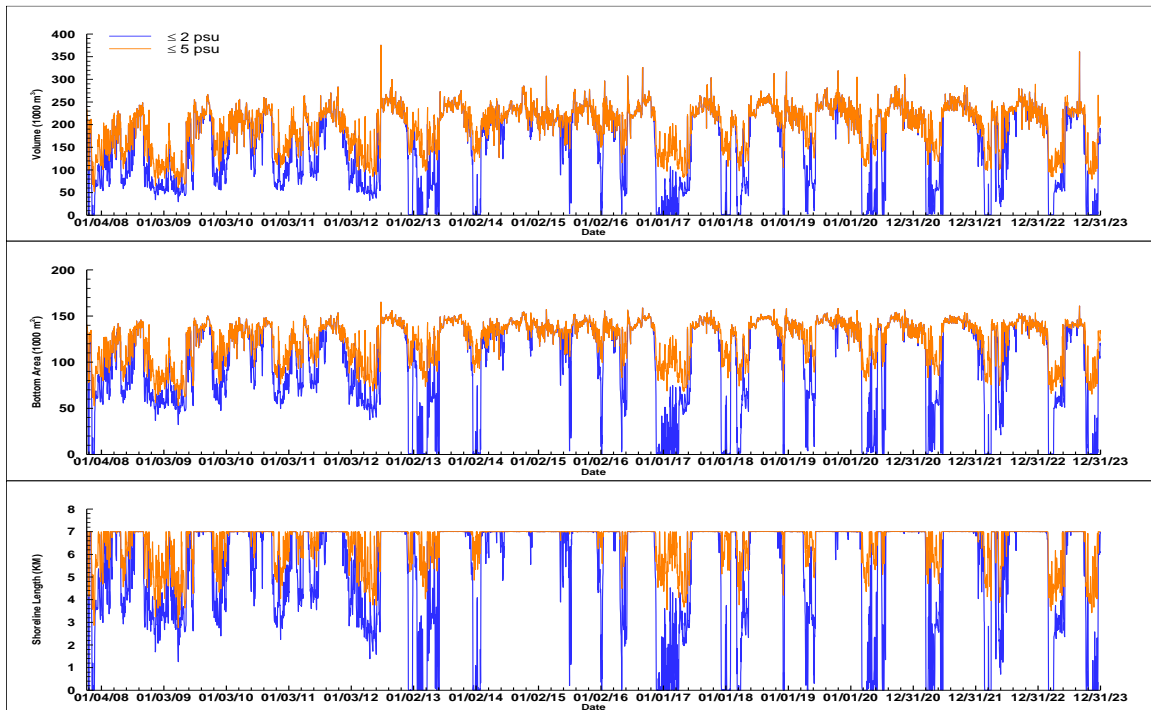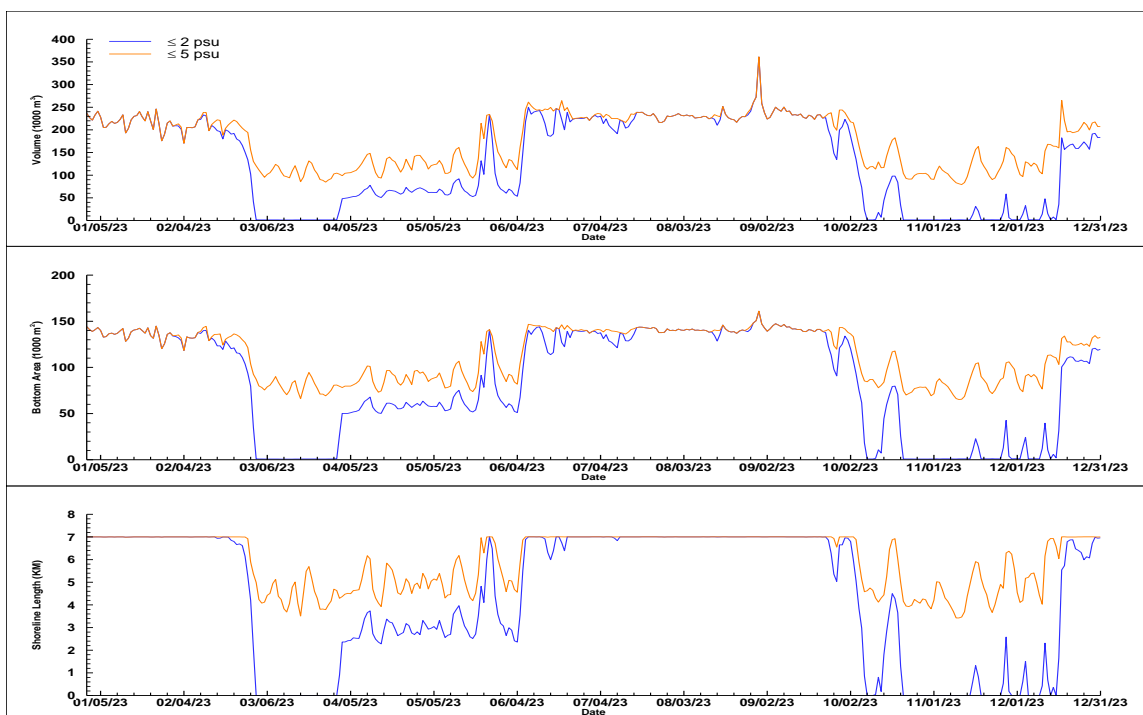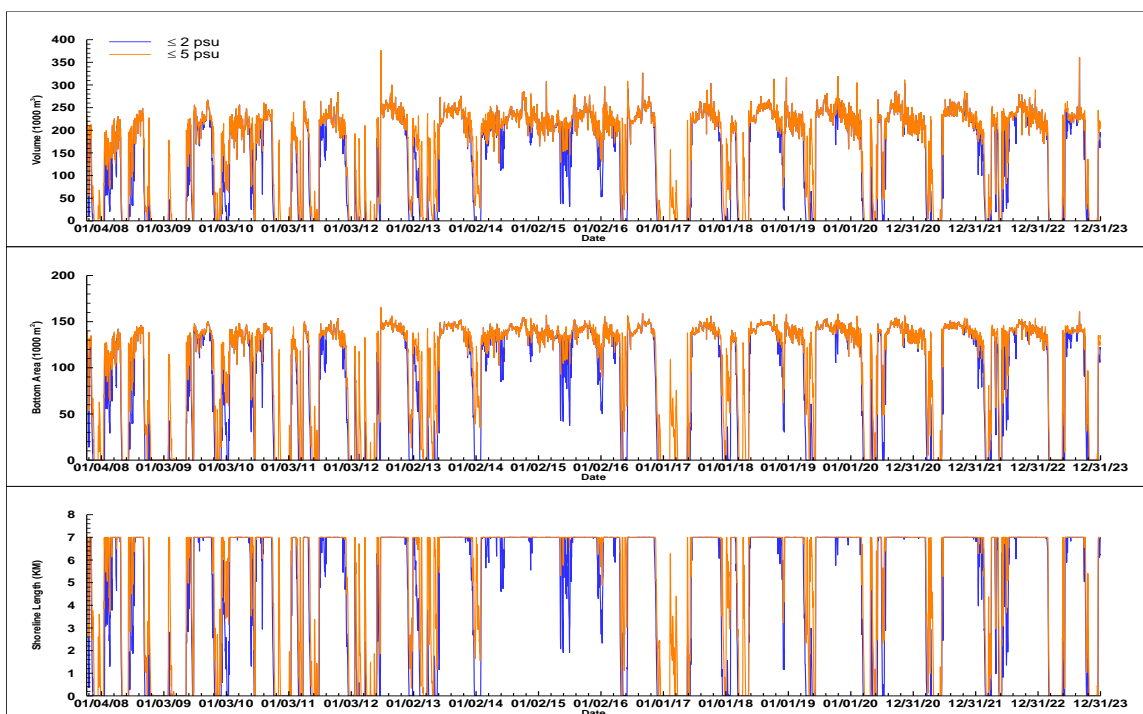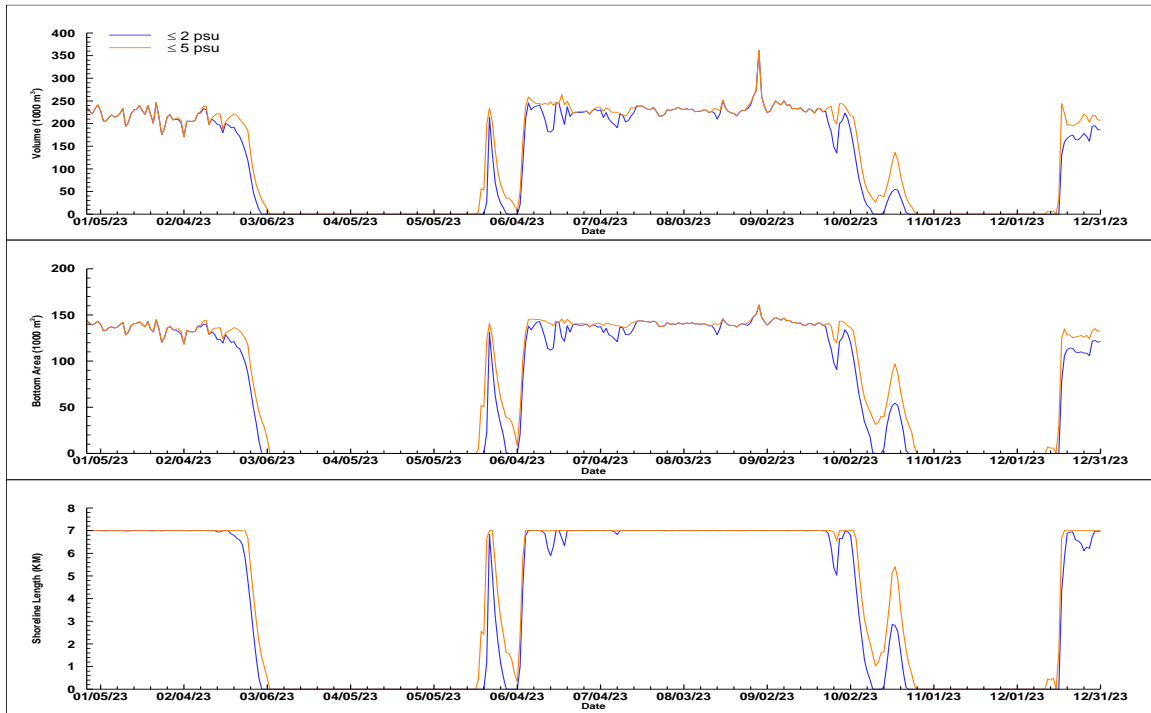
Figure 23. Simulated water volumes (top), bottom areas (middle), and shoreline lengths (bottom) of ≤ 2 psu (blue) and ≤ 5 psu (orange) between the dam and the confluence of Sulphur Springs run in the LHR during January – December 2023 for the no MFL flow condition.

Simulated time series of the low salinity habitats could be summarized with cumulative distribution functions (CDF), which then can be easily compared and used to illustrate the differences of simulated habitats among various flow scenarios. Figs. 24, 25, and 26 are comparisons of CDFs of simulated water volume, bottom area, and shoreline length, respectively for salinity ≤ 2 psu in the upstream segment during October 2007 – December 2023. Results of the existing flow condition are plotted with blue lines, while those of the MFL flow condition are plotted with red lines and CDFs for the no MFL flow condition are in green lines. As the area bounded by the y-axis and the CDF curve represents the average value of the time series, differences among these average values can be easily observed and identified simply by looking at the areas bounded by the y-axis and the various CDF curves.

Figs. 27, 28, and 29 are comparisons of CDFs of simulated water volume, bottom area, and shoreline length, respectively for salinity ≤ 5 psu during October 2007 – December 2023 in the same upstream segment as that shown in Figs. 24 – 26. Because the full MFL implementation was supposed to be carried out starting on January 1, 2023, CDF plots for these 12 months were generated specifically to verify the true full implementation of the MFLs for the LHR. These CDF plots are shown in Figs. 30 -35 in the same order as those in Figs. 24 – 29. As can be seen from these figures, CDFs for the existing and MFL scenarios are basically identical, suggesting that MFL rules for the LHR were indeed fully implemented since the first day of 2023.

Figure 24. CDFs of simulated ≤ 2 psu water volume for the existing, MFL, and no MFL flow conditions during Oct 2007 – Dec 2023 in the LHR between the dam and the Sulphur Springs confluence.

Figure 25. CDFs of simulated ≤ 2 psu bottom area for the existing, MFL, and no MFL flow conditions during Oct 2007 – Dec 2023 in the LHR between the dam and the Sulphur Springs confluence.

Figure 26. CDFs of simulated ≤ 2 psu shoreline length for the existing, MFL, and no MFL flow conditions during Oct 2007 – Dec 2023 in the LHR between the dam and the Sulphur Springs confluence.
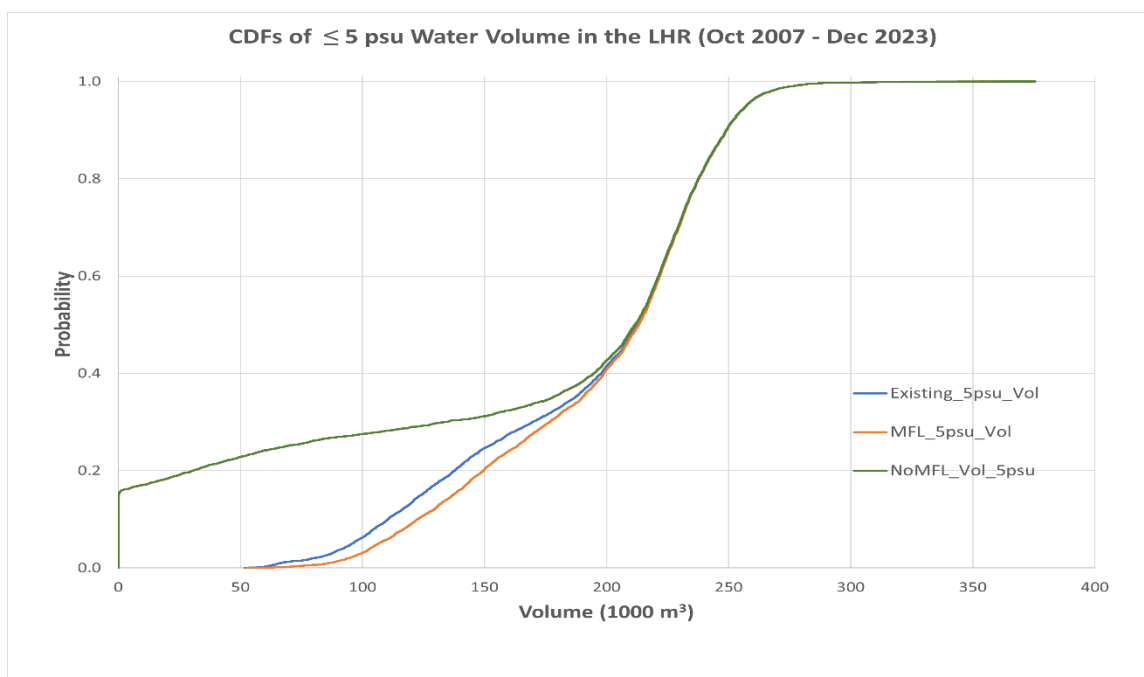
Figure 27. CDFs of simulated ≤ 5 psu water volume for the existing, MFL, and no MFL flow conditions during Oct 2007 – Dec 2023 in the LHR between the dam and the Sulphur Springs confluence.
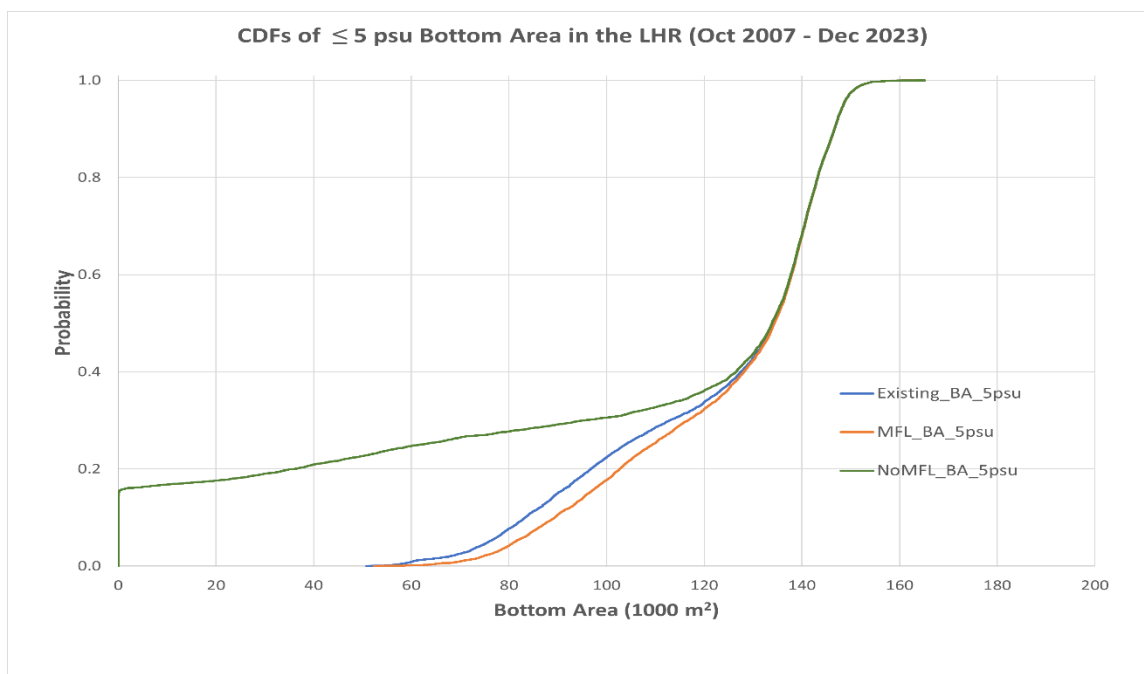
Figure 28. CDFs of simulated ≤ 5 psu bottom area for the existing, MFL, and no MFL flow conditions during Oct 2007 – Dec 2023 in the LHR between the dam and the Sulphur Springs confluence.
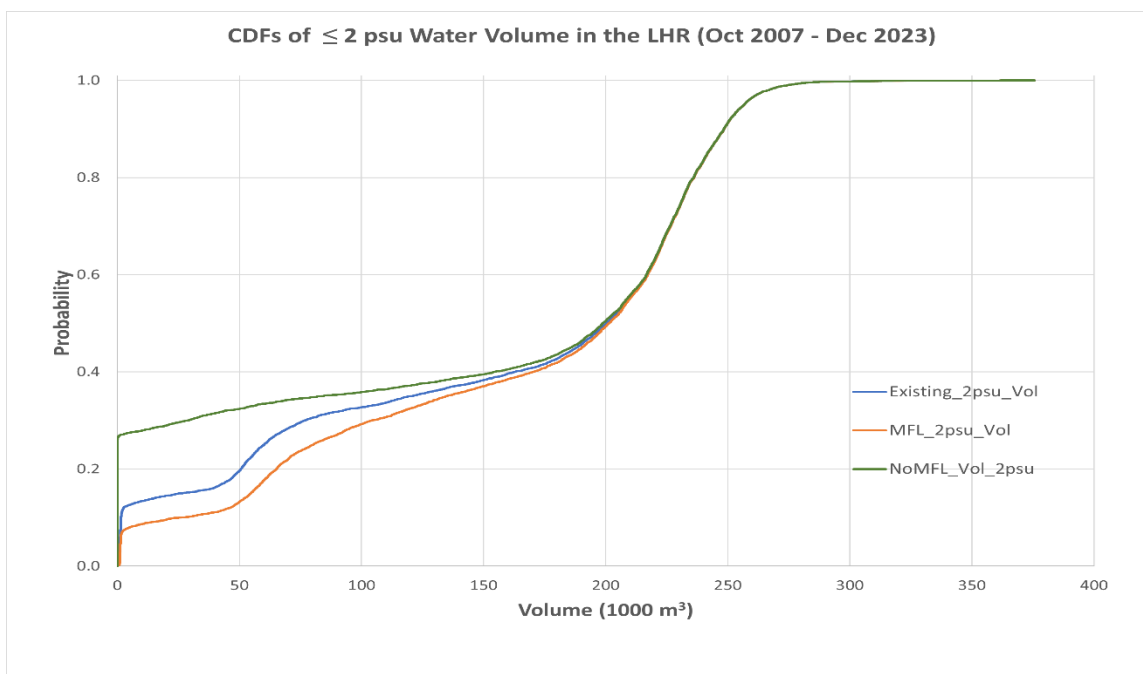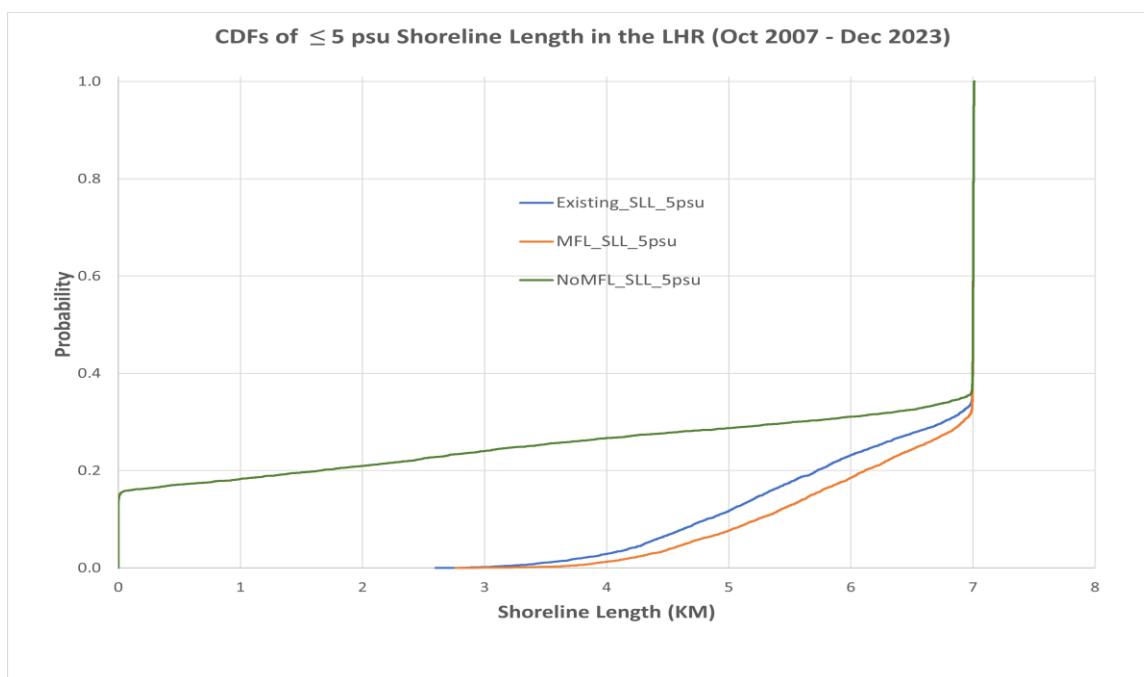

Figure 29. CDFs of simulated ≤ 5 psu shoreline length for the existing, MFL, and no MFL flow conditions during Oct 2007 – Dec 2023 in the LHR between the dam and the Sulphur Springs confluence.
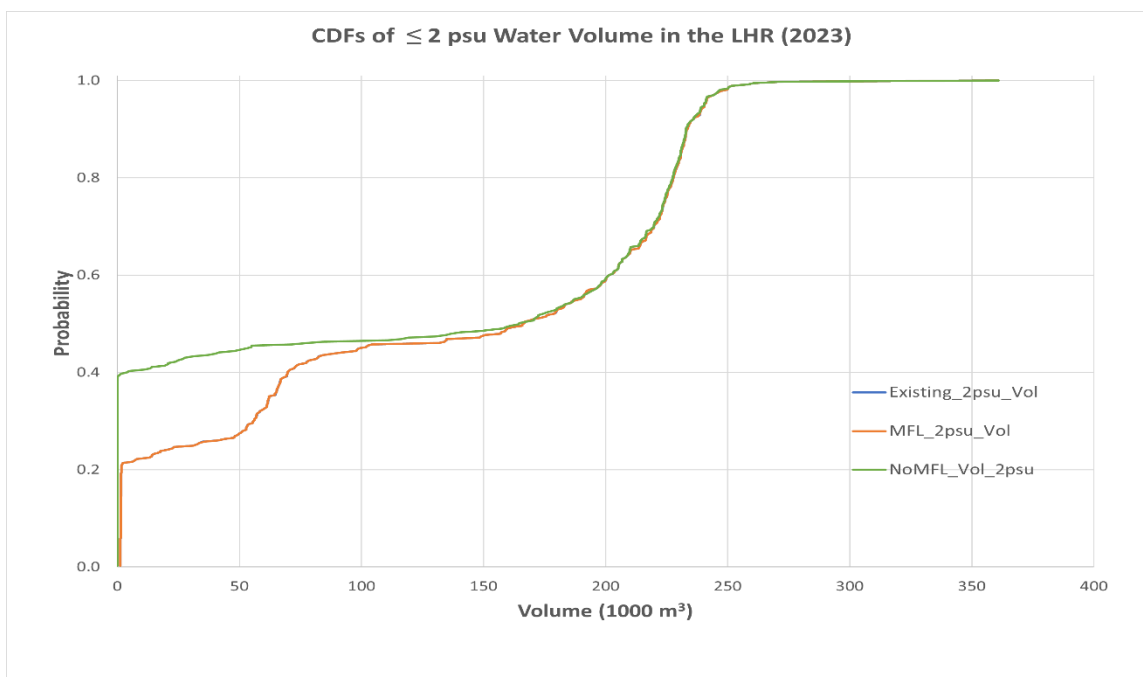
Figure 30. CDFs of simulated ≤ 2 psu volume for the existing, MFL, and no MFL flow conditions in 2023 in the LHR between the dam and the Sulphur Springs confluence.
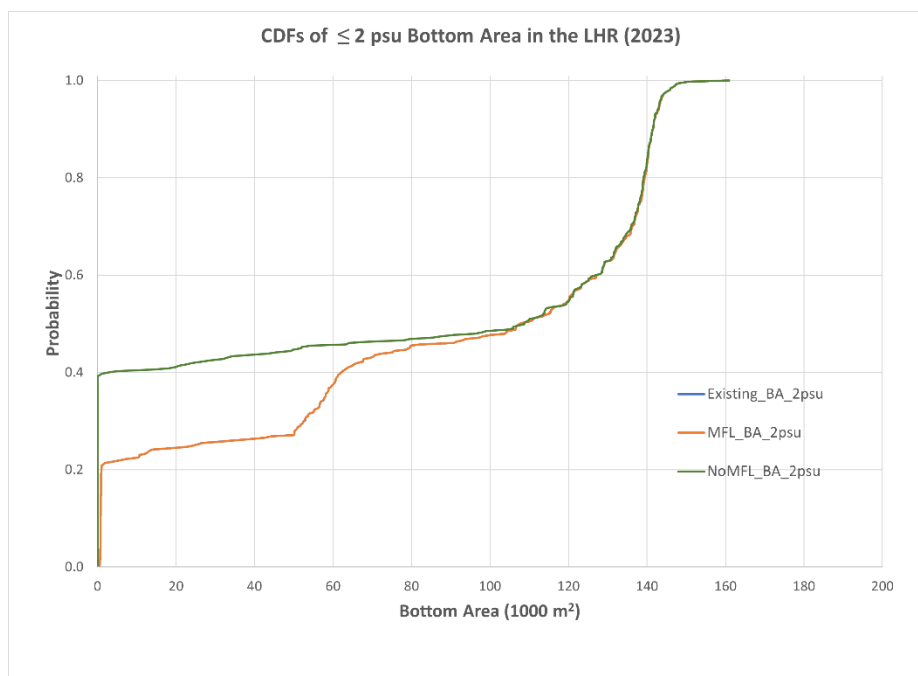
Figure 31. CDFs of simulated ≤ 2 psu bottom area for the existing, MFL, and no MFL flow conditions in 2023 in the LHR between the dam and the Sulphur Springs confluence.
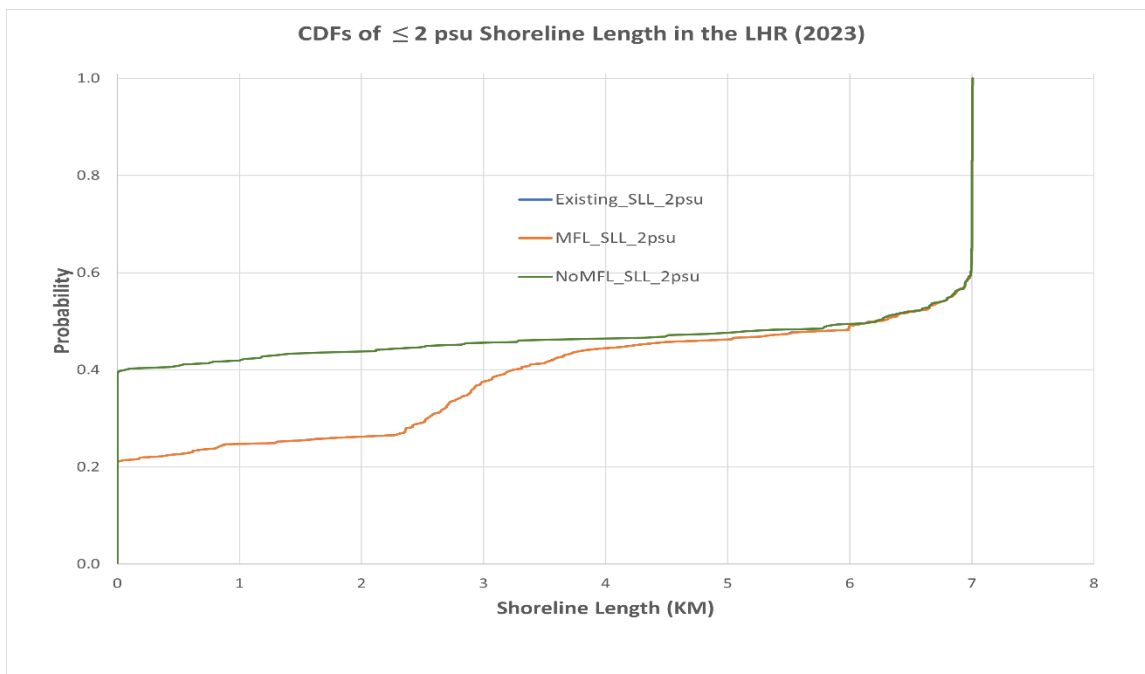
Figure 32. CDFs of simulated ≤ 2 psu shoreline length for the existing, MFL, and no MFL flow conditions in 2023 in the LHR between the dam and the Sulphur Springs confluence.

Figure 33. CDFs of simulated ≤ 5 psu volume for the existing, MFL, and no MFL flow conditions in 2023 in the LHR between the dam and the Sulphur Springs confluence.
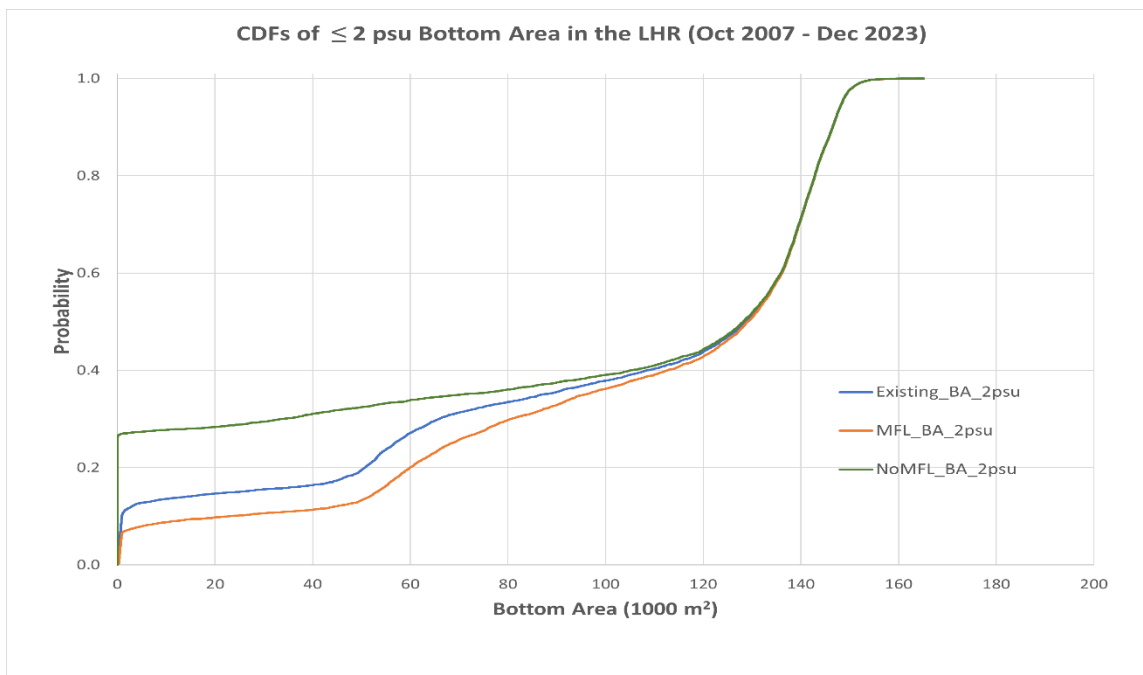
Figure 34. CDFs of simulated ≤ 5 psu bottom area for the existing, MFL, and no MFL flow conditions in 2023 in the LHR between the dam and the Sulphur Springs confluence.
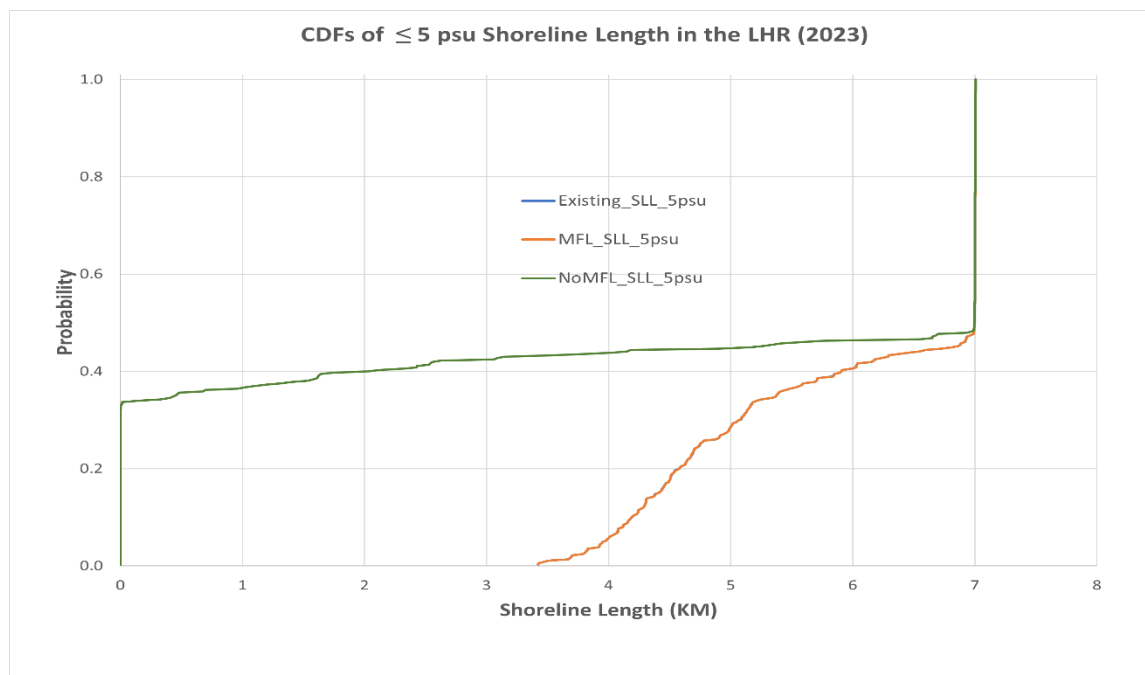
Figure 35. CDFs of simulated ≤ 2 psu shoreline length for the existing, MFL, and no MFL flow conditions in 2023 in the LHR between the dam and the Sulphur Springs confluence.

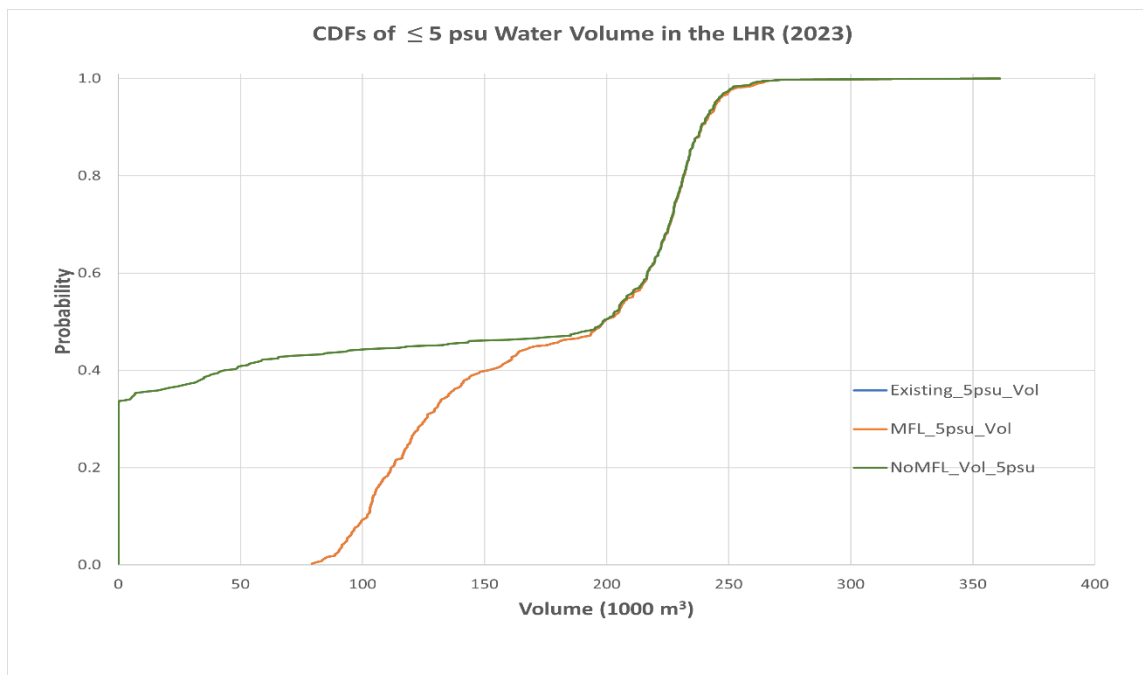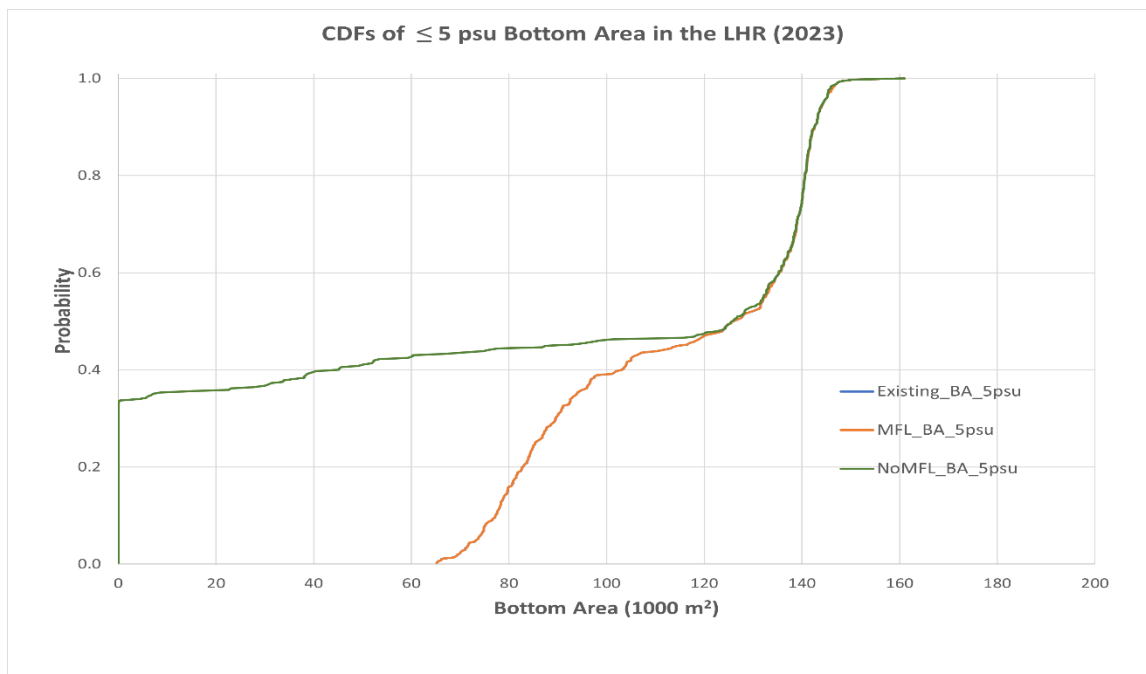Tables 7 – 9 are average and median volumes, bottom areas, and shoreline lengths for salinity ≤ 2 psu between the dam and the SS confluence in the LHR for the 195-month simulation period from October 2007 to December 2023 and for the 12-month period in 2023. Ratios of the low salinity habitats for the existing and no MFL scenarios to the corresponding habitats for the MFL scenario are also given in the tables.

Table 7. Average and median volumes for salinity ≤ 2 psu between the dam and the Sulphur Springs confluence in the LHR during the 195-month period from October 2007 to December 2023 and in 2023. Ratios to results of the MFL scenario are also included.

≤ 2 psu	Oct 2007 – Dec 2023		Jan - Dec 2023	
	Volume (1000 m³)	Ratio to MFL	Volume (1000 m³)	Ratio to MFL
Average				
Existing	155.89	0.957	130.96	1.000
MFL	162.94		130.96	
No MFL	143.85	0.883	117.37	0.896
Median				
Existing	200.31	0.995	166.30	1.000
MFL	201.36		166.27	
No MFL	198.71	0.987	164.49	0.989

Table 8. Average and median bottom areas for salinity ≤ 2 psu between the dam and the Sulphur Springs confluence in the LHR during the 195-month period from October 2007 to December 2023 and in 2023. Ratios to results of the MFL scenario are also included.

≤ 2 psu	Oct 2007 – Dec 2023		Jan - Dec 2023	
	Bottom Area (1000 m²)	Ratio to MFL	Bottom Area (1000 m³)	Ratio to MFL
Average				
Existing	99.64	0.951	84.50	1.000
MFL	104.78		84.50	
No MFL	90.10	0.860	73.28	0.867
Median				
Existing	128.62	0.996	107.63	1.000
MFL	129.10		107.65	
No MFL	128.21	0.993	108.71	1.010

On average, the river segment between the dam and the SS confluence had about 155,890 m³ of ≤ 2 psu water during October 2007 – December 2023. If the MFL rules were fully implemented, the average ≤ 2 psu volume would be 162,940 m³ during the 195-month period.

However, if no MFL were implemented, the river segment would only have 143,850 m³ of ≤ 2 psu water. In terms of ≤ 2 psu volume, the existing flow condition represented about 95% of the full MFL flow condition during October 2007 – December 2023, while the no MFL flow condition would represent 88% of it during the same period. In 2023, results of simulated ≤ 2 psu volume for the existing and MFL flow conditions were basically the same, which is expected. If no MFL flows were released, the average of ≤ 2 psu volume in 2023 would be about 90% of that for the full MFL implementation.

Median ≤ 2 psu volumes for the three flow scenarios were very close during October 2007 – December 2023. Ratios of ≤ 2 psu volumes for the existing and no MFL flow conditions to that of the full MFL flow condition were 99% or higher for the 195-month period. The same was true during the 12 months of 2023, with differences among the three medians of ≤ 2 psu volume being about 1% or less.

Characteristics of average and median ≤ 2 psu bottom areas and shoreline lengths during October 2007 – December 2023 and during the 12 months of 2023 are similar to those of average and median ≤ 2 psu volumes. Averages of ≤ 2 psu bottom area and shoreline length for the existing flow condition were about 5% lower than those for the MFL flow condition. Under the no MFL flow condition, however, averages of ≤ 2 psu bottom area and shoreline length were respectively 14% and 15% lower than those under the MFL flow condition. Differences of median ≤ 2 psu bottom areas and shoreline lengths among the three flow conditions were very small. These differences were generally less than 1% for the 195-month simulation period and basically 0% for the 12 months of 2023. The slightly odd numbers for the medians of ≤ 2 psu bottom area and shoreline length under the no MFL flow condition in 2023 were due to the non-smooth nature of their corresponding CDFs. A close exam of the CDFs showed that both the 49th and 51st percentiles of ≤ 2 psu bottom area and shoreline for the no MFL flow condition were smaller than those for the MFL flow condition, but the medians for the no MFL flow condition were slightly higher than those for the MFL flow condition in 2023.

Table 9. Average and median shoreline lengths for salinity ≤ 2 psu between the dam and the Sulphur Springs confluence in the LHR during the 195-month period from October 2007 to December 2023 and in 2023. Ratios to results of the MFL scenario are also included.

≤ 2 psu	Oct 2007 – Dec 2023		Jan - Dec 2023	
	Shoreline (KM)	Ratio to MFL	Shoreline (KM)	Ratio to MFL
Average				
Existing	5.12	0.947	4.36	1.000
MFL	5.41		4.36	
No MFL	4.59	0.848	3.78	0.868
Median				
Existing	7.00	1.000	6.21	1.000
MFL	7.00		6.21	
No MFL	7.00	1.000	6.22	1.001

Tables 10 – 12 are average volumes, bottom areas, and shoreline lengths for salinity ≤ 5 psu between the dam and the SS confluence in the LHR for the 195-month period from October 2007 to December 2023 and for the 12-month period in 2023. Like Tables 7 – 9, ratios of the low salinity habitats for the existing and no MFL scenarios to the corresponding habitats for the MFL scenarios are also given in the tables.

Table 10. Average and median volumes for salinity ≤ 5 psu between the dam and the Sulphur Springs confluence in the LHR during the 195-month period from October 2007 to December 2023 and in 2023. Ratios to results of the MFL scenario are also included.

≤ 5 psu	Oct 2007 – Dec 2023		Jan - Dec 2023	
	Volume (1000 m³)	Ratio to MFL	Volume (1000 m³)	Ratio to MFL
Average				
Existing	194.05	0.980	177.75	1.000
MFL	198.06		177.75	
No MFL	163.78	0.827	128.57	0.723
Median				
Existing	212.73	0.998	198.87	1.000
MFL	213.17		198.87	
No MFL	211.58	0.993	198.52	0.998

Table 11. Average and median bottom areas for salinity ≤ 5 psu between the dam and the Sulphur Springs confluence in the LHR during the 195-month period from October 2007 to December 2023 and in 2023. Ratios to results of the MFL scenario are also included.

≤ 5 psu	Oct 2007 – Dec 2023		Jan - Dec 2023	
	Bottom Area (1000 m²)	Ratio to MFL	Bottom Area (1000 m²)	Ratio to MFL
Average				
Existing	123.22	0.984	114.39	1.000
MFL	125.18		114.38	
No MFL	102.95	0.822	80.12	0.700
Median				
Existing	134.18	0.999	125.91	1.000
MFL	134.33		125.91	
No MFL	133.88	0.997	125.74	0.999

Generally, characteristics for ≤ 5 psu averages and medians are similar to those for ≤ 2 psu averages and medians. For example, averages were lower than medians for the entire simulation

period from October 2007 to December 2023 and for the 12 months of 2023. On average, the existing flow condition was able to create no less than 98% of the required ≤ 5 psu salinity habitats in the river segment between the dam and the SS confluence. Without any MFL flows, there would only be 80 – 83% of the required average ≤ 5 psu salinity habitats in the upstream river segment. During the 12 months in 2023, there would only be 67 – 72% of the required average ≤ 5 psu salinity habitats for the no MFL flow condition. Median ≤ 5 psu salinity habitats had similar values under the three flow conditions, with the differences among them being < 1%.

Table 12. Average and median shoreline lengths for salinity ≤ 5 psu between the dam and the Sulphur Springs confluence in the LHR during the 195-month period from October 2007 to December 2023 and in 2023. Ratios to results of the MFL scenario are also included.

≤ 5 psu	Oct 2007 – Dec 2023		Jan - Dec 2023	
	Shoreline (KM)	Ratio to MFL	Shoreline (KM)	Ratio to MFL
Average				
Existing	6.47	0.982	6.02	1.000
MFL	6.58		6.02	
No MFL	5.25	0.798	4.06	0.674
Median				
Existing	7.00	1.000	7.00	1.000
MFL	7.00		7.00	
No MFL	7.00	1.000	7.00	1.000

Because the simulation period was long enough to include some long-term rainfall variabilities in the region, annual average low salinity habitats were calculated to assess the implementation of the LHR MFL rules for each of the 16 years, especially for dry years. Furthermore, to reduce the effect of large flows on the MFL assessment, our attention was placed on days when reservoir flows over the Tampa dam, gaged by the USGS, were low and an MFL implementation was required. For simplicity, these low flow days are called MFL-required days.

Table 13 lists annual averages of ≤ 2 psu and ≤ 5 psu water volumes between the dam and the Sulphur Springs confluence in the LHR during MFL-required days under the existing, MFL, and no MFL flow conditions. From the table, one can see that 2015 was a relatively wet year and had the highest values of ≤ 2 psu and ≤ 5 psu water volumes under any of the three flow conditions. On the other hand, 2023 was quite dry and had the lowest values of the low salinity habitats. Under the no MFL flow condition, the average ≤ 2 psu water volume during the MFL-required days in 2023 was only 8,280 m^3, which was only about 6.3% of that in 2015. Nevertheless, 2023 had the biggest improvement of the ≤ 2 psu water volume during the MFL-required days with a full MFL implementation, which expanded the salinity habitat to 36,090 m^3, representing an increase of 335.9%. The improvement of ≤ 5 psu water volume during the MFL-required days caused by a full MFL implementation was even more significant in 2023, when the salinity habitat was increased from 19,720 m^3 to 123,130 m^3, or a 524.4% increase.

Table 13. Annual average water volumes (1000 m³) during MFL-required days for salinity ≤ 2 psu and ≤ 5 psu between the dam and the Sulphur Springs confluence in the LHR during January 2008 - December 2023 under the existing, MFL, and no MFL flow conditions.

Year	Salinity ≤ 2 psu			Salinity ≤ 5 psu		
	Existing	MFL	No MFL	Existing	MFL	No MFL
2008	85.19	95.54	30.26	135.64	145.35	60.44
2009	78.00	87.19	23.75	125.81	134.45	54.26
2010	77.59	103.10	20.10	140.26	160.65	62.82
2011	88.34	118.92	34.67	152.22	174.51	71.80
2012	45.85	70.38	14.21	129.43	145.91	42.86
2013	33.40	54.25	33.94	154.63	160.05	98.69
2014	61.60	78.59	63.93	174.61	183.18	140.66
2015	101.05	155.39	131.07	198.36	202.77	198.23
2016	29.30	51.47	22.35	150.01	158.73	92.32
2017	34.60	45.30	10.29	135.84	143.54	38.74
2018	39.06	51.46	18.85	149.03	154.42	76.78
2019	53.12	79.67	20.85	176.82	182.51	109.50
2020	34.19	41.41	26.48	159.24	164.04	73.95
2021	35.49	58.63	19.59	162.06	168.96	65.01
2022	57.23	66.04	39.49	152.61	156.87	85.15
2023	36.08	36.09	8.28	123.14	123.13	19.72

Table 14 contains annual averages of ≤ 2 psu and ≤ 5 psu bottom areas between the dam and the Sulphur Springs confluence in the LHR during MFL-required days under the existing, MFL, and no MFL flow conditions, while Table 15 has the corresponding annual averages of ≤ 2 psu and ≤ 5 psu shoreline lengths. Consistent with ≤ 2 psu and ≤ 5 psu water volumes listed in Table 13, 2015 had the highest values of ≤ 2 psu and ≤ 5 psu bottom areas and shoreline lengths under any of the three flow conditions, while 2023 had the lowest values of the low salinity habitats. Under the no MFL flow condition, the average ≤ 2 psu bottom area and shoreline length during the MFL-required days in 2023 were 7,230 m² and 0.35 KM, respectively, which were only about 7.7% and 6.8% of those in 2015. Again, 2023 had the biggest improvement of the salinity habitats with a MFL full implementation, which improved the average ≤ 2 psu bottom area to 30,470 m² and the average ≤ 2 psu shoreline length to 1.54 KM during the MFL-required days, representing a 321.4% increase for ≤ 2 psu bottom area and a 340.0% increase for ≤ 2 psu shoreline length. The improvement was even larger for ≤ 5 psu bottom area and shoreline length during the MFL-required days in 2023. From Tables 14 and 15, one can find that a full MFL implementation yielded a 463.1% increase of ≤ 5 psu bottom area and a 522.8% increase of ≤ 5 psu shoreline length during the MFL-required days in 2023.

Table 14. Annual average bottom areas (1000 m^2) during MFL-required days for salinity ≤ 2 psu and ≤ 5 psu between the dam and the Sulphur Springs confluence in the LHR during January 2008 - December 2023 under the existing, MFL, and no MFL flow conditions.

Year	Salinity ≤ 2 psu			Salinity ≤ 5 psu		
	Existing	MFL	No MFL	Existing	MFL	No MFL
2008	70.37	76.07	24.04	95.83	100.56	43.16
2009	66.22	71.45	19.14	90.91	95.21	38.76
2010	66.25	80.06	17.21	98.12	108.04	45.27
2011	71.80	88.24	26.26	104.06	114.86	51.46
2012	39.61	59.31	11.67	92.43	100.57	32.69
2013	22.49	41.00	26.90	105.63	108.28	70.37
2014	40.06	53.12	43.62	115.06	119.23	97.61
2015	61.76	102.50	93.32	126.95	129.20	126.85
2016	20.56	39.75	19.45	102.24	106.29	65.77
2017	28.80	36.97	7.60	95.85	99.58	30.15
2018	29.68	40.10	15.68	102.60	105.17	55.70
2019	40.59	63.23	17.98	114.04	116.66	75.99
2020	21.52	28.03	20.18	106.46	108.70	52.94
2021	24.99	45.24	14.99	107.75	111.00	46.77
2022	39.96	48.48	32.08	102.66	104.72	61.19
2023	30.47	30.47	7.23	87.86	87.85	15.60

Table 15. Annual average shoreline lengths (KM) during MFL-required days for salinity ≤ 2 psu and ≤ 5 psu between the dam and the Sulphur Springs confluence in the LHR during January 2008 - December 2023 under the existing, MFL, and no MFL flow conditions.

Year	Salinity ≤ 2 psu			Salinity ≤ 5 psu		
	Existing	MFL	No MFL	Existing	MFL	No MFL
2008	4.00	4.37	1.37	5.66	5.94	2.45
2009	3.79	4.13	1.06	5.40	5.67	2.18
2010	3.70	4.59	0.93	5.71	6.27	2.56
2011	3.98	5.01	1.44	5.98	6.59	2.79
2012	2.14	3.20	0.61	5.31	5.81	1.75
2013	1.21	2.22	1.44	6.09	6.24	3.91
2014	2.23	2.93	2.39	6.47	6.70	5.28
2015	3.57	5.65	5.18	6.90	6.97	6.89

2016	1.12	2.07	0.99	5.76	6.02	3.50
2017	1.47	1.96	0.39	5.50	5.73	1.58
2018	1.56	2.13	0.81	5.93	6.09	3.09
2019	2.04	3.18	0.86	6.26	6.41	4.04
2020	1.15	1.47	1.06	5.94	6.08	2.83
2021	1.30	2.33	0.75	5.97	6.16	2.44
2022	2.11	2.47	1.61	5.68	5.81	3.24
2023	1.54	1.54	0.35	4.92	4.92	0.79

Salinity distributions for the upstream portion of the LHR are included in Appendix A. The first 9 maps are distributions of the average top-layer, bottom-layer, and depth-averaged salinities during the 195-month simulation period (October 2007 – December 2023.) Distributions of the average top-layer, bottom-layer, and depth-averaged salinities during January – December 2023 are shown in the second 9 maps in the appendix.

5.2   Simulated Thermal Habitats for Manatees

Thermal habitats were calculated for the thermal refuge for manatees, which was defined as the entire SS run and a 50-meter box in the LHR that is centered at the SS confluence (SWFWMD, 2004). Because an adult manatee needs 3.8 feet of water for it to be entirely submerged, the thermal habitat calculation excluded any areas where the favorable thermal habitat has a depth of < 3.8 feet.

Manatees cannot stay in cold water for a long period of time. It was found that the mortality rate of manatee could significantly increase if staying in water < 20 °C longer than 4 days (Rouhani et al., 2007). If the water temperature is further decreased to below 15 °C, manatees would have a hard time surviving after 4 hours (Janicki Environmental and Applied Technology & Management, 2007.) As such, available water volumes and surface areas that are ≥ 20 °C and ≥ 15 °C (or between 15 °C and 20 °C) need to be calculated and analyzed.

Time series of simulated volumes and surface areas for temperature ≥ 20 °C and for temperature between 15 °C and 20 °C in the thermal refuge for manatees during October 2007 – December 2023 for the existing, MFL, and no MFL flow conditions are presented in Figs. 36, 38, and 40, respectively. Corresponding time series plots during January – December 2023 for the three flow scenarios are presented in Figs. 37, 39, and 41, respectively. Red lines in these figures are for temperature ≥ 20 °C, while green lines are for temperature between 15 °C and 20 °C.

From the figures, one can see that the thermal refuge for manatees is dominated by warm water with a temperature of ≥ 20 °C. A relatively small amount of thermal habitat for temperature between 15 °C and 20 °C existed during cold days of the manatee season, defined as a 5-month period from November to March. Because the SS flow has a relatively stable temperature at around 25.5°C, it is unlikely that thermal habitats for temperature between 15 °C and 20 °C existed in the spring run, especially upstream of the weir structure.
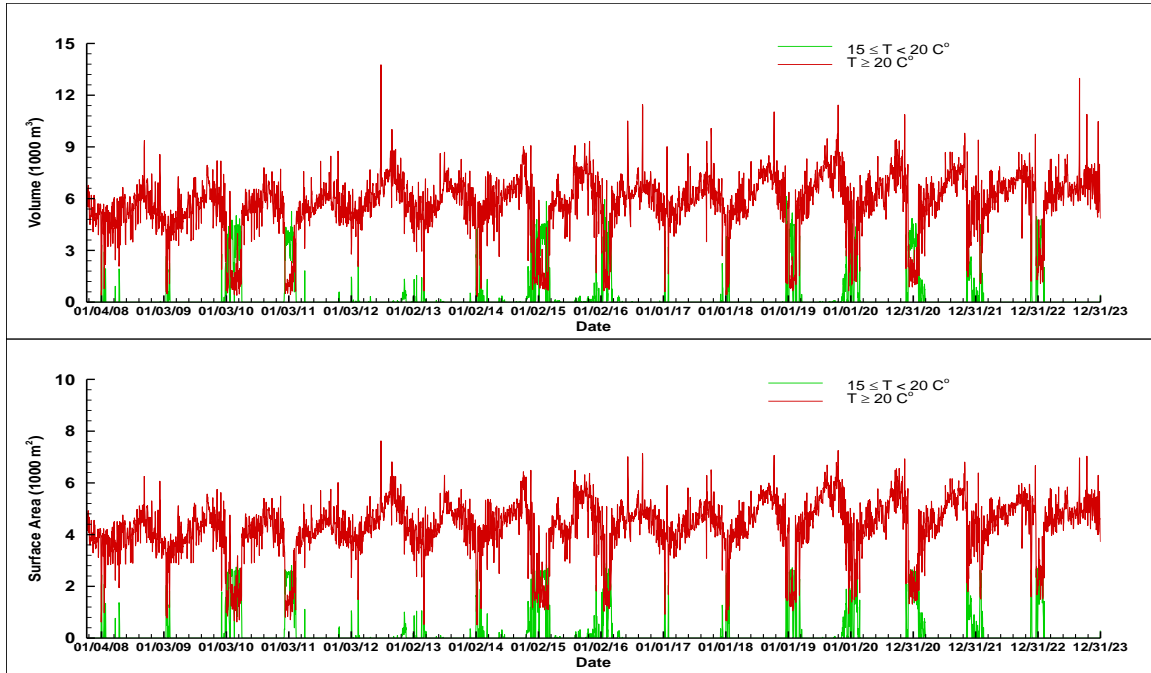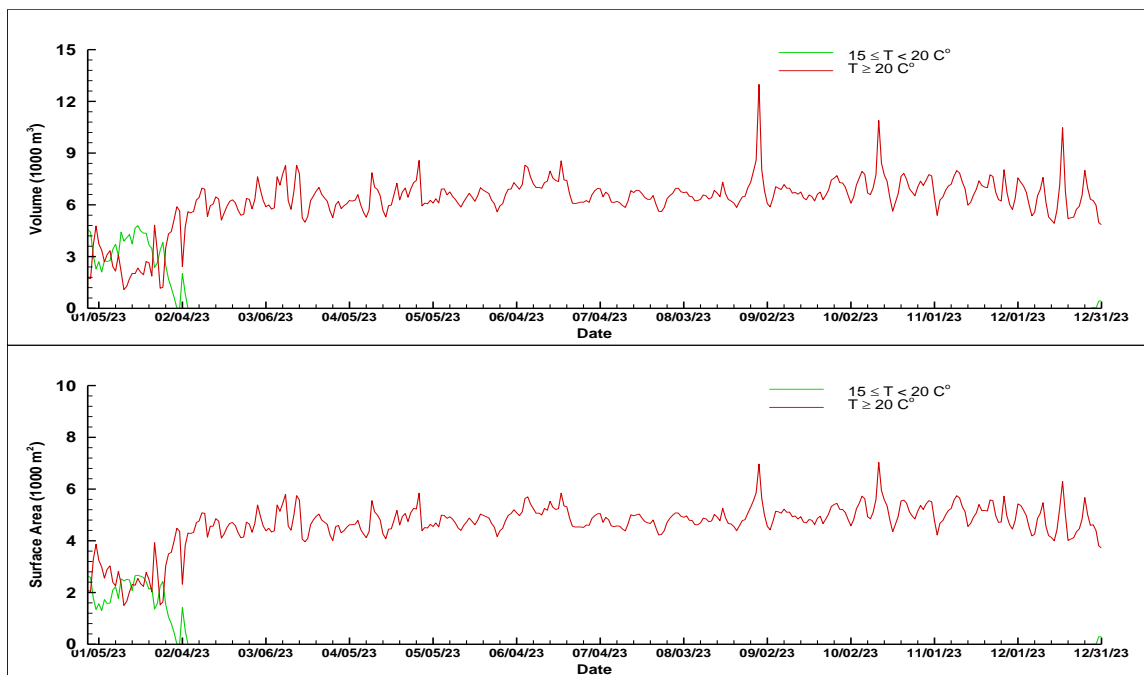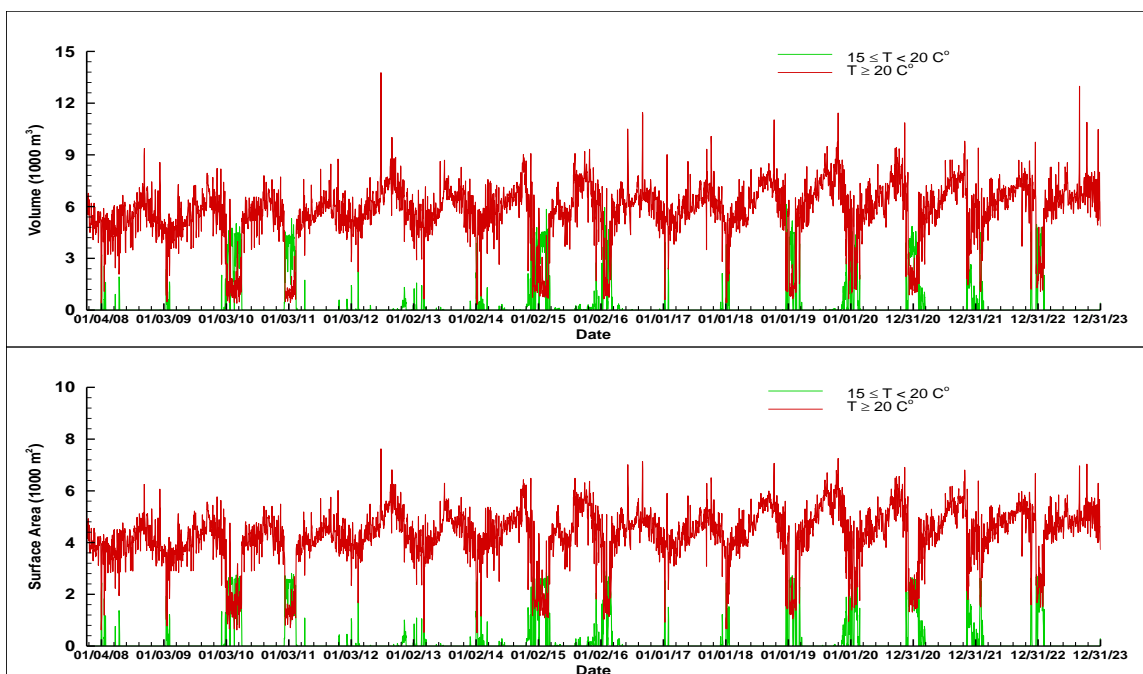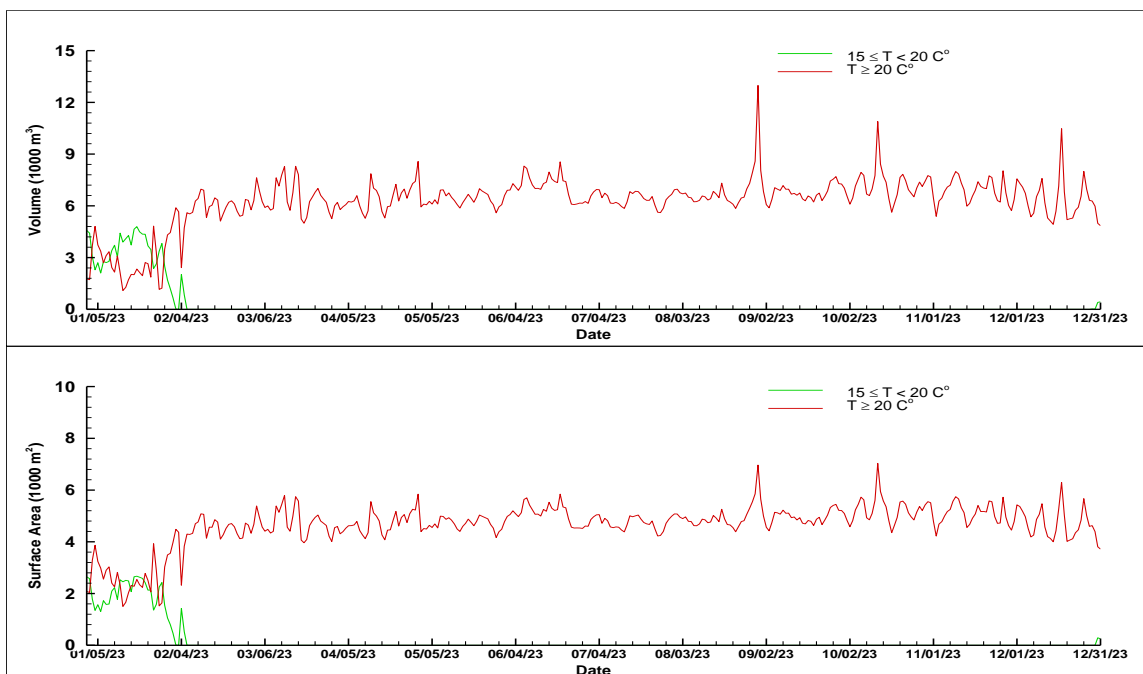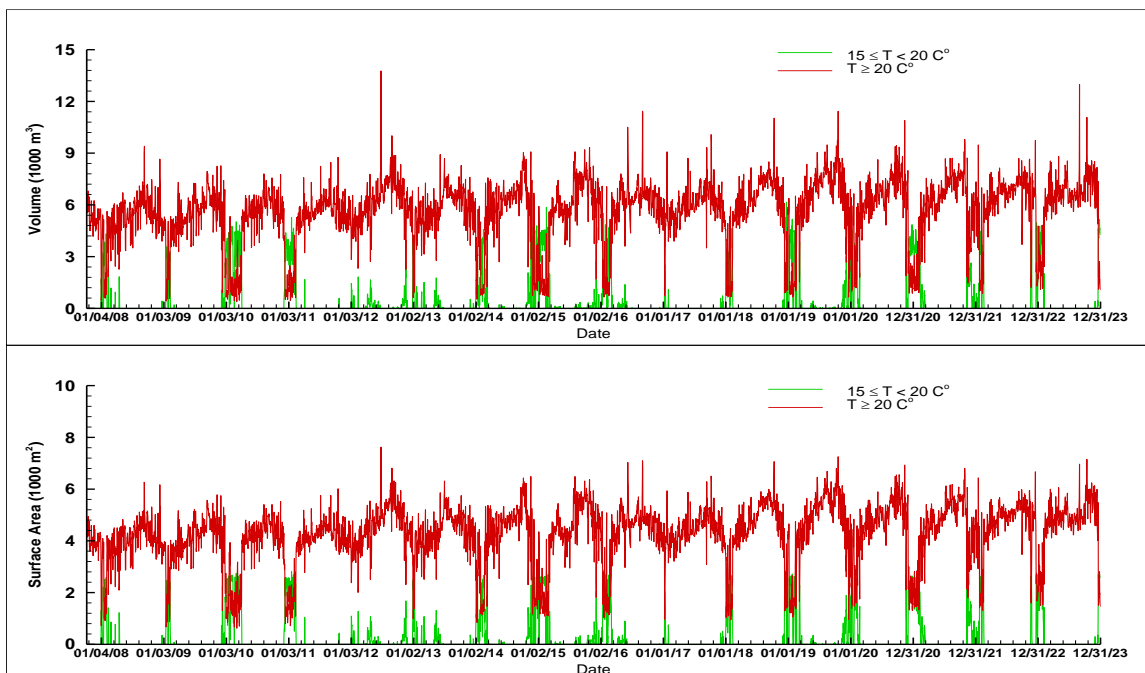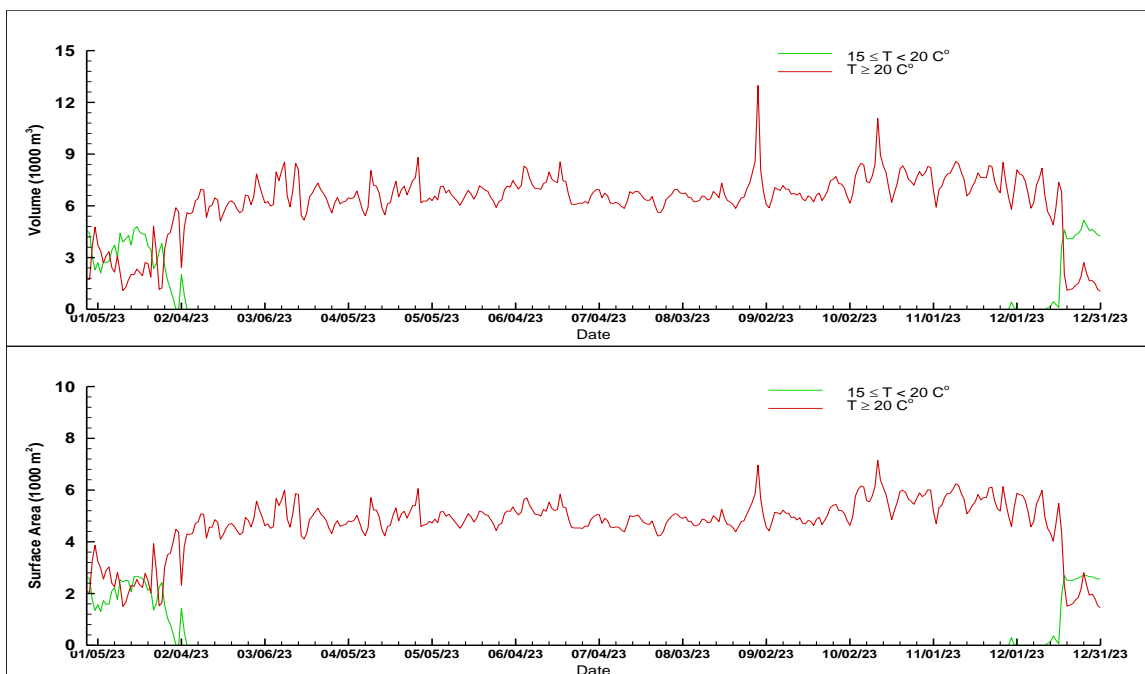
Figure 36. Simulated thermal habitats for manatees in the Sulphur Springs run and a 50-m box of the LHR at the Sulphur Springs confluence during October 2007 – December 2023 for the Existing flow condition.

Figs. B–1, B–3, and B-5 in Appendix B are time series plots of simulated thermal habitats for manatees during October 2007 – December 2023 for the existing, MFL, and no MFL flow conditions, respectively, while Figs. B–2, B–4, and B-6 are thermal habitats during January – December 2023 for the three flow conditions. These figures are for the Sulphur Springs run only, a main part of the refuge for manatees, and they demonstrate that thermal habitats in the SS run are almost always ≥ 20 ºC and thermal habitats for temperature between 15 ºC and 20 ºC barely existed in the SS run. Under the existing and MFL flow conditions, thermal habitats for temperature between 15 ºC and 20 ºC only existed shortly during very cold days in early 2012 and 2013. These small amounts of 15 – 20 ºC thermal habitats were in the most downstream grid of the spring run, which is below the weir in the spring run. Under the no MFL flow condition, there was no thermal habitat that is below 20 ºC, simply because no Sulphur Springs water would be pumped to the base of the dam and all SS discharges would be entering the LHR through the spring run. The relatively larger flow rate in the SS under the no MFL flow condition pushed any < 20 ºC thermal habitats in the most downstream grid in the run to the LHR. A comparison of Figs. B-1 – B-6 with Figs. 36 – 41 proves that thermal habitats for temperature between 15 ºC and 20 ºC exist mostly in the 50-m box in the LHR.

Simulated temperatures over the water column were averaged to obtain depth-averaged temperatures for all the model grids. Top-layer, bottom-layer, and depth-averaged temperatures were averaged over the manatee seasons of the 195-month simulation period as well as over the manatee season of 2023. Consequently, distributions of average top-layer, bottom-layer, and depth-

48

averaged temperatures could be generated. These temperature distributions are shown in Appendix C, with Figs. C-1 – C-9 being average temperatures during manatee seasons of the 195-month period (October 2007 - December 22023) and Figs. C-10 - C-18 being average temperatures during the manatee season of 2023.

Figure 37. Simulated thermal habitats for manatees in the Sulphur Springs run and a 50-m box of the LHR at the Sulphur Springs confluence during 2023 for the Existing flow condition.

Similar to the discussion about the low salinity habitats, the above thermal habitat time series can be best summarized with CDF plots. As thermal habitats for manatees are only critical to manatees during cold days, CDFs were obtained using simulated thermal habitats during the manatee season only, namely the 5-month period from November to March.

Figs. 42 and 43 are CDF plots of ≥ 20 ºC volume and surface area, respectively in the thermal refuge for manatees of the LHR, which include the SS run and a 50-m box at the confluence of the spring run. Blue lines are for the existing flow condition, while orange and green lines are for MFL and no MFL flow conditions. Again, areas bounded by the y-axis and the CDF curves in these CDF plots represent the average thermal habitats. The difference among the three flow scenarios can be easily identified. CDFs for the MFL scenario and the existing scenario are very close, but those of the no MFL scenario are different.

Figure 38. Simulated thermal habitats for manatees in the Sulphur Springs run and a 50-m box of the LHR at the Sulphur Springs confluence during October 2007 – December 2023 for the MFL flow condition.

Figure 39. Simulated thermal habitats for manatees in the Sulphur Springs run and a 50-m box of the LHR at the Sulphur Springs confluence during January – December 2023 for the MFL flow condition.

Figure 40. Simulated thermal habitats for manatees in the Sulphur Springs run and a 50-m box of the LHR at the Sulphur Springs confluence during October 2007 – December 2023 for the no MFL flow condition.

Figure 41. Simulated thermal habitats for manatees in the Sulphur Springs run and a 50-m box of the LHR at the Sulphur Springs confluence during January – December 2023 for the no MFL flow condition.

51

As mentioned before, the thermal refuge for manatees is generally dominated by water ≥ 20 ºC, especially in the spring run. Thermal habitats with temperatures below 20 ºC mainly occur in the 50-m box, which is assumed to be the plume of the Sulphur Springs flow. The fact that thermal habitats < 20 ºC existed primarily in the 50-m box suggests that the Sulphur Springs plume is quite different from the 50-m box in the LHR. Because of the interactions among the bathymetry of the river, tides, and flows entering the river, the plume of the SS flow is very dynamic, with its shape changing constantly. Generally, the plume is greatly asymmetric relative to the confluence of the spring run, with its length scale in the upstream direction being much shorter than that in the downstream station. During a flood tide, the upstream end of the plume will be pushed to a more upstream position, with a relatively shorter total length of the plume. On the other hand, during an ebb tide, the downstream end of the plume will be pushed to a more downstream position, with a relatively longer total plume length. Furthermore, it is likely that during an ebb tide, the plume of the SS flow exists entirely at the downstream side of the confluence of the SS run. The flow received by the river at the dam also affects the shape of the plume. A large flow will push the plume more downstream, with an elongated shape, while a small flow will allow the plume to be transported to a more upstream position during the flood tide. In any case, the assumption of a 50-m box that is 25 m in both the upstream and downstream directions is an over-simplification of the shape of the plume of the Sulphur Springs flow in the LHR.
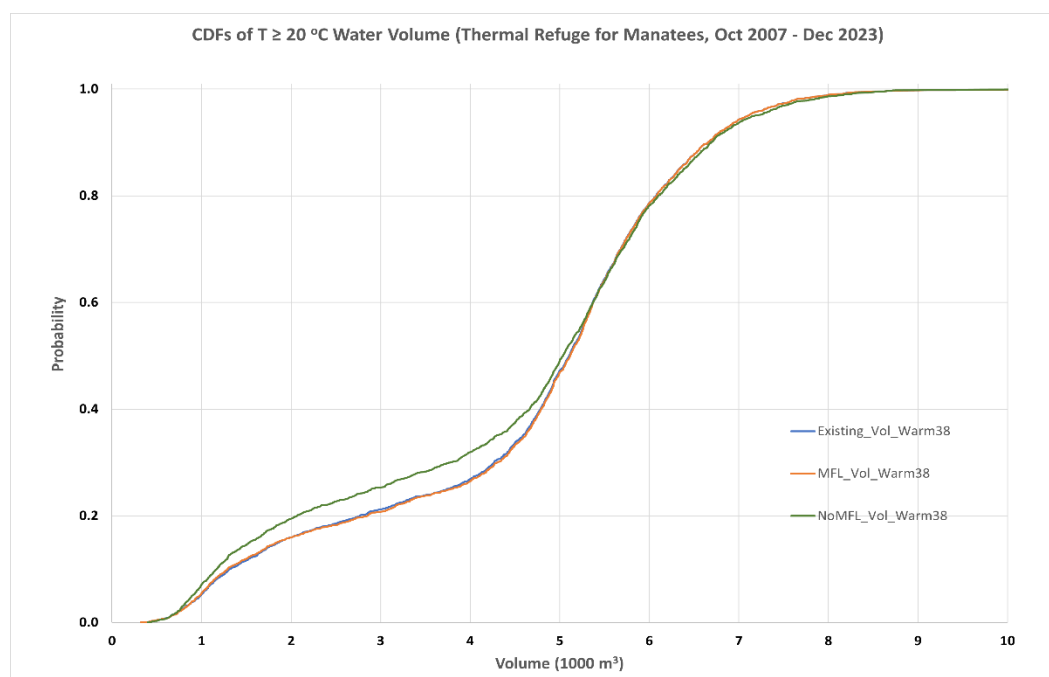
Figure 42. CDFs of ≥ 20 ºC water volume for the existing, MFL, and no MFL flow conditions during the manatee seasons of the simulation period between October 2007 and December 2023 in the thermal refuge for manatees of the LHR.
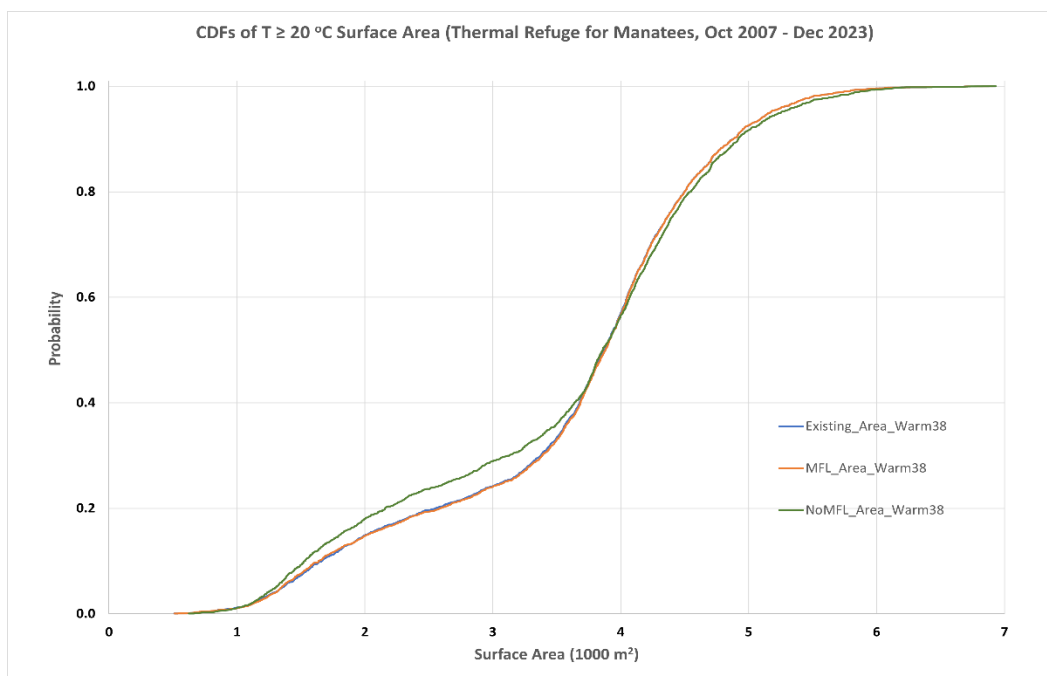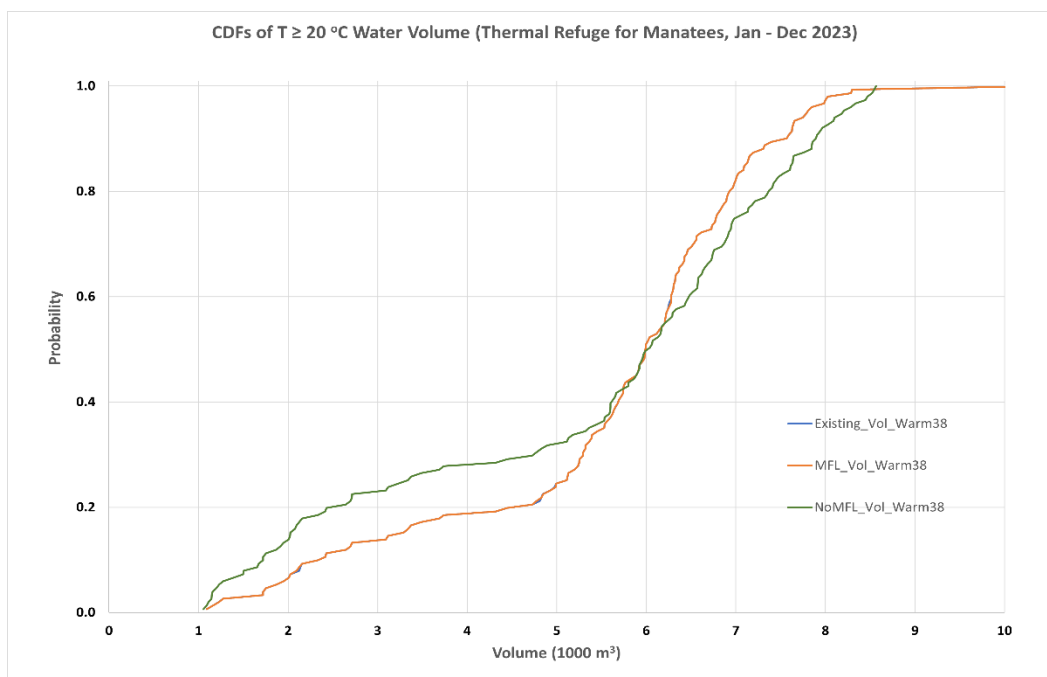
Figure 43. CDFs of ≥ 20 ºC surface area for the existing, MFL, and no MFL flow conditions during the manatee seasons of the simulation period between October 2007 and December 2023 in the thermal refuge for manatees of the LHR.

Figure 44. CDFs of ≥ 20 ºC water volume for the existing, MFL, and no MFL flow conditions during the manatee season of 2023 in the thermal refuge for manatees of the LHR.
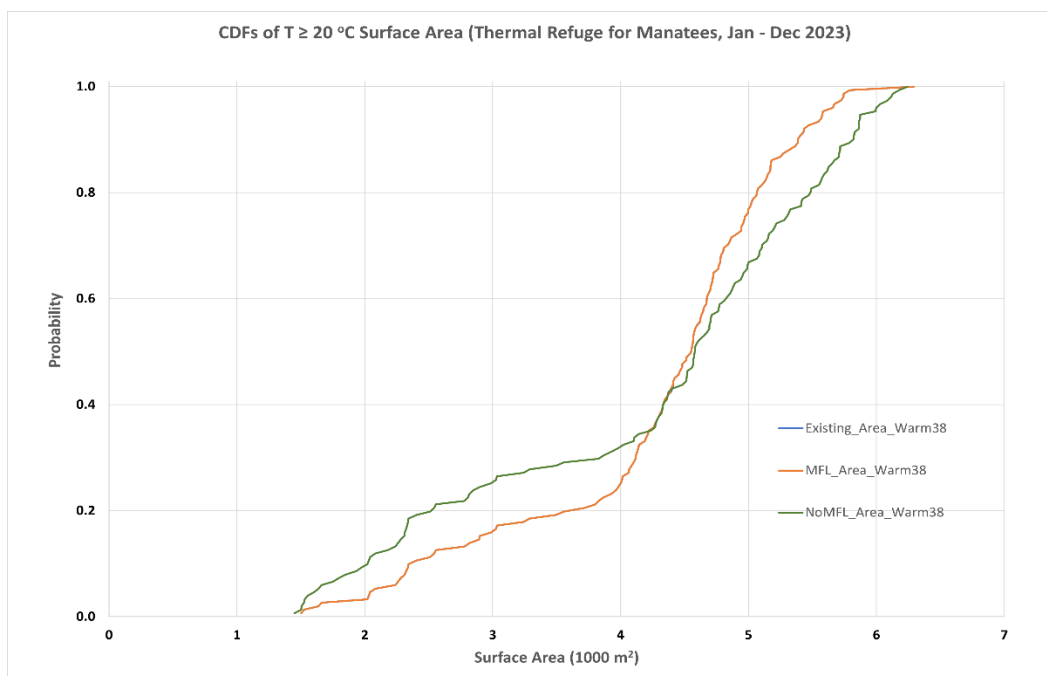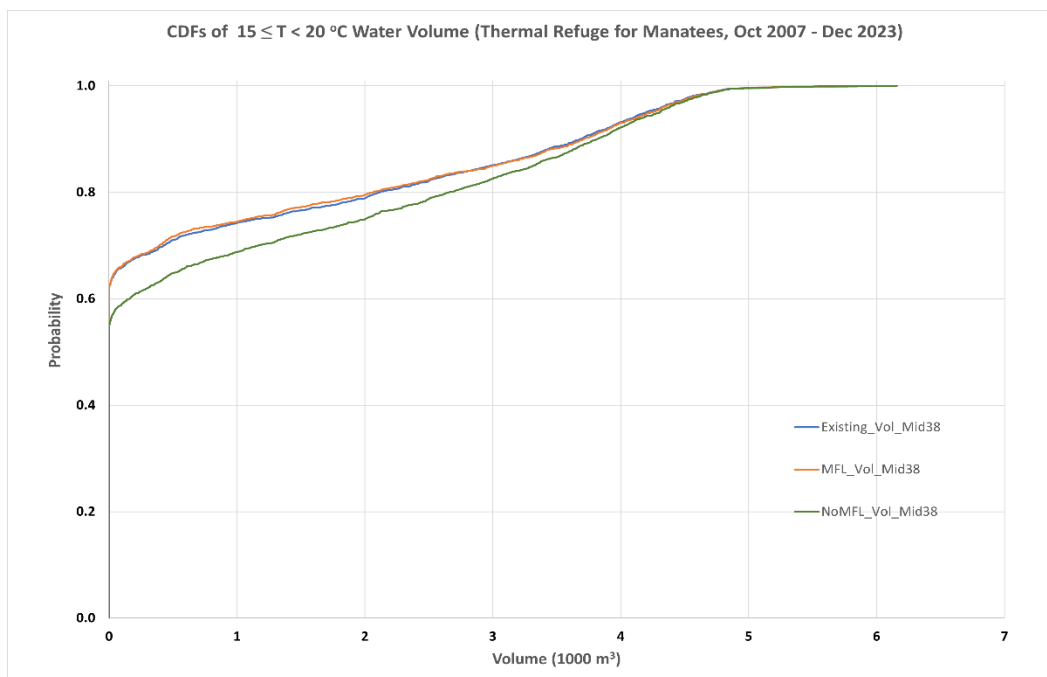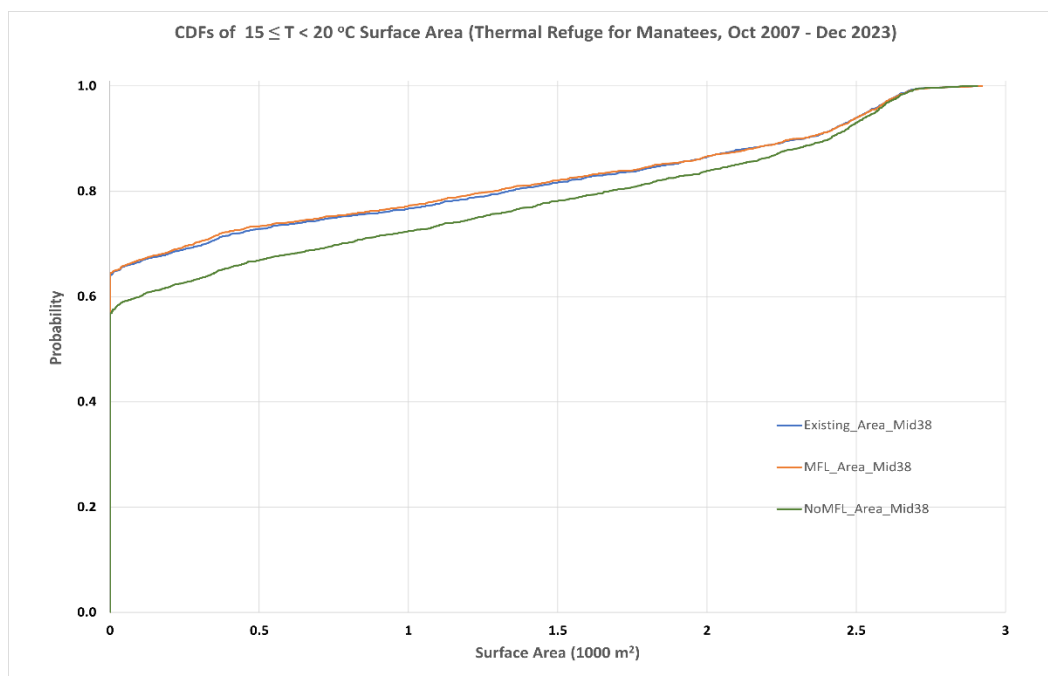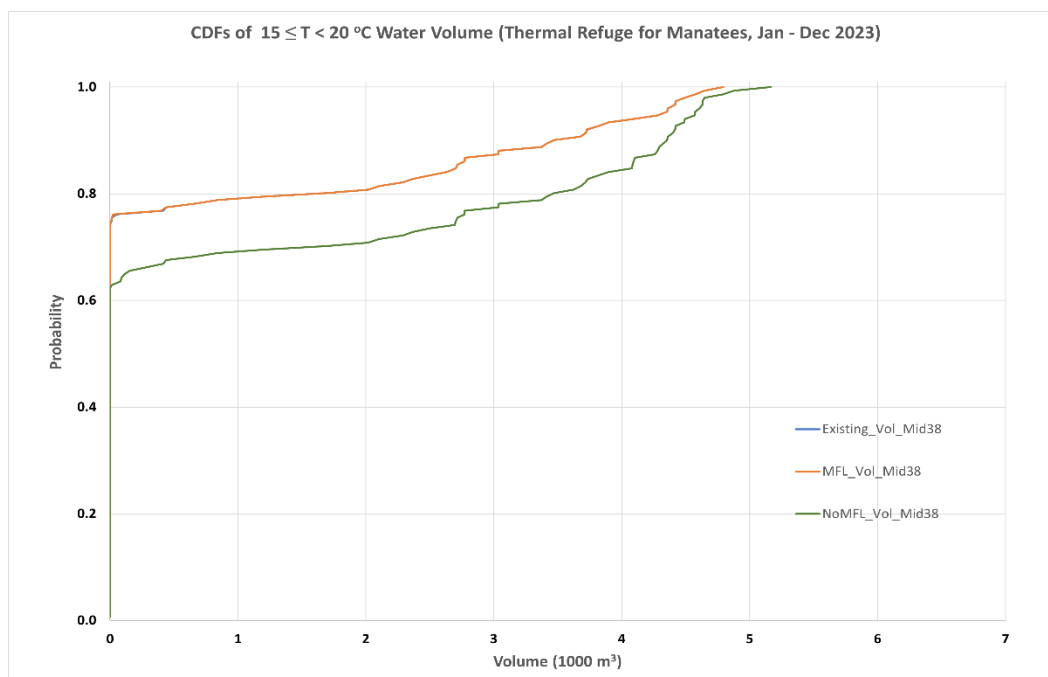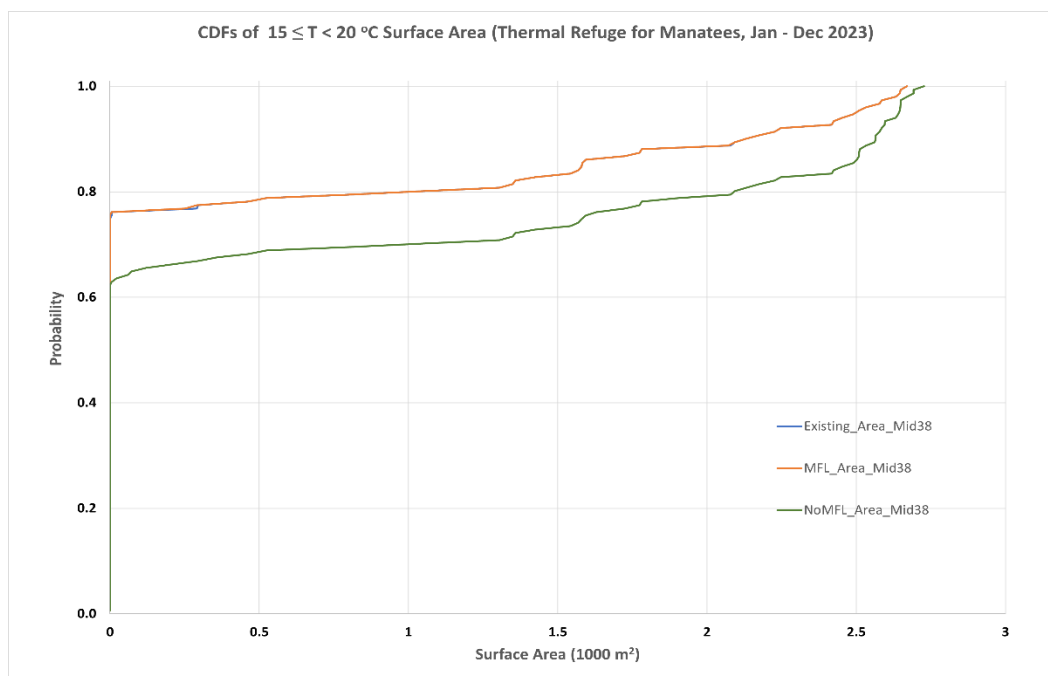
Figure 45. CDFs of ≥ 20 ºC surface area for the existing, MFL, and no MFL flow conditions during the manatee season of 2023 in the thermal refuge for manatees of the LHR.

Figure 46. CDFs of water volume for temperature between 15 ºC and 20 ºC for the existing, MFL, and no MFL flow conditions during the manatee seasons of the simulation period between October 2007 and December 2023 in the thermal refuge for manatees of the LHR.

Figure 47. CDFs of surface area for temperature between 15 ºC and 20 ºC for the existing, MFL, and no MFL flow conditions during the manatee seasons of the simulation period between October 2007 and December 2023 in the thermal refuge for manatees of the LHR.

Figure 48. CDFs of water volume for temperature between 15 ºC and 20 ºC for the existing, MFL, and no MFL flow conditions during the manatee season of 2023 in the thermal refuge for manatees of the LHR.

Figure 49. CDFs of surface area for temperature between 15 ºC and 20 ºC for the existing, MFL, and no MFL flow conditions during the manatee season of 2023 in the thermal refuge for manatees of the LHR.

The dynamics of the plume of the SS flow in the LHR and the fixed 50-m box that is assumed to be the refuge for manatees are partially responsible for the differences of the CDFs among the three flow scenarios shown in Figs. 42 – 49. Because of the asymmetric nature of the plume of the Sulphur Springs flow in the LHR, the downstream half of the 50-m box would contain mostly the plume water, while the upstream half could be filled mainly with water that is not a part of SS flow plume. The relatively smaller ≥ 20 ºC volume and surface area under the no MFL flow condition (see Figs. 42 and 43) were not necessarily caused by a smaller plume of the SS flow. In contrast, the plume under the no MFL condition could be bigger than that under the existing or MFL flow condition. Because of a larger flow in the spring run, the flume becomes severely asymmetric with relation to the spring run confluence, with most of it being in the downstream direction. As a result, a large portion of the plume could be downstream of the 50-m box in the LHR and not counted in the thermal habitat calculation. Under the existing and MFL flow conditions, however, the routing of the SS flow to the base of the dam will cause water in the upstream side of the spring run confluence warmer during cold days and thus the upstream half of the 50-m box will contain more ≥ 20 ºC water volume and surface area.

Figs. 42 and 43 demonstrate that the ranges of the middle 50% (25th percentile to 75th percentile) for ≥ 20 ºC thermal habitats under the no MFL flow condition are larger than those under the existing and MFL flow conditions. The 25th percentiles of ≥ 20 ºC volume and surface area for the no MFL scenario are lower than those for the existing and MFL scenarios, while the 75th percentiles for the no MFL scenario are slightly higher than those for the existing and MFL scenarios. In other words, the middle halves of ≥ 20 ºC thermal habitats would be more centered around their median values under the existing and MFL flow conditions than under the no MFL

flow condition. This phenomenon is attributed to the definition of the thermal refuge for manatees in the LHR and the use of the SS flow at the base of the dam for the MFL implementation.

Because the upstream portion of the LHR barely experiences water temperature below 15 ºC, sums of the thermal habitats for temperature ≥ 20 ºC and for temperature between 15 ºC and 20 ºC under the three flow scenarios should approximately match to each other, except for those that could be caused by the 3.8' depth requirement. As such, the relatively smaller ≥ 20 ºC thermal habitats in the manatee seasons of the 195-month simulation period (October 2007 – December 2023) under the no MFL flow condition explain the relatively larger thermal habitats for temperature between 15 ºC and 20 ºC for the no MFL scenario, as shown in Figs. 46 and 47.

The manatee season (January – March and November – December) of 2023 was atypical because of a relatively drier condition and the full implementation of the MFL since January 2023. From Figs. 44 – 45 and 48 – 49, one can see that CDFs of the thermal habitats for the existing and MFL flow conditions are basically identical, suggesting that a full MFL implementation was indeed achieved for the LHR in 2023. A drier than normal condition required more flows other than routing the SS flow to the base of the dam to be released/pumped to the upstream boundary of the LHR. These additional flows caused the CDFs of the thermal habitats under the no MFL flow condition to differ substantially from those under the existing and MFL flow conditions. Nevertheless, the averages of ≥ 20 ºC water volume and surface area under the no MFL flow condition were only slightly lower than those under the existing and MFL flow conditions, as indicated by the areas bounded by the CDF curves and the vertical axis in Figs. 44 and 45. On the other hand, the averages of thermal habitats for temperature between 15 ºC and 20 ºC under the no MFL flow condition were significantly higher than those under the existing and MFL flow conditions. This can also be visually seen from the areas that are bounded by the CDF curves and the vertical axis in Figs. 48 and 49.

6. Conclusions

An updated LAMFE model for the LHR was developed using the recently surveyed bathymetric data and LiDAR data. Same as previous LAMFE models for the LHR, the new LAMFE model simulates hydrodynamics and salinity transport processes in the LHR, from the base of the Tampa dam to Platt Street near downtown Tampa, where the LHR meets the Hillsborough Bay. One of the improvements is that the new LAMFE model for the LHR includes a temperature routine, which allows the simulation of thermal dynamics in the estuary. Another improvement is the inclusion of the SS run in the simulation domain.

The simulation domain was discretized with 154 cross sections, resulting in 144 longitudinal grids in the main stem of the LHR and 7 longitudinal grids in the SS run. This is the third improvement of the new LAMFE model for the LHR, because the previous LAMFE models for the estuary used only 88 longitudinal grids to discretize the LHR main stem. In the vertical direction, the new model used a similar resolution to discretize the water depth as that used in previous LAMFE models.

The updated LAMFE model was calibrated and verified against measured field data in the LHR and SS run during a 5-year period between 10/25/2017 and 10/12/2021. Based on the availability of measured variables, the second half of the 5-year period, 4/15/2020 – 10/12/2021, was chosen for model calibration. By tuning a limited number of model parameters, the best match of model results with measured real-time data of water level, salinity, and temperature was obtained at the District station in the LHR and four USGS stations, including the I-275, Hannah's Whirl, and Rowlett Park stations in the LHR and the SS run station. The calibrated LAMFE model for the LHR was verified against real-time collected at the four USGS stations during 10/25/2017 – 4/14/2020.

After the model was calibrated and verified, it was used to conduct scenario runs for the existing, MFL, and no MFL flow conditions. Model results of water level, salinity, and temperature for all grid cells were saved to output files at an interval of 30 minutes. Several post-processing programs were created to process the model results, so that salinity habitats for various isohalines and thermal habitats for temperature ≥ 20 ºC and $15 - 20$ ºC can be calculated. The salinity habitat calculation was carried out for the river segment between the dam and the confluence of the SS run, while the thermal habitat calculation was for the refuge for manatees, which was defined as the spring run plus a 50-m box of the LHR at the confluence of the spring run.

An analysis of the low salinity habitats shows that on average, the existing flow condition was able to produce 95% or more of ≤ 2 psu volume, bottom area, and shoreline length that are supposed to exist under the fully implemented MFL flow condition during October 2007 – December 2023. In 2023, the existing flow condition produced 100% of ≤ 2 psu salinity habitats of the fully implemented MFL flow condition, verifying the full implementation of the MFLs since January 1, 2023. For average ≤ 5 psu salinity habitats, the existing flow condition guaranteed about 98% of the water volume, bottom area, and shoreline of these under the MFL flow condition during October 2007 – December 2023. Again, the existing flow condition in 2023 created 100% of ≤ 5 psu salinity habitats of the MFL flow condition because of the full implementation of the MFLs since January 1, 2023.

If there were no MFL rules implemented, the river segment between the dam and the SS run would have 12% less of average ≤ 2 psu volume, 14% less of average ≤ 2 psu bottom area,

58

and 15% less of average ≤ 2 psu shoreline length than those of the fully implemented MFL scenario. For ≤ 5 psu salinity habitats, the deficits become 17%, 18%, and 20% for volume, bottom area, and shoreline length, respectively.

Annual low salinity habitats during MFL-required days were analyzed for each of the 16 years. Effects of the MFL implementation on low salinity habitats during wet and dry years can be very different. A full implementation of MFL rules may lead to a fair improvement of low salinity habitats during a wet year, it could result in a very impressive increase of low salinity habitats during a dry year. For example, 2015 was a relatively wet year and would have the highest values of ≤ 2 psu and ≤ 5 psu water volumes under the no MFL flow condition, while 2023 was very dry and had the lowest ≤ 2 psu and ≤ 5 psu water volumes (more than one order of magnitude smaller than those of 2015 for the no MFL flow condition.) A full MFL implementation could bring about 19% increase for ≤ 2 psu water volume and only about 2% increase of ≤ 5 psu water volume in 2015. However, it could generate a 336% increase of the ≤ 2 psu water volume and a 524% increase of ≤ 5 psu water volume during the MFL-required days in 2023.

Comparisons of simulated thermal habitats in the refuge for manatees show that effects of the implementation of the MFLs on various thermal habitats for manatees are complicated, not just because of the complexity of the MFL rules for the LHR and the SS run, but also because of the dynamic nature of the plume of the SS flow in the LHR. While the refuge for manatees is a fixed area, the shape and extent of the plume vary constantly, depending on many factors such as tides, SS flow in the run, SS flow routed to the base of the dam, freshwater flow entering the river at the dam, ungagged flows, boundary conditions at the Platt Street, as well as meteorological conditions. Simulated results suggest that the spring run temperature barely drops below 20 ºC, which occurs only below the weir structure for the existing and MFL flow conditions. For the no MFL flow condition, no < 20 ºC thermal habitats exist in the entire spring run. In any case, calculated thermal habitats for temperature between 15 ºC and 20 ºC in the refuge for manatees mainly or entirely exist in the 50-m box in the LHR.

Because of the huge discrepancy of the refuge for manatee and the actual shape and extent of the plume of the SS flow, a detailed analysis of calculated thermal habitats in the refuge area for different flow scenarios is not an easy task and becomes fruitless if this discrepancy is not considered, because the refuge for manatees sometimes can only cover a small portion of the actual plume. Nevertheless, differences of calculated thermal habitats for manatees in the refuge are not significant among the three flow scenarios, under which there are more than enough ≥ 20 ºC volume and surface area for the number of manatees normally observed in the SS area.

7. References

Brater, E. F. and King, H. W., 1982. *Handbook of Hydraulics for the Solution of Hydraulic Engineering Problems*, sixth Edition, McGraw-Hill Book Company, New York.

Chen, X., M.S. Flannery, 1997. Use of a Hydrodynamic Model for Establishing a Minimum Freshwater Flow to the Lower Hillsborough River Estuary, Estuarine and Coastal Modeling: Proceeding of the 5th International Conference, Alexandria, VA, 663 – 678.

Chen, X. 1999. Appendix O. Study of salt transport in the Lower Hillsborough River using a laterally averaged two-dimensional hydrodynamic model. SWIM Section, SWFWMD.

Chen, X. 2003. An efficient finite difference scheme for free-surface flows in narrow rivers and estuaries. International Journal for Numerical Methods in Fluids 42:233–247.

Chen, X. 2004a. Simulating Hydrodynamics and Salinity Transport in the Lower Hillsborough River During February 2001 - December 2002. SWFWMD. 71pp.

Chen, X. 2004b. Using a piecewise linear bottom to fit the bed variation in a laterally averaged, z-co-ordinate hydrodynamic model. International Journal for Numerical Methods in Fluids 44:1185–1205.

Chen, X., Flannery, M.S., and Moore, D.L. 2000. Response Times of Salinity in Relation to Changes in Freshwater Inflows in the Lower Hillsborough River, Florida, *Estuaries* Vol. 23, No. 5, p. 735–742.

Cox, R.A., McCartney, M.J., and Culkin F. 1970. The specific gravity/salinity/temperature relationship in natural seawater. *Deep-Sea Research* 17:679‑689.

HSW Engineering, 1992. *Tampa Bypass Canal and Hillsborough River Biologic Monitoring Assessment Program*; Task I, Tampa.

Janicki Environmental, Inc., Applied Technology & Management. 2007. *Impacts of Withdrawals on the Thermal Regime of the Weeki Wachee River*. Prepared for Southwest Florida Water Management District, Tampa, Fla 33637.

Rouhani, S., Sucsy, P., Hall, G., Osburn, W., and Wild, M. 2007. *Analysis of Blue Spring Discharge Data to Determine a Minimum Flow Regime*. Prepared for St. Johns River Water Management District, Palatka, Fla. 32178.

Skinner, C., Bloetscher, F., and Pathak, C.S. 2009. Comparison of NEXRAD and Rain Gauge Precipitation Measurements in South Florida, *Journal of Hydrologic Engineering*, , 14(3): 248-260, DOI: 10.1061/(ASCE)1084-0699(2009)14:3(248).

SWFWMD, 2004. *The Determination of Minimum Flows for Sulphur Springs, Tampa, Florida*, Brooksville, Florida. September 28, 2004.

SWFWMD & Atkins North America, Inc., 2015. *A Hydrobiological Assessment of the Phased Implementation of Minimum Flows for the Lower Hillsborough River,* Brooksville, Florida. April 24, 2015.

SWFWMD, 2006. *Lower Hillsborough River Low Flow Study Results and Minimum Flow Recommendation*, Brooksville, Florida. August 31, 2006.

Water & Air Research, Inc., 2020. *A Hydrobiological Evaluation of the Minimum Flows for the Lower Hillsborough River for the Second Five-Year Assessment Period - October 2012 to May 2018*, Report submitted to SWFWMD, May 2020.

Willmott, C.J., 1981. On the validation of models. Physical Geography 2, 184-194.

George F. Young, Inc., 2021. Lower Hillsborough River Bathymetric Data Collection, Report of Survey. Lakewood Ranch, FL 34211, 3pp.

1. Appendix A. Salinity Distributions

The following 18 maps contain distributions of the average top-layer, bottom-layer, and depth-averaged salinities during October 2007 – December 2023 (the first 9 maps) and during January - December 2023 (the second 9 maps.)
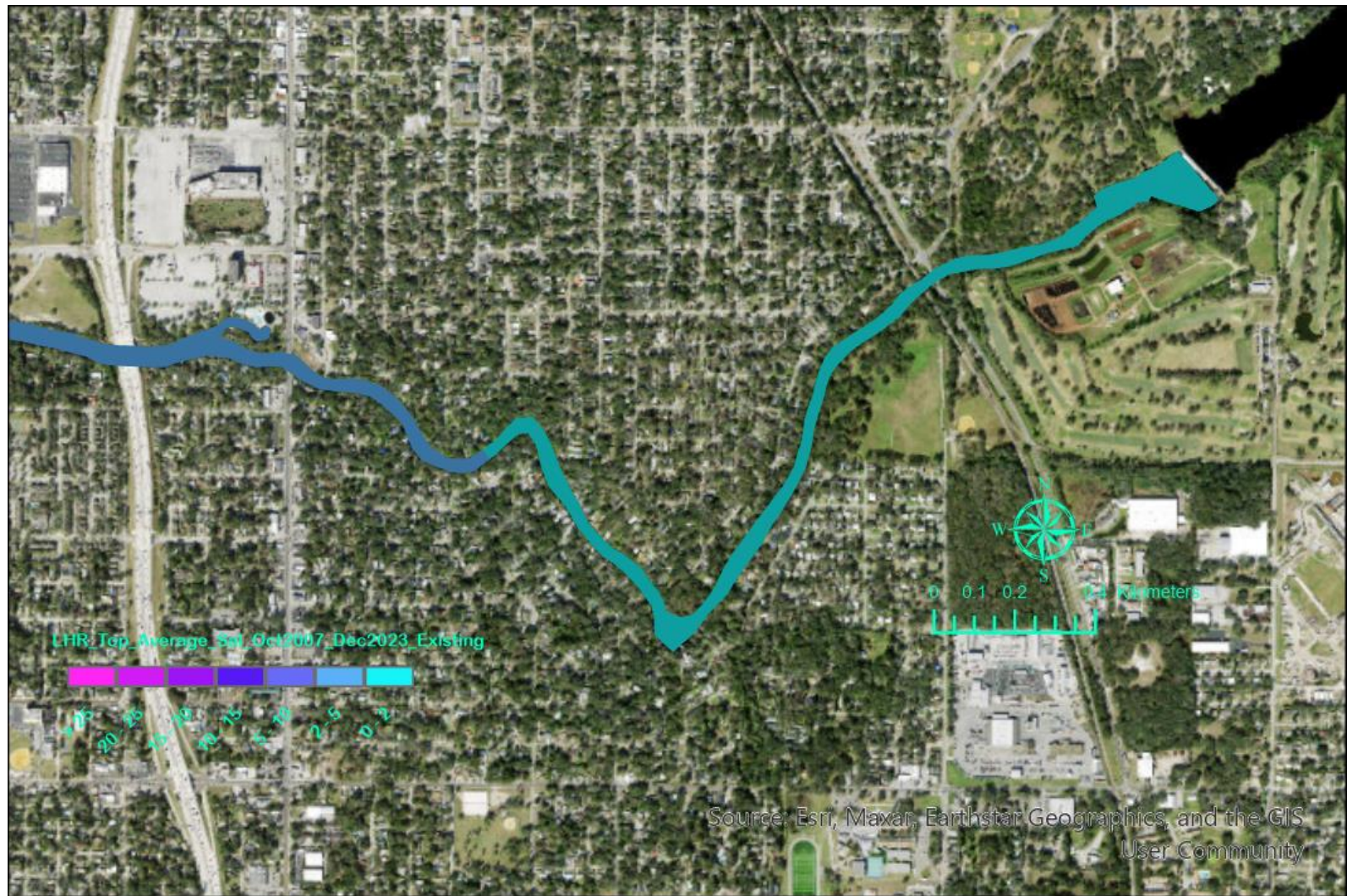
Figure A - 1. Average top–layer salinity in the upstream reach of the LHR during October 2007 – December 2023 for the existing flow condition.
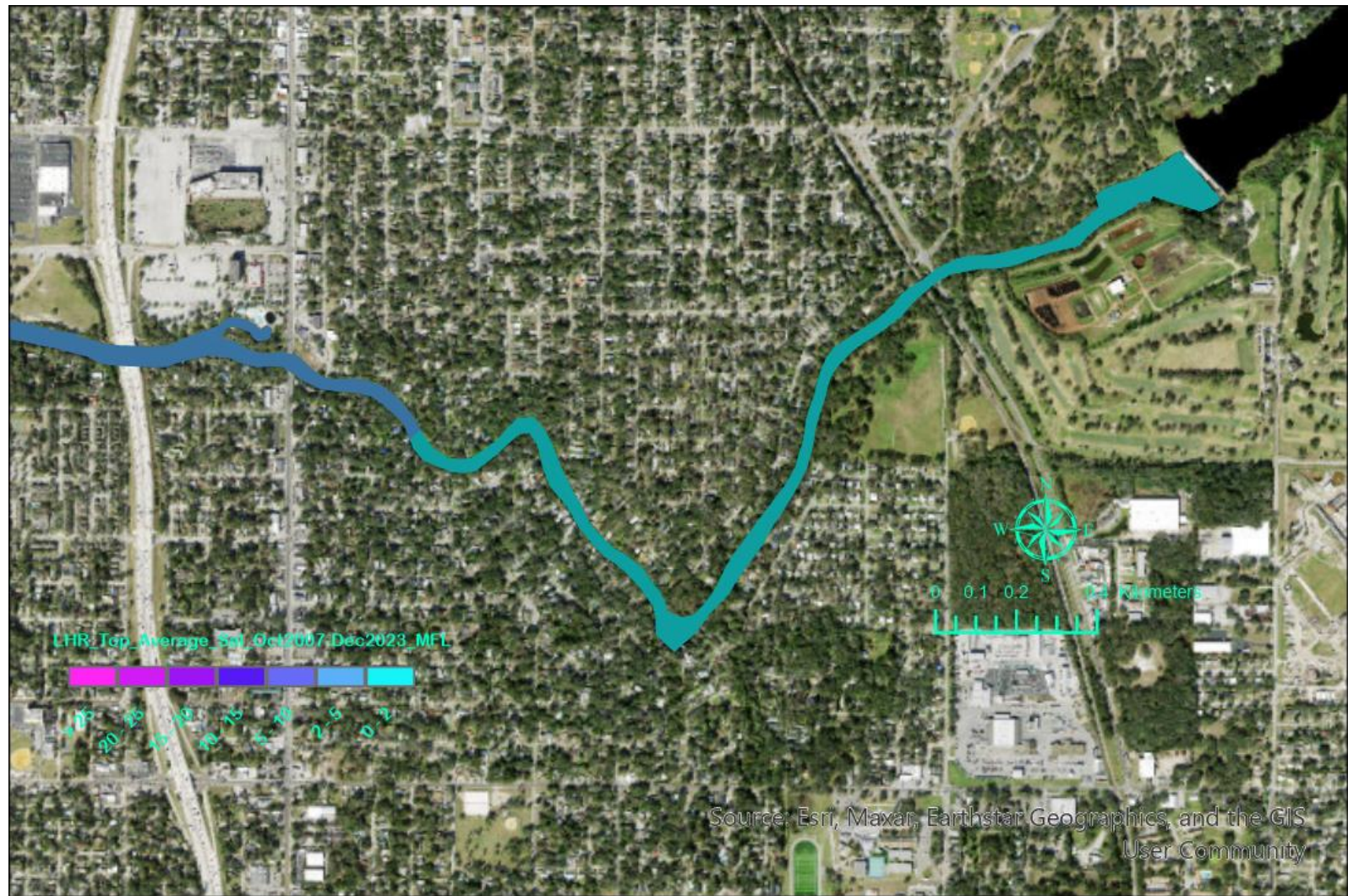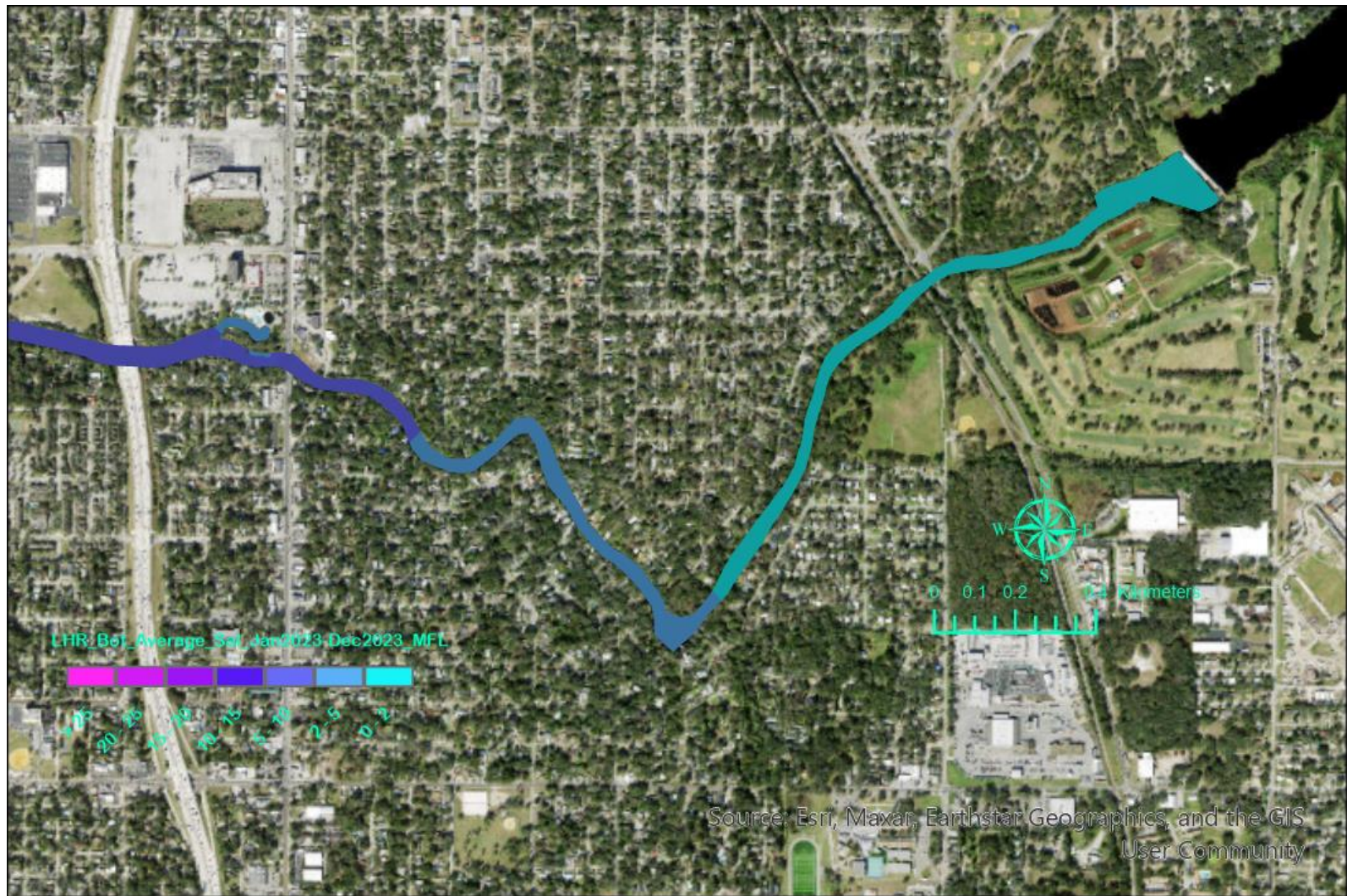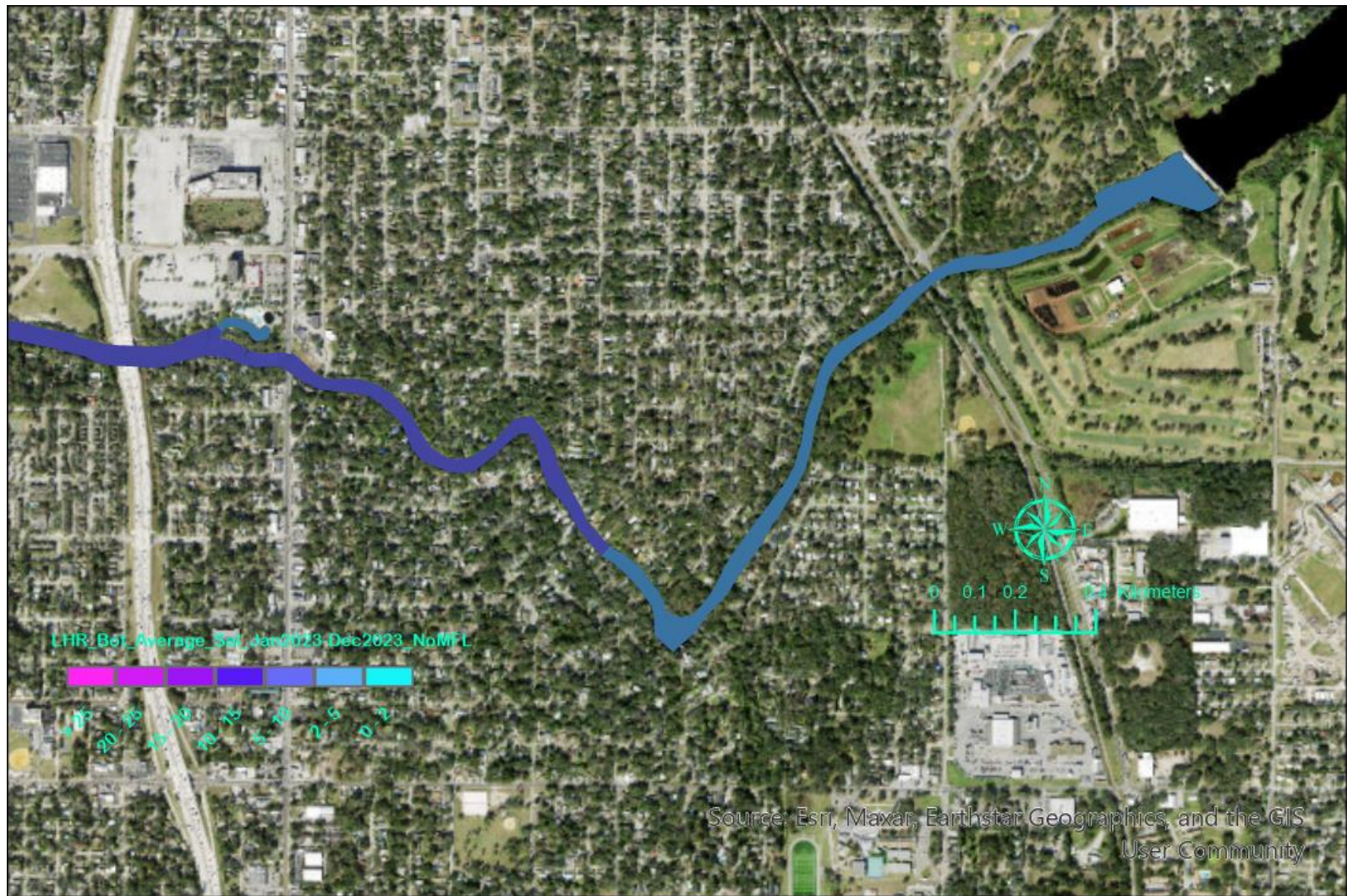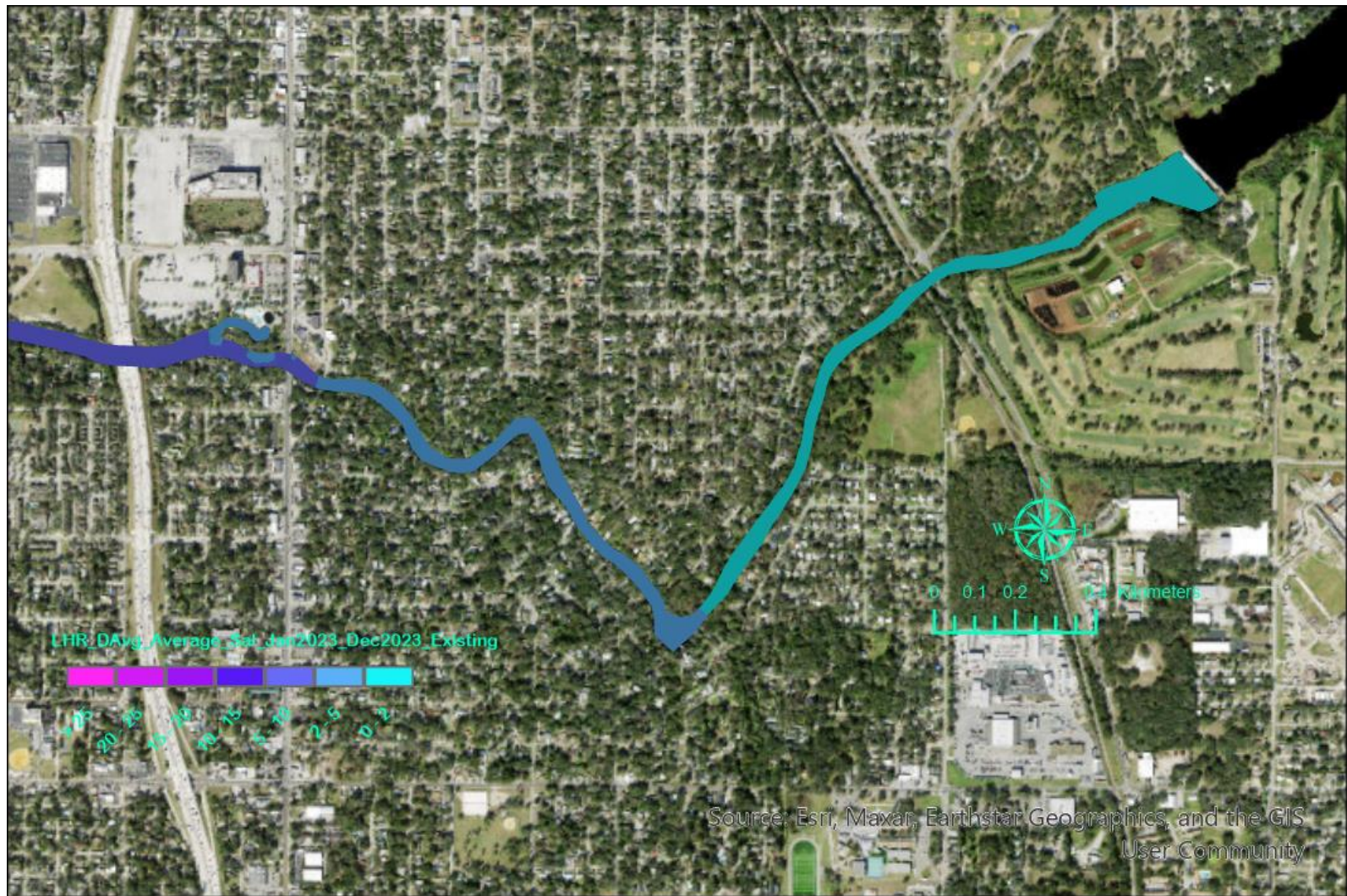
Figure A - 2. Average top–layer salinity in the upstream reach of the LHR during October 2007 – December 2023 for the MFL flow condition.
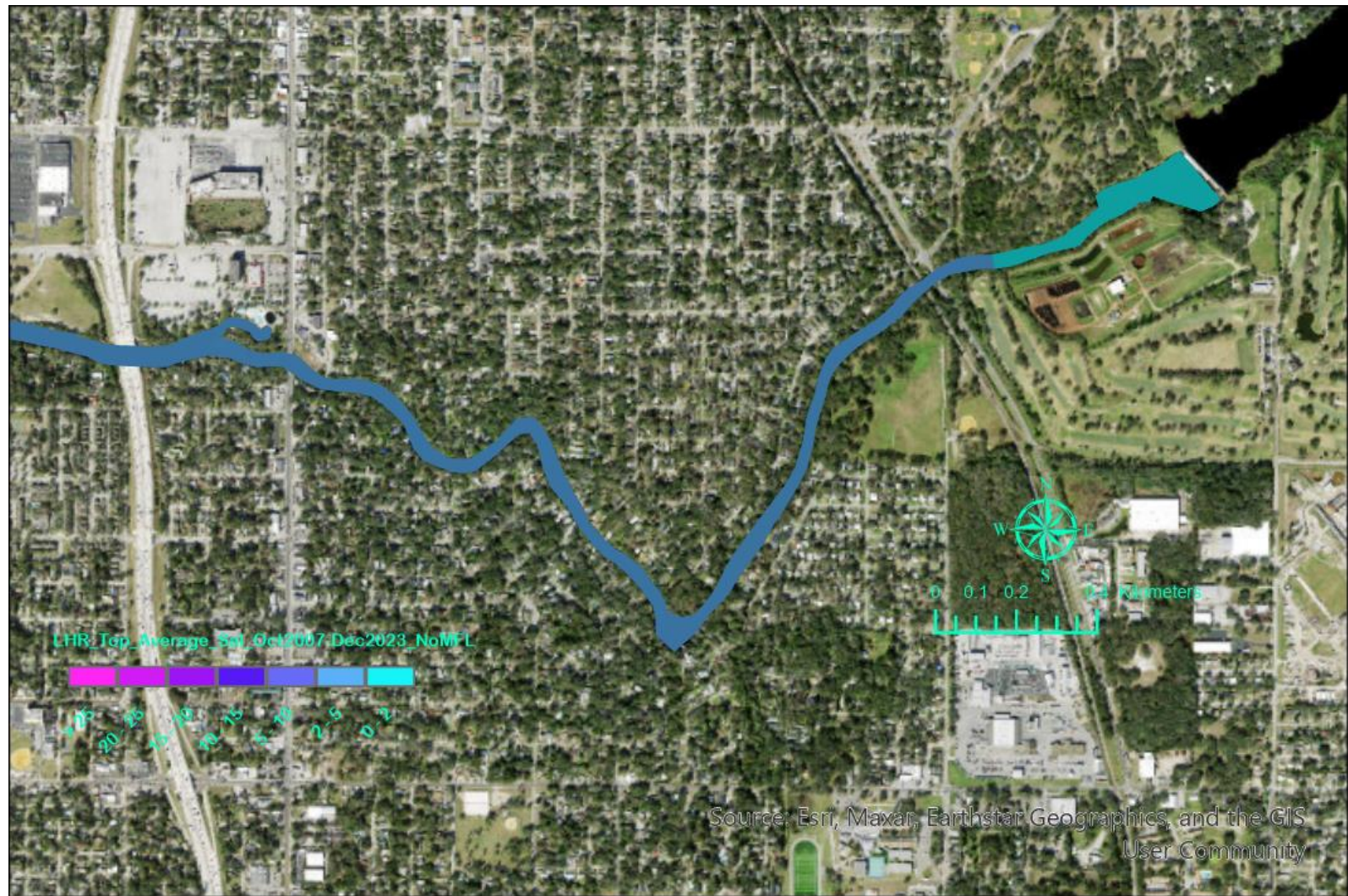
Figure A - 3. Average top–layer salinity in the upstream reach of the LHR during October 2007 – December 2023 for the no MFL flow condition.
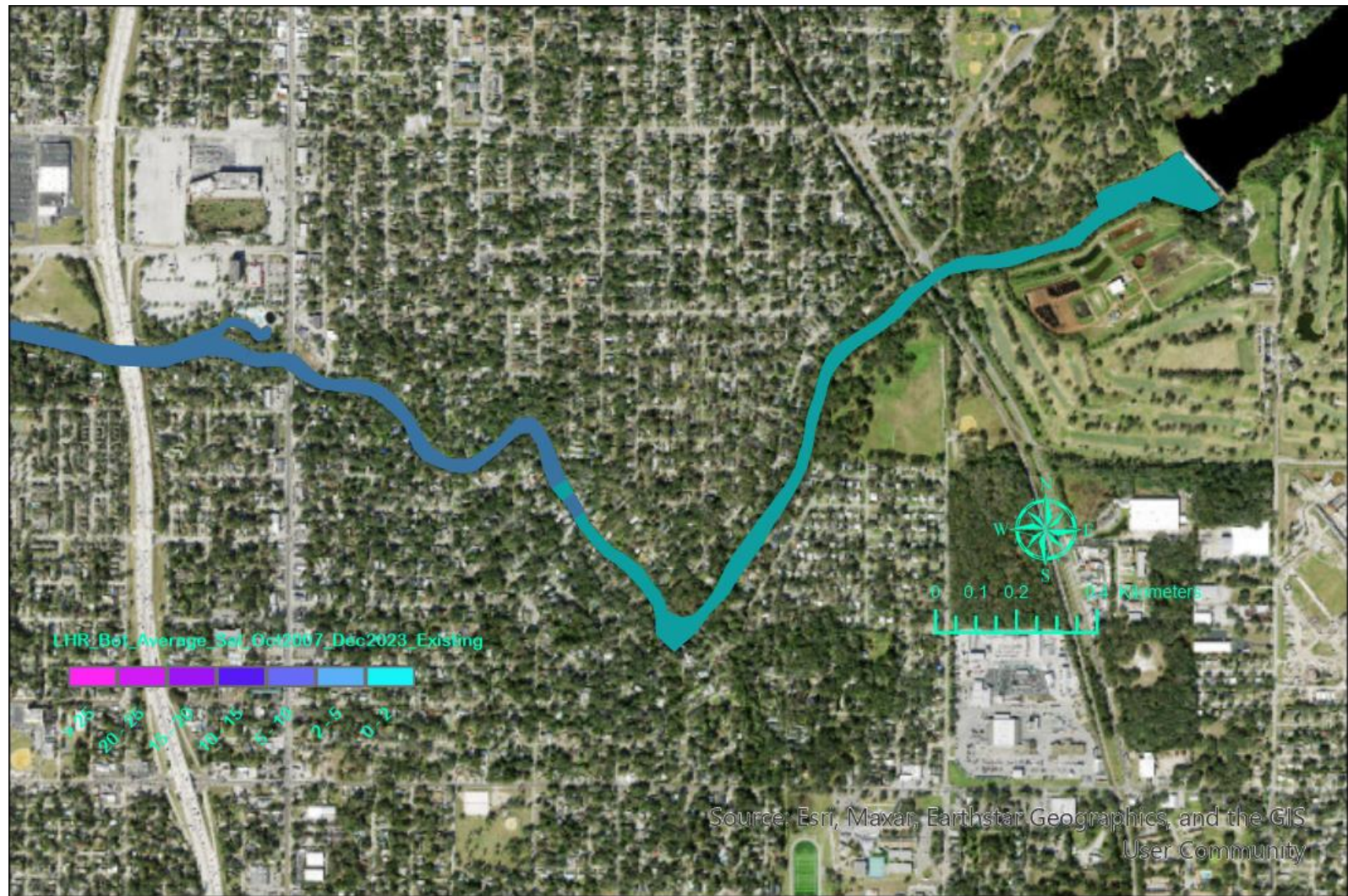
Figure A - 4. Average bottom–layer salinity in the upstream reach of the LHR during October 2007 – December 2023 for the existing flow condition.
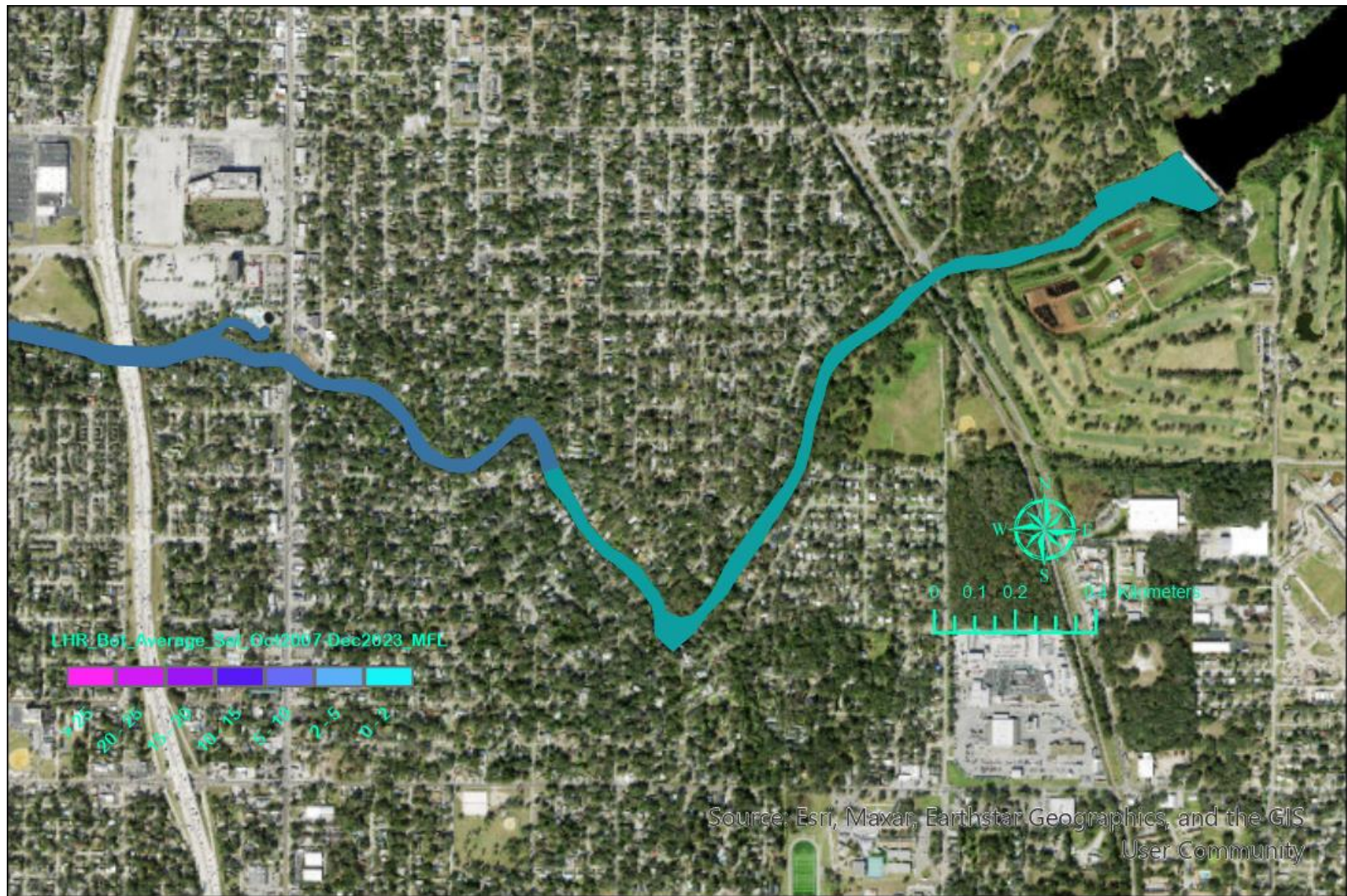
Figure A - 5. Average bottom–layer salinity in the upstream reach of the LHR during October 2007 – December 2023 for the MFL flow condition.

Figure A - 6. Average bottom–layer salinity in the upstream reach of the LHR during October 2007 – December 2023 for the no MFL flow condition.
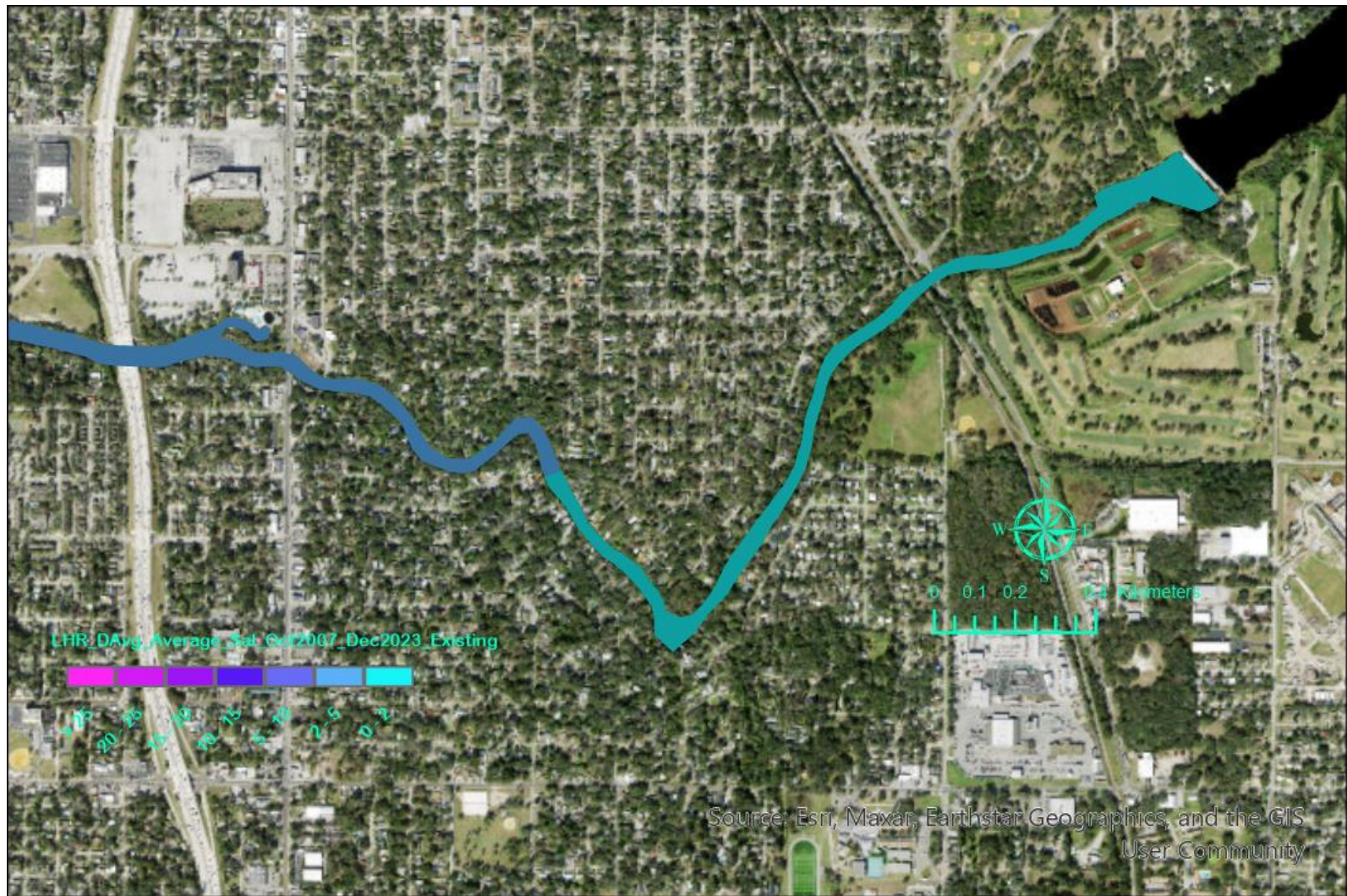
Figure A - 7. Average depth-averaged salinity in the upstream reach of the LHR during October 2007 – December 2023 for the existing flow condition.
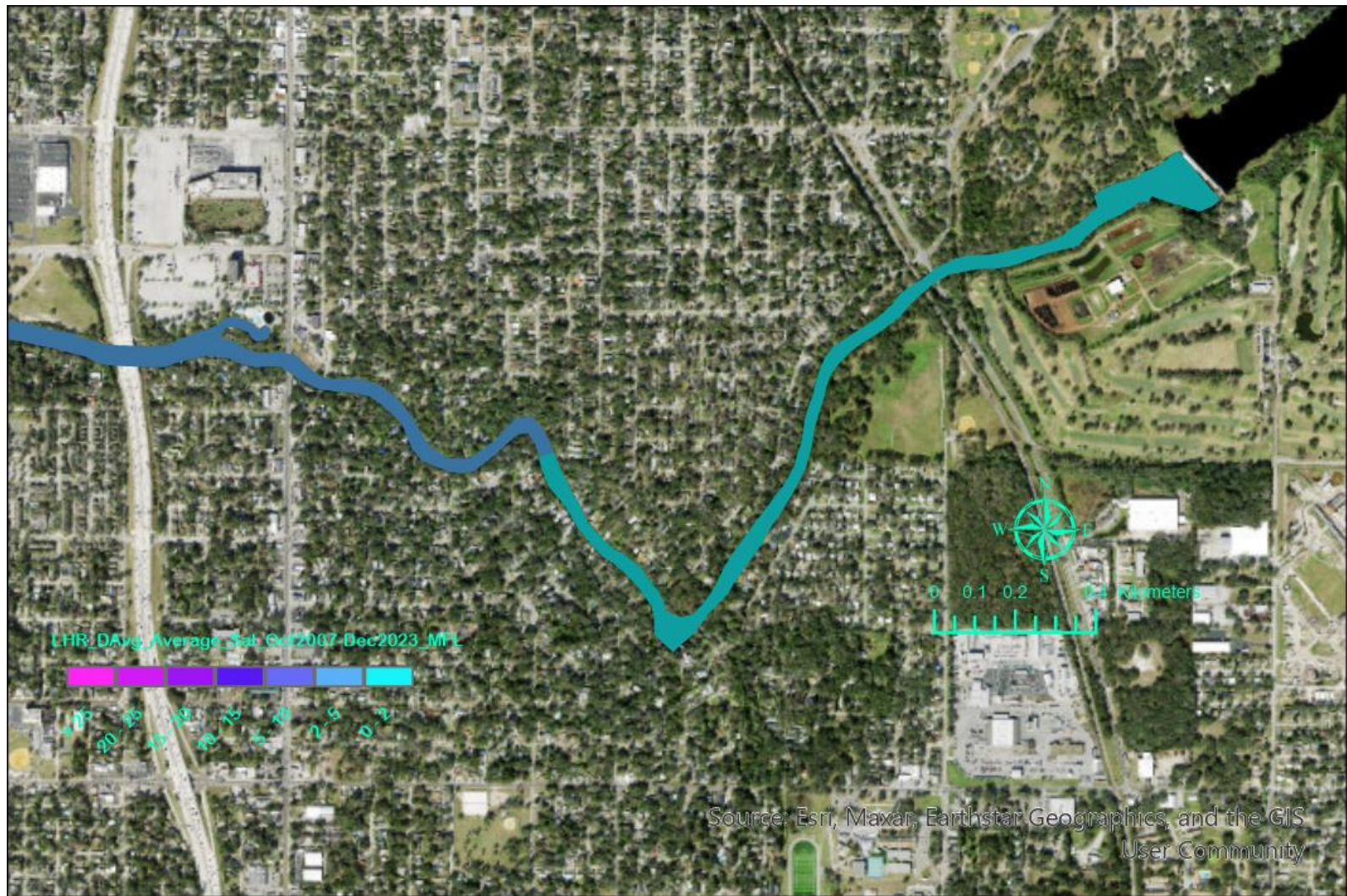
Figure A - 8. Average depth-averaged salinity in the upstream reach of the LHR during October 2007 – December 2023 for the MFL flow condition.

Figure A - 9. Average depth-averaged salinity in the upstream reach of the LHR during October 2007 – December 2023 for the no MFL flow condition.
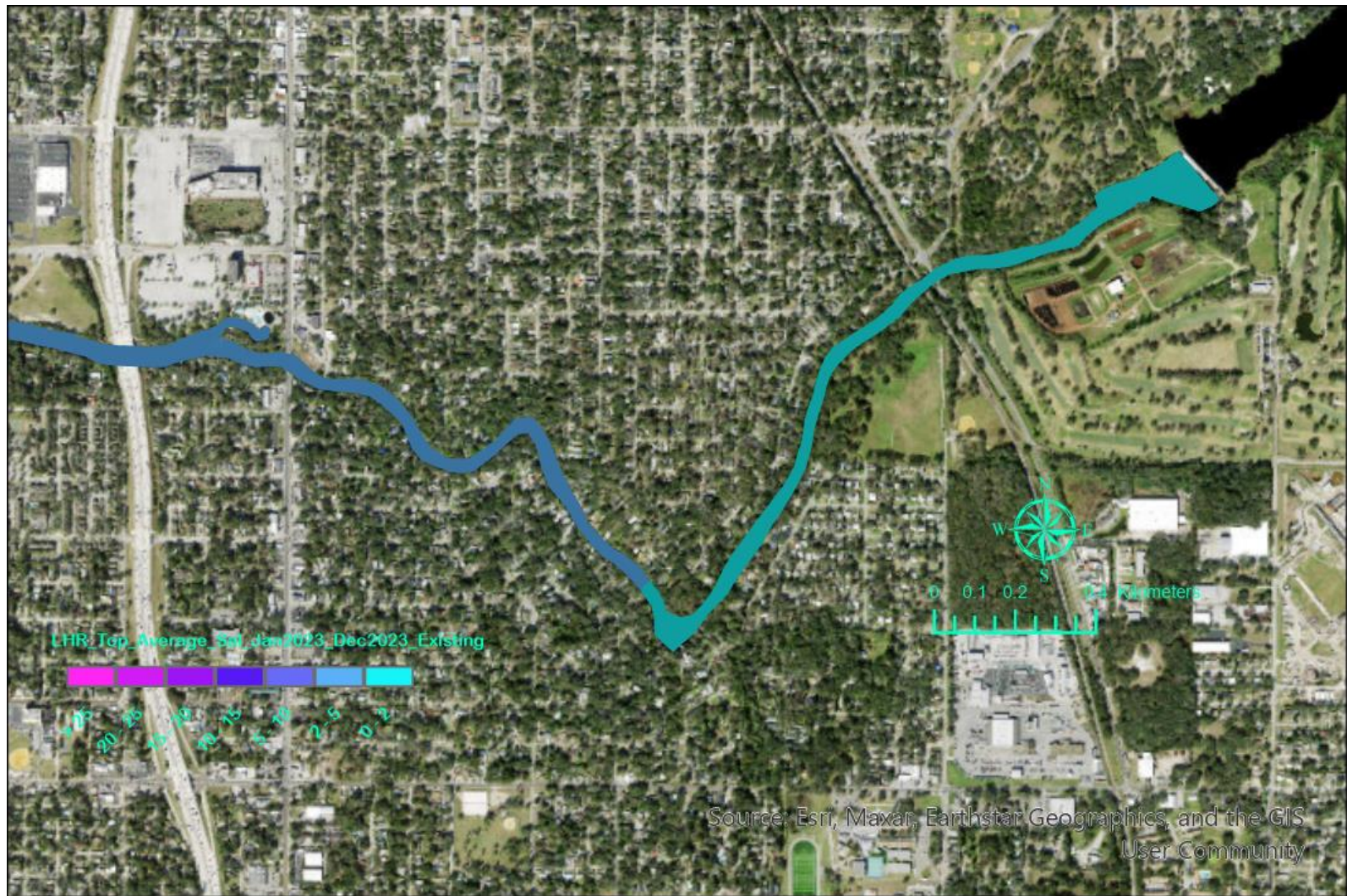
Figure A - 10. Average top-layer salinity in the upstream reach of the LHR during January - December 2023 for the existing flow condition.
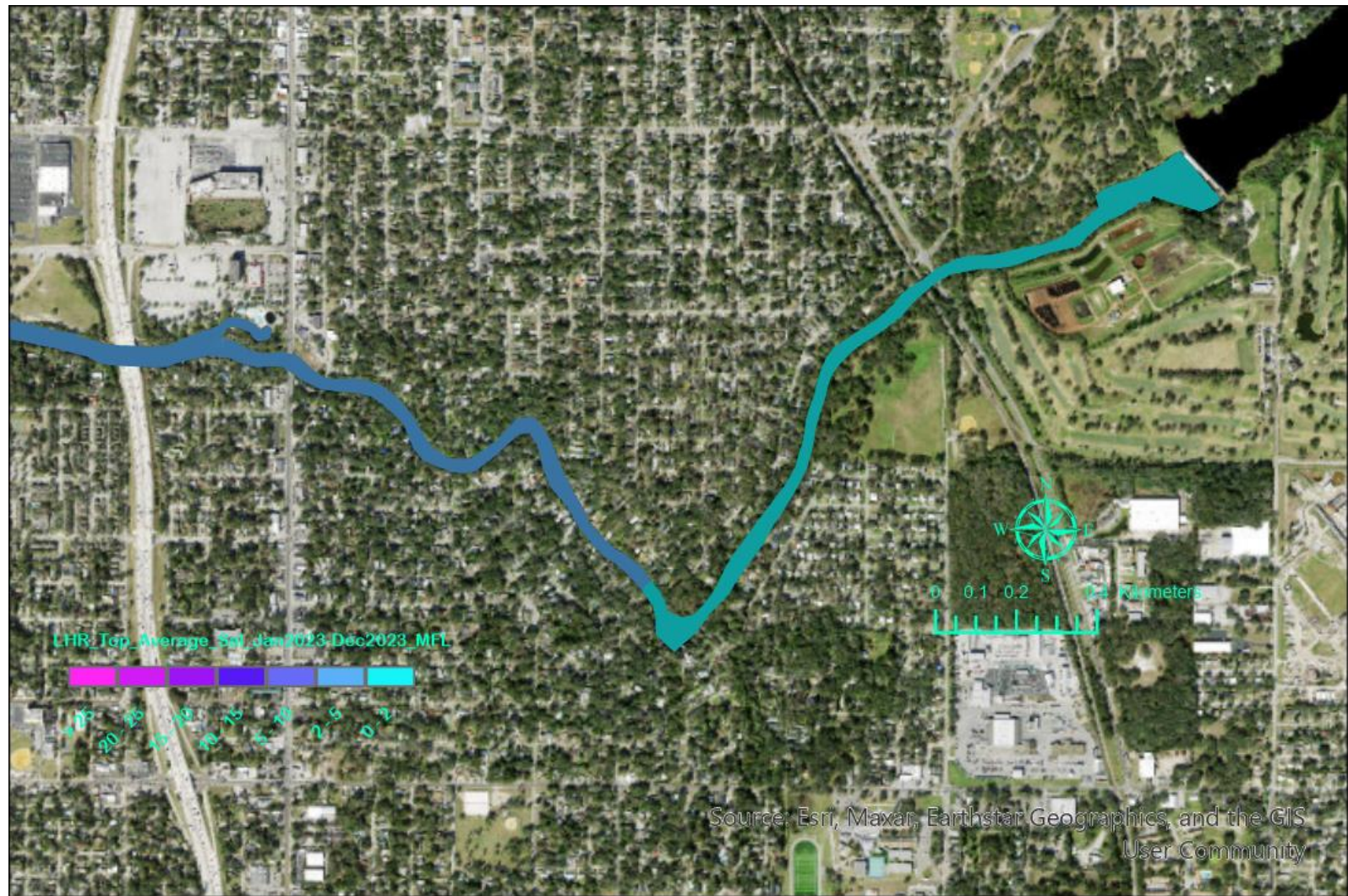
Figure A - 11. Average top-layer salinity in the upstream reach of the LHR during January - December 2023 for the MFL flow condition.
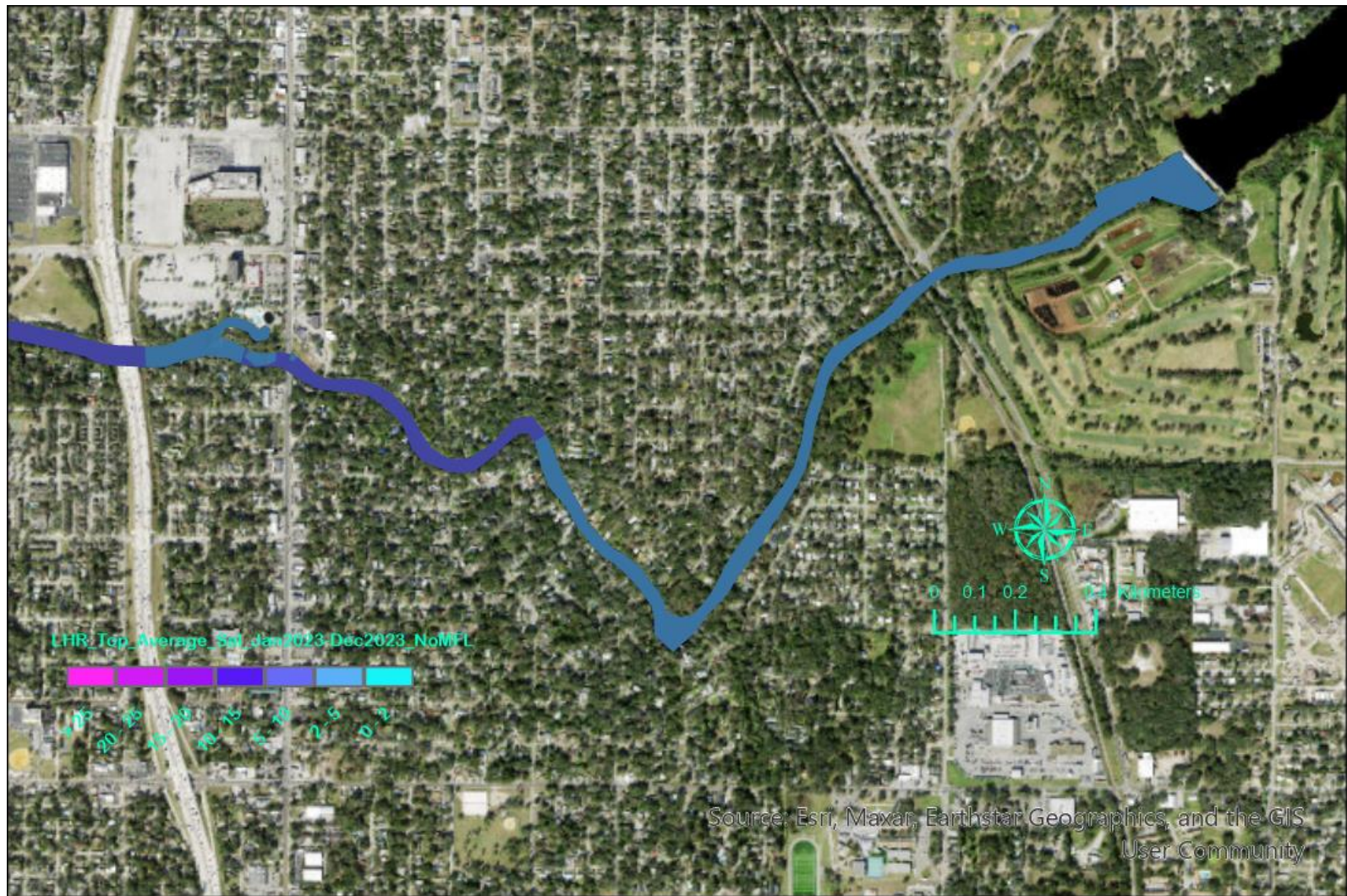
Figure A - 12. Average top-layer salinity in the upstream reach of the LHR during January - December 2023 for the no MFL flow condition.
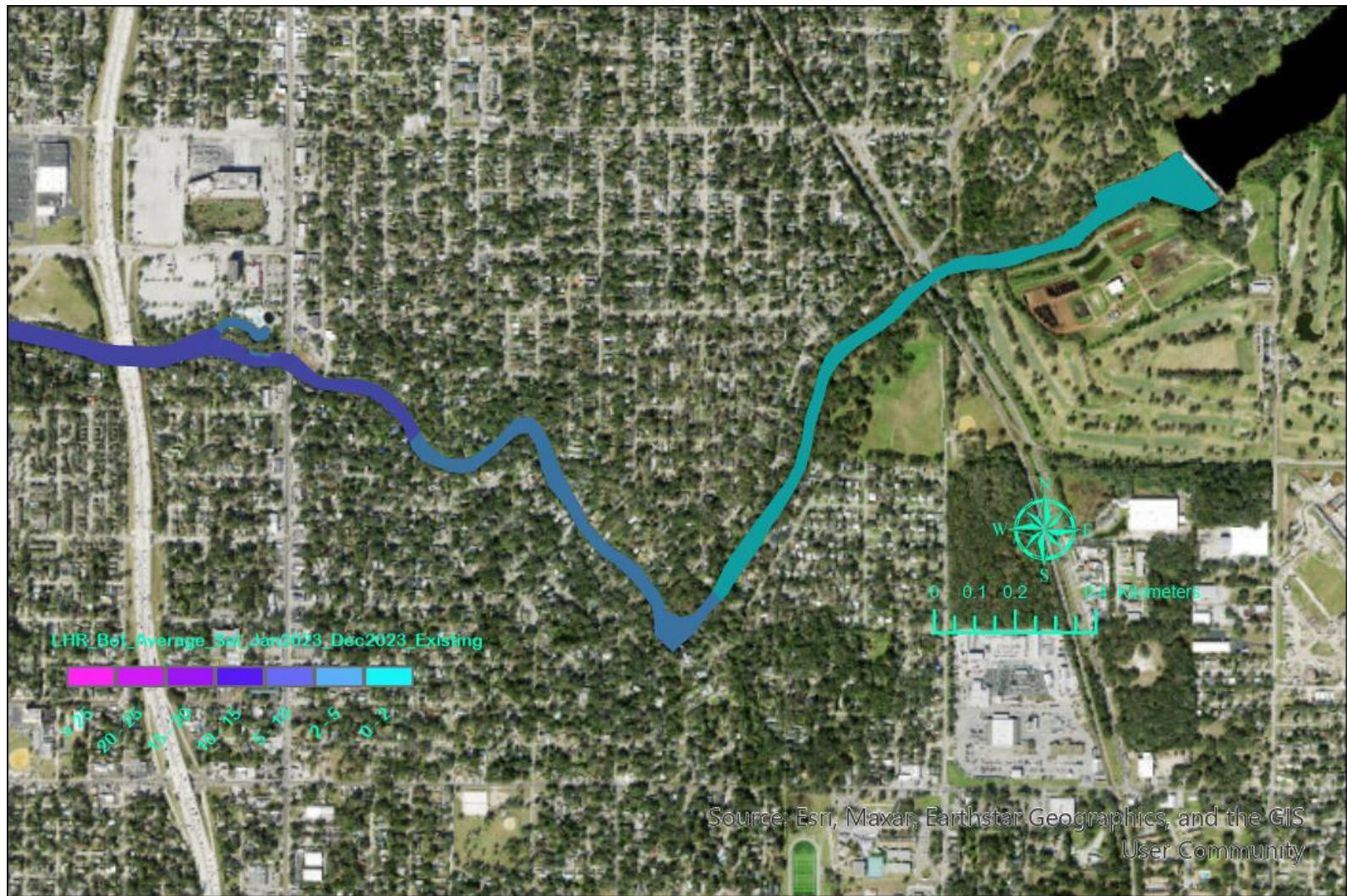
Figure A - 13. Average bottom-layer salinity in the upstream reach of the LHR during January - December 2023 for the existing flow condition.

Figure A - 14. Average bottom-layer salinity in the upstream reach of the LHR during January - December 2023 for the MFL flow condition.

Figure A - 15. Average bottom-layer salinity in the upstream reach of the LHR during January - December 2023 for the no MFL flow condition.

Figure A - 16. Average depth-averaged salinity in the upstream reach of the LHR during January - December 2023 for the existing flow condition.
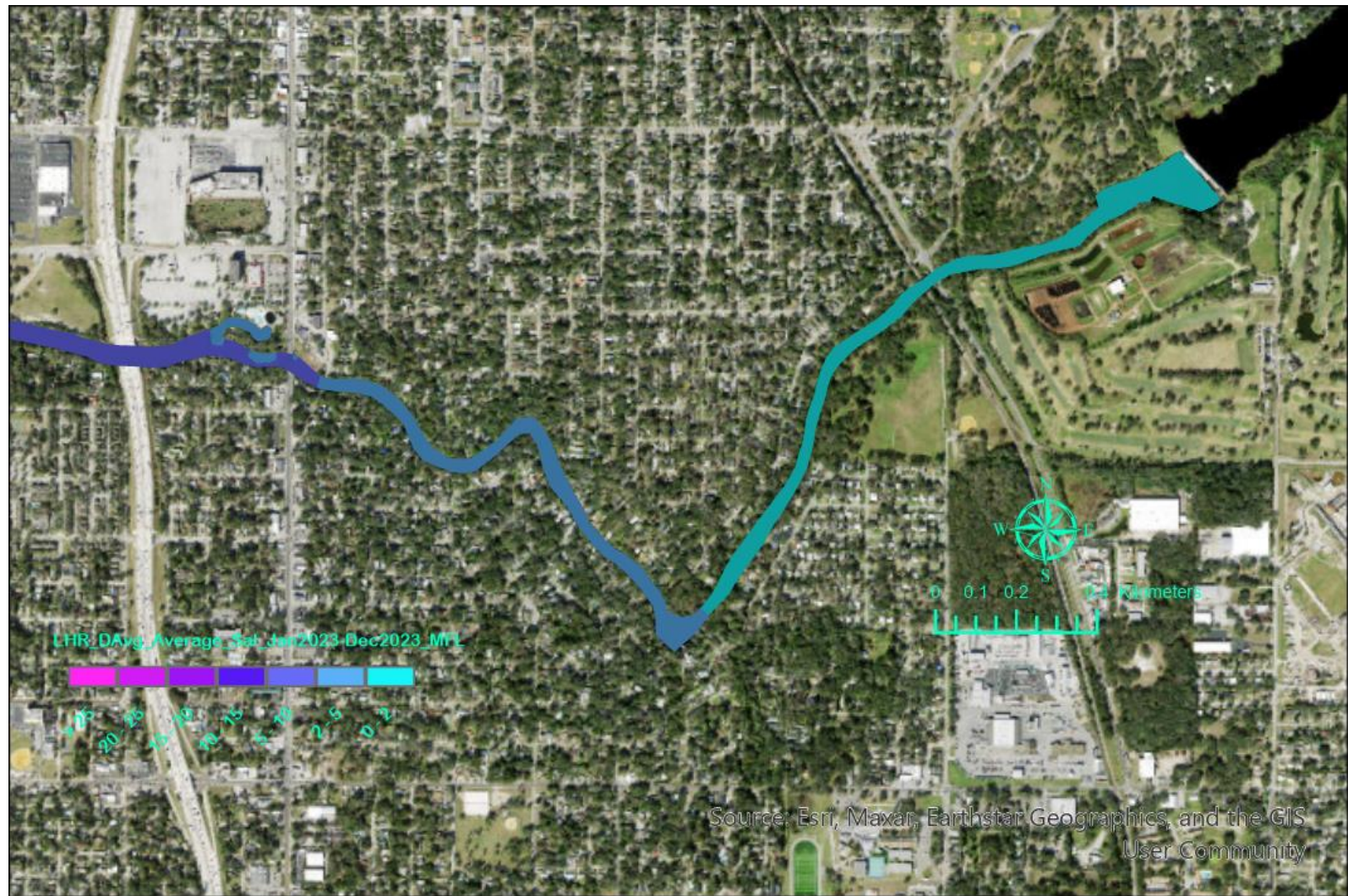
Figure A - 17. Average depth-averaged salinity in the upstream reach of the LHR during January - December 2023 for the MFL flow condition.

Figure A - 18. Average depth-averaged salinity in the upstream reach of the LHR during January - December 2023 for the no MFL flow condition.

2. Appendix B. Thermal Habitats in the Spring Run Only
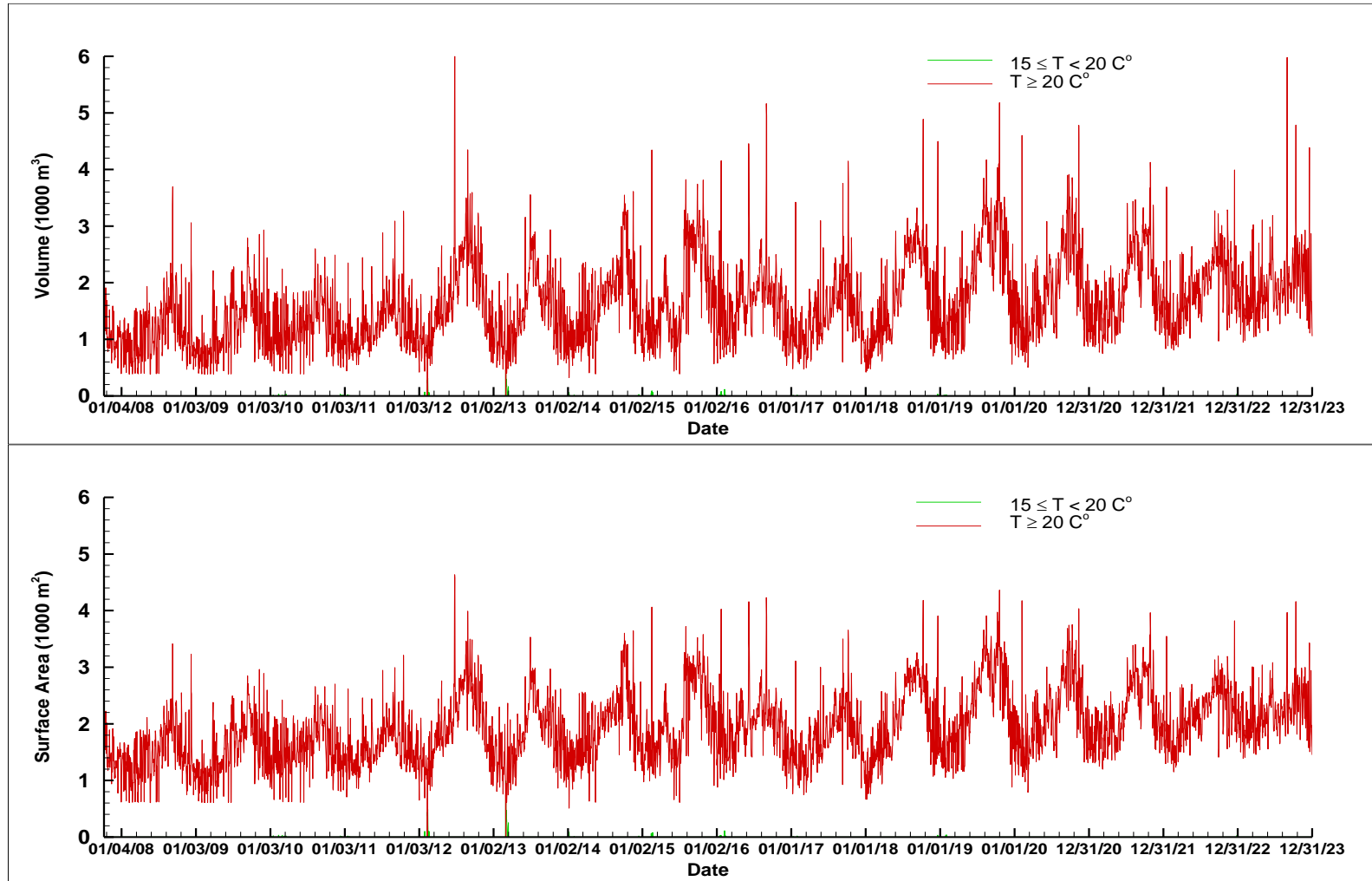
Figure B - 1. Simulated thermal habitats for manatees in the Sulphur Springs run only during October 2007 – December 2023 for the existing flow condition.
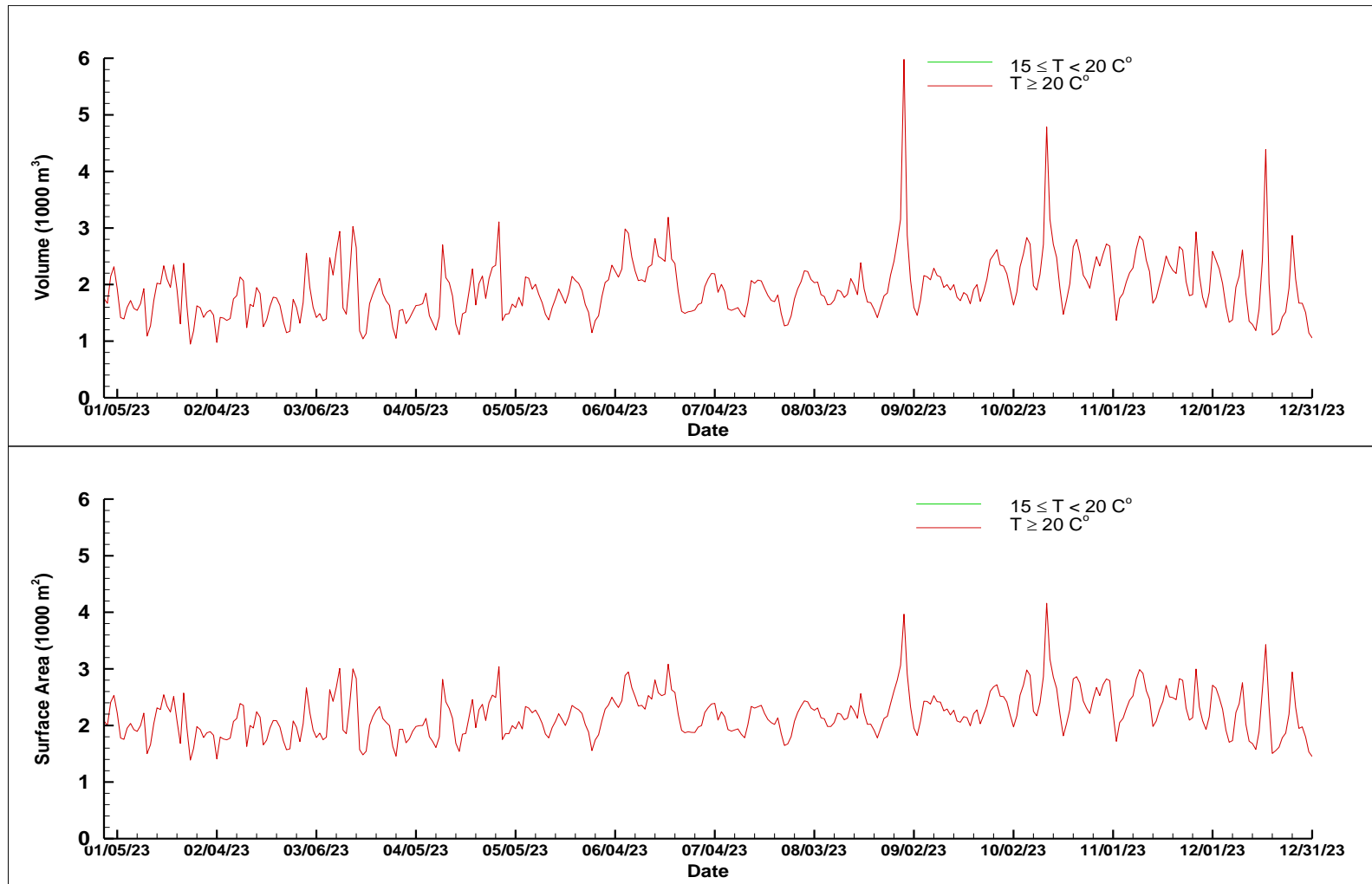
Figure B - 2. Simulated thermal habitats for manatees in the Sulphur Springs run only during January – December 2023 for the existing flow condition.
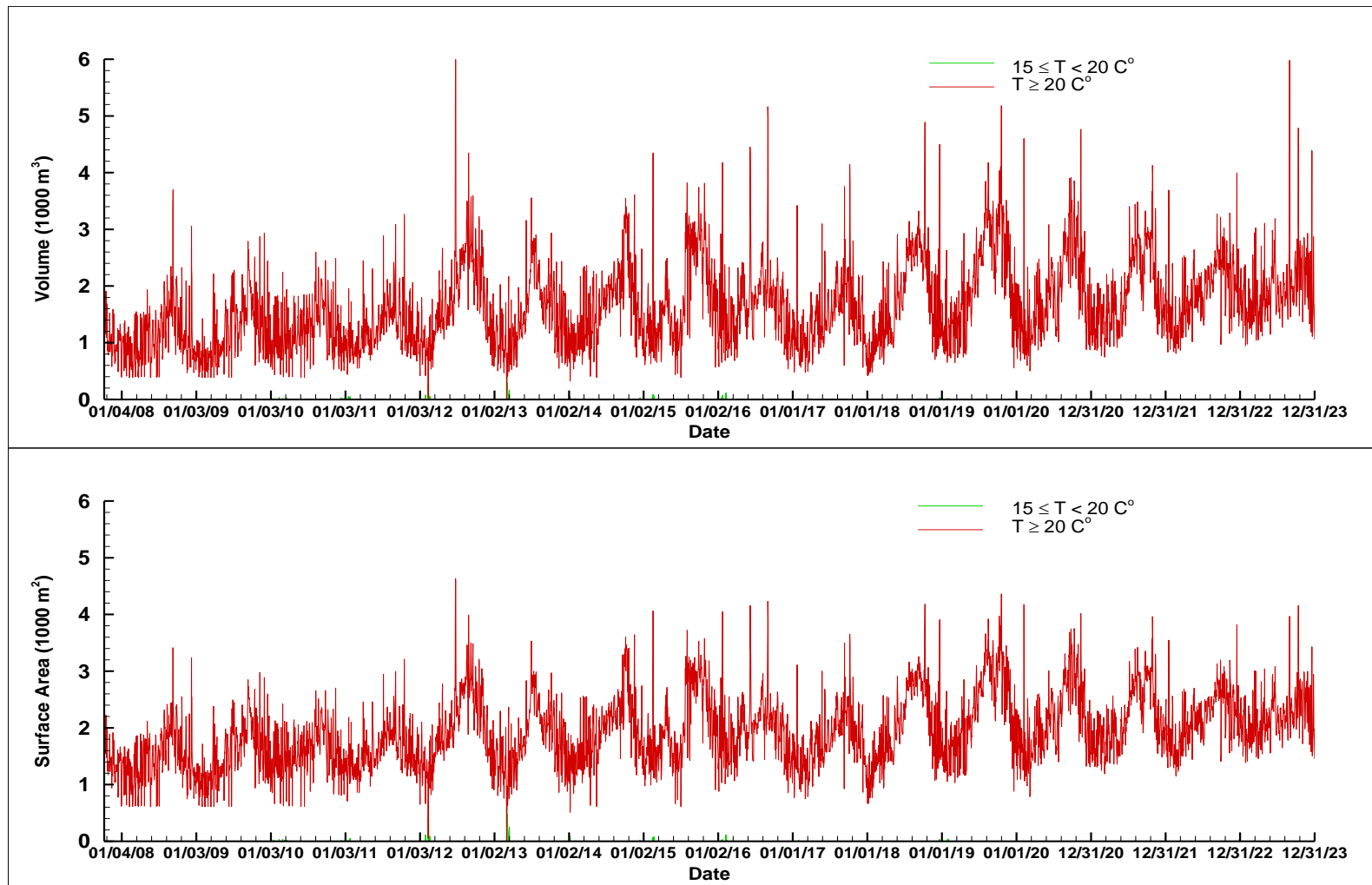
Figure B - 3. Simulated thermal habitats for manatees in the Sulphur Springs run only during October 2007 – December 2023 for the MFL flow condition.
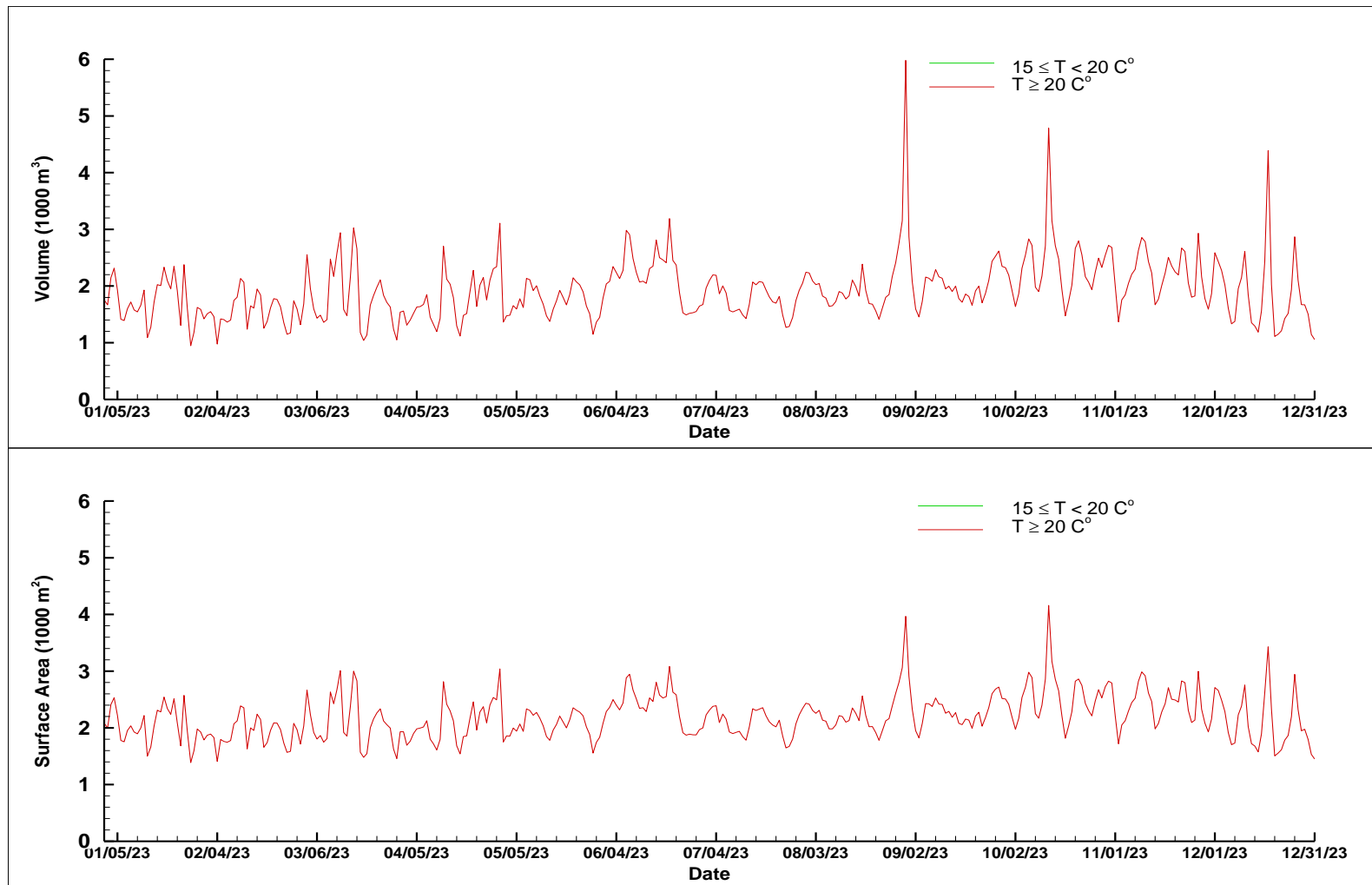
Figure B - 4. Simulated thermal habitats for manatees in the Sulphur Springs run only during January – December 2023 for the MFL flow condition.
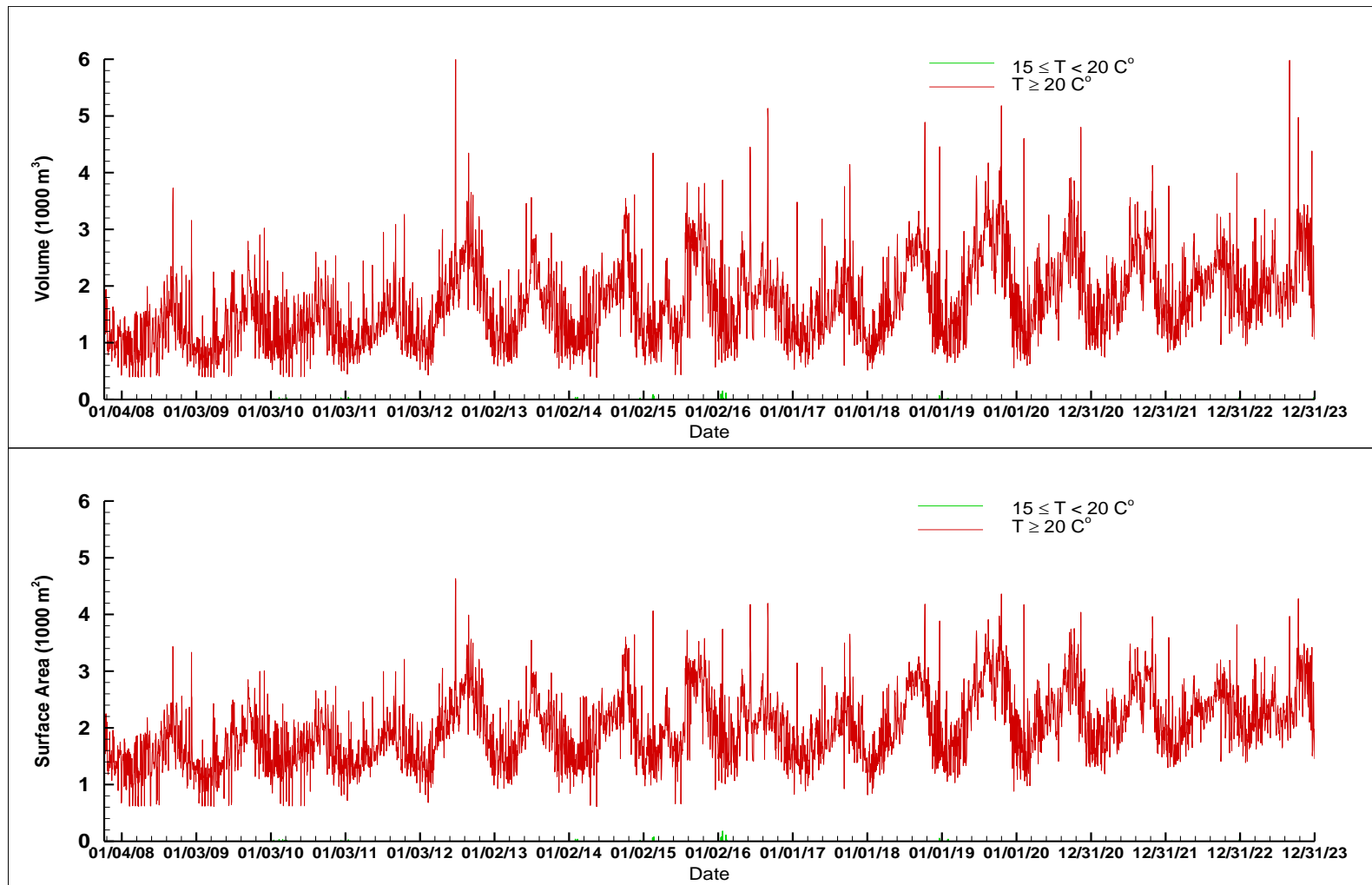
Figure B - 5. Simulated thermal habitats for manatees in the Sulphur Springs run only during October 2007 – December 2023 for the no MFL flow condition.
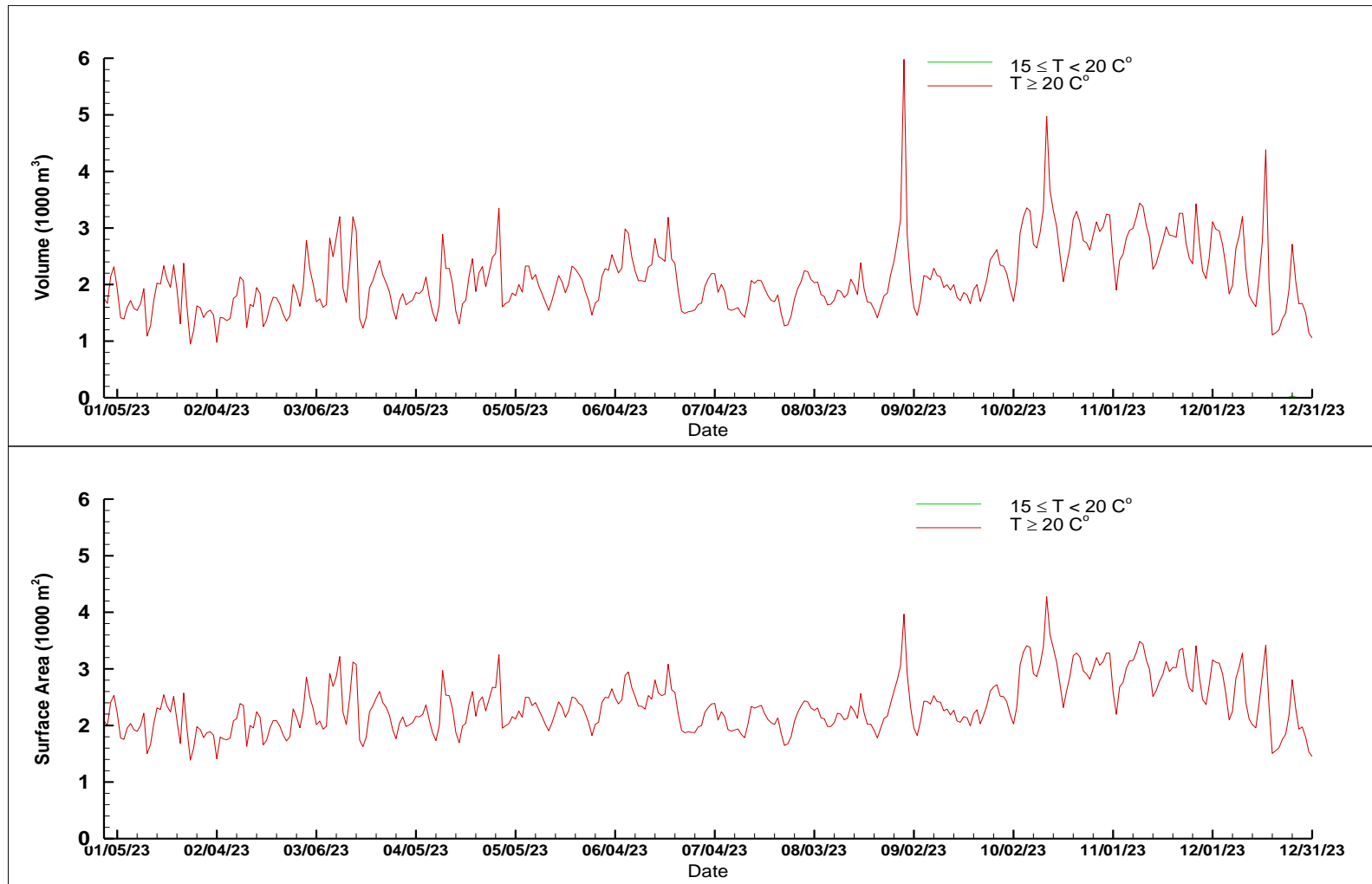
Figure B - 6. Simulated thermal habitats for manatees in the Sulphur Springs run only during January – December 2023 for the no MFL flow condition.

3. Appendix C. Temperature Distributions

The following 18 maps contain distributions of the average top-layer, bottom-layer, and depth-averaged temperatures during manatee seasons of the 195-month simulation period, October 2007 – December 2023 (Figs. C – 1 – C – 9) and the manatee season of 2023 (Figs. C – 10 – C – 18)
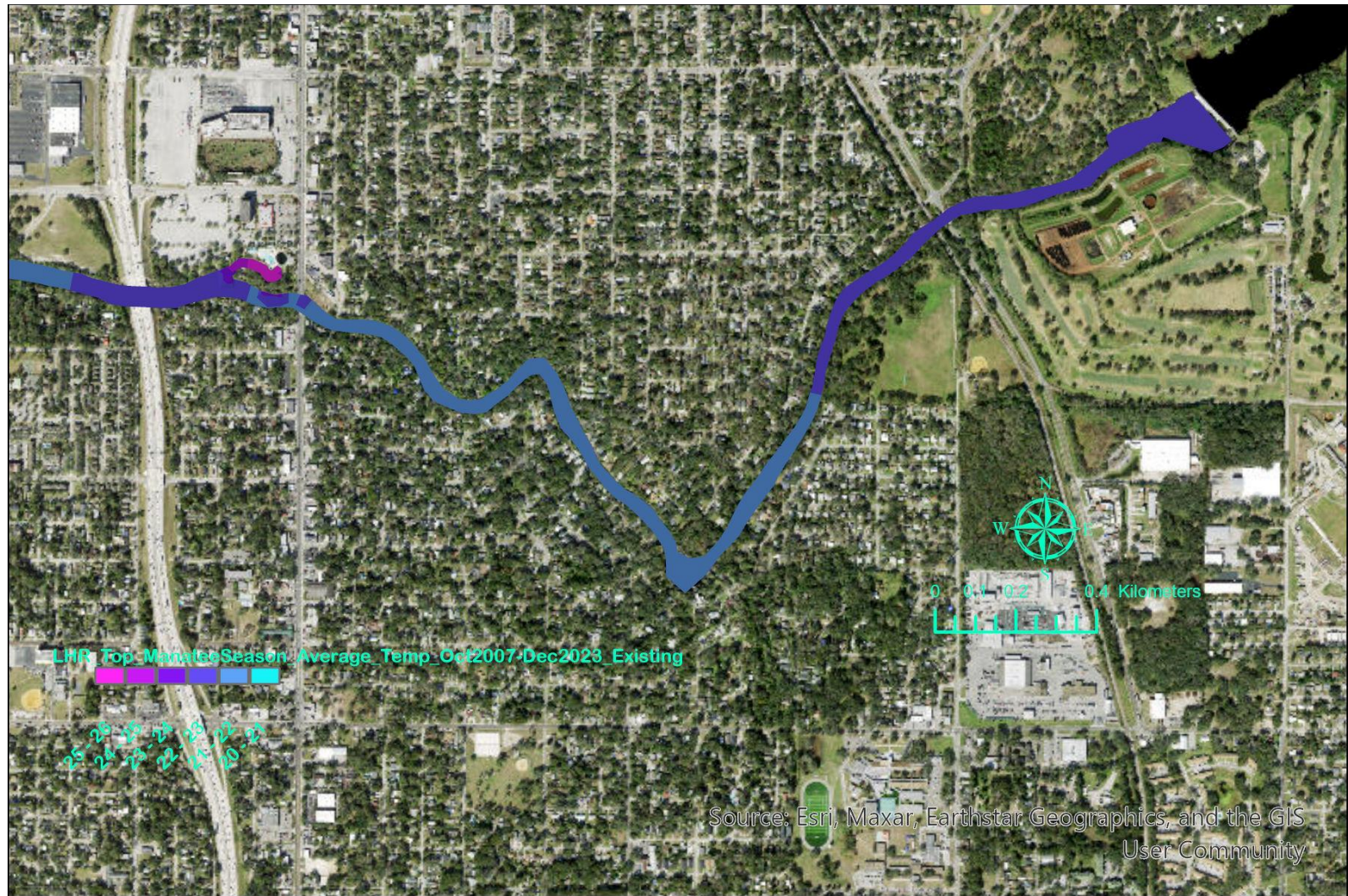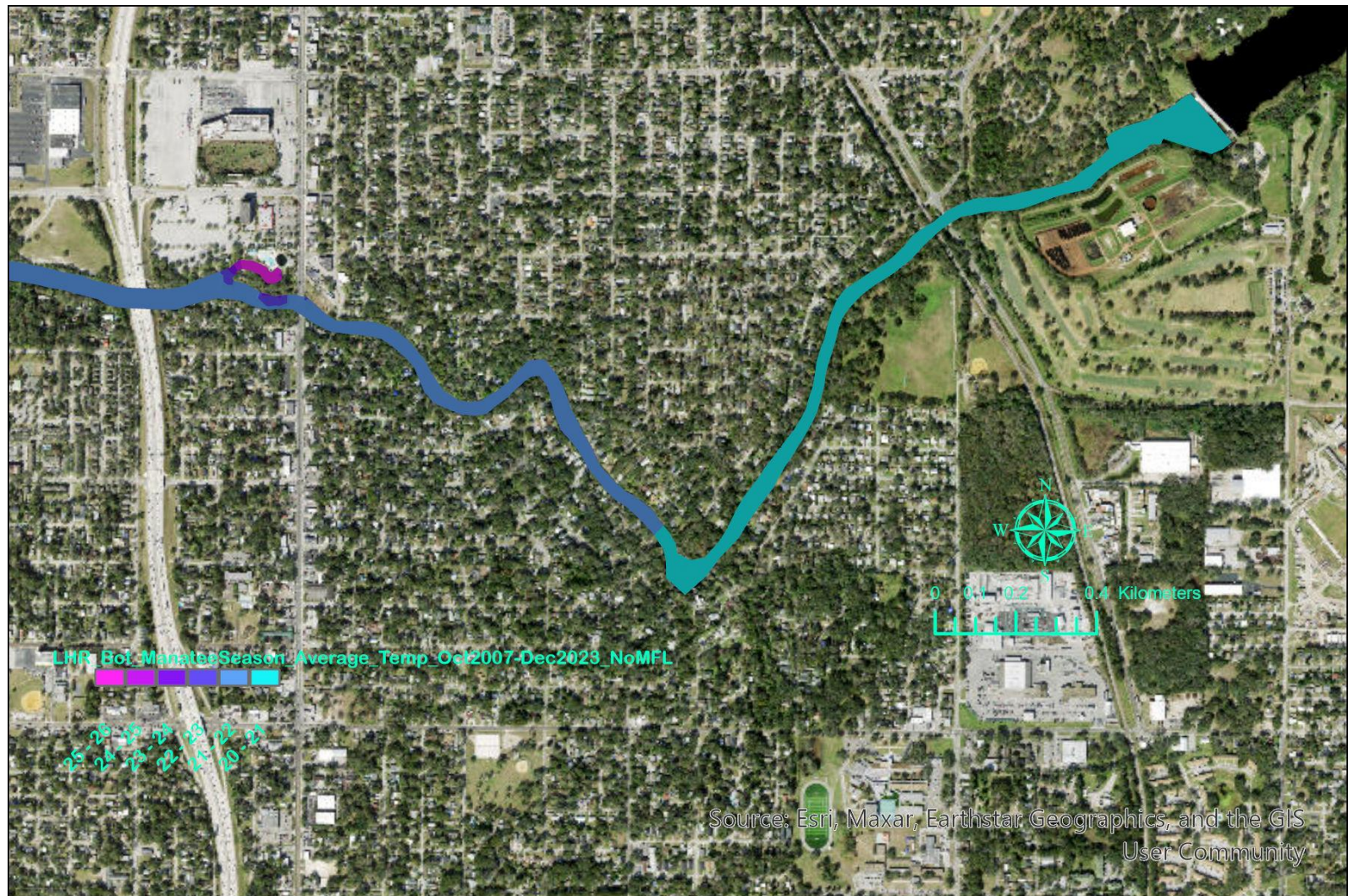
Figure C - 1. Average top-layer temperature in the upstream reach of the LHR during manatee seasons of the 195-month simulation period from October 2007 to December 2023 for the existing flow condition.
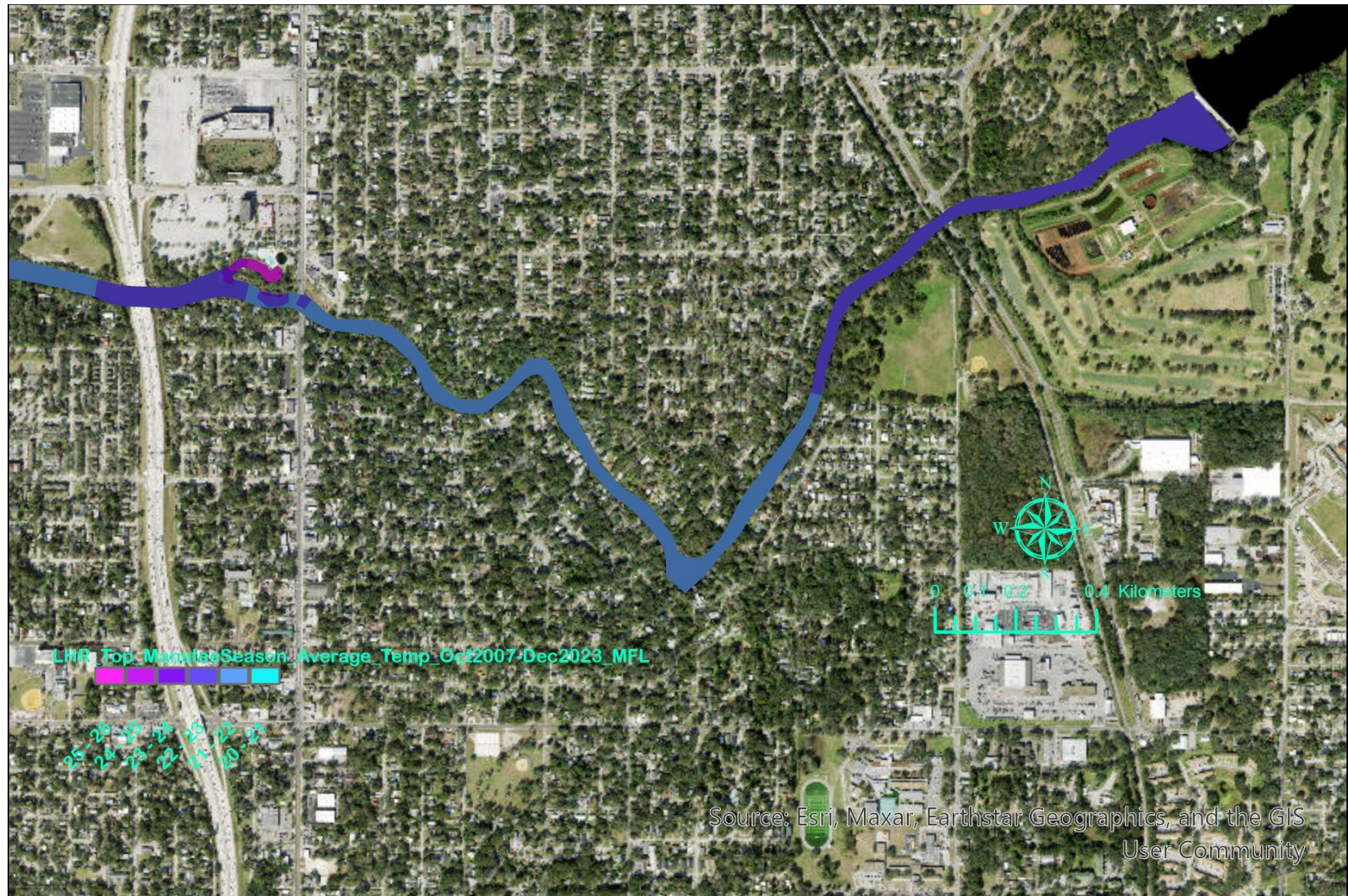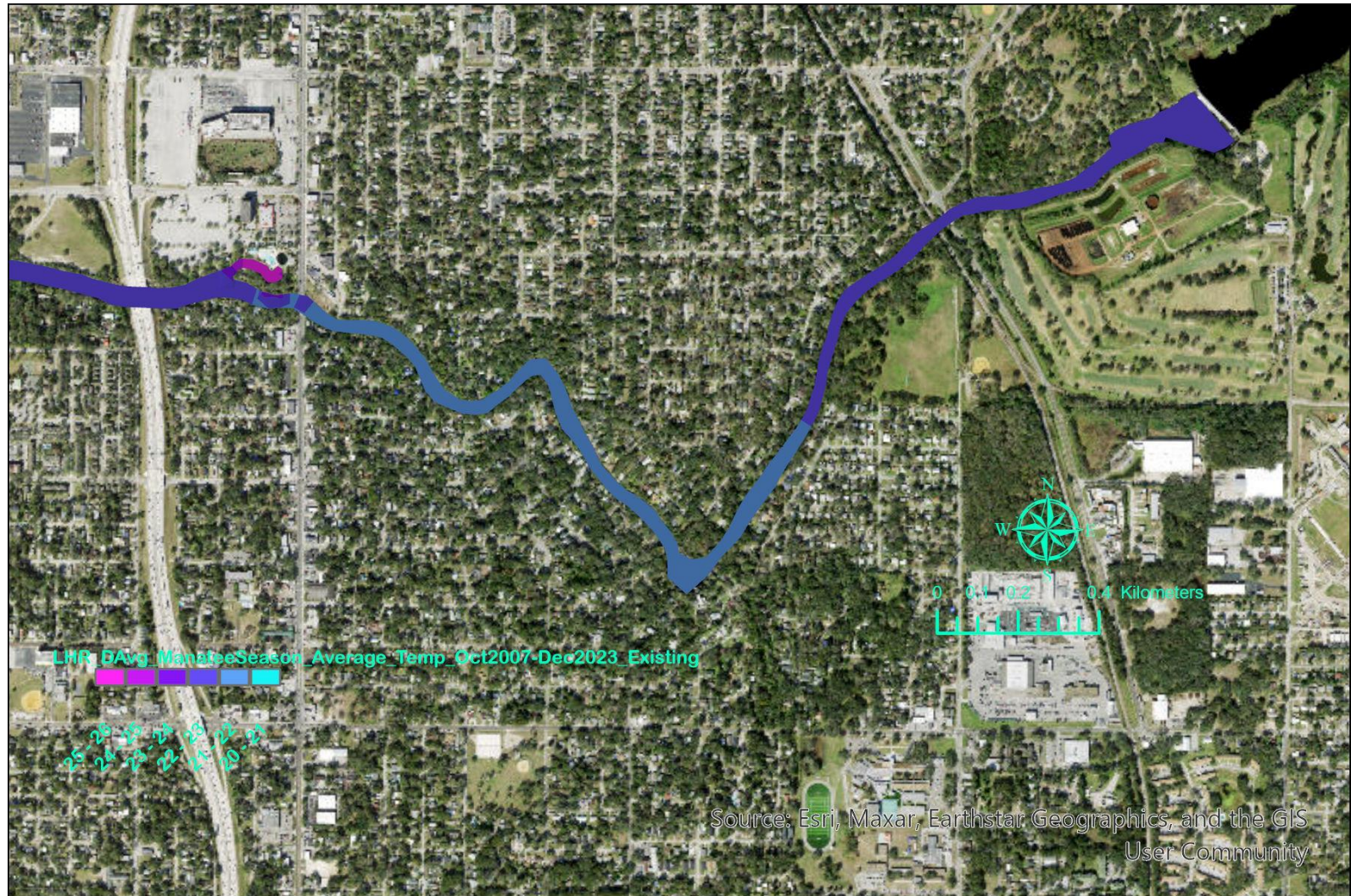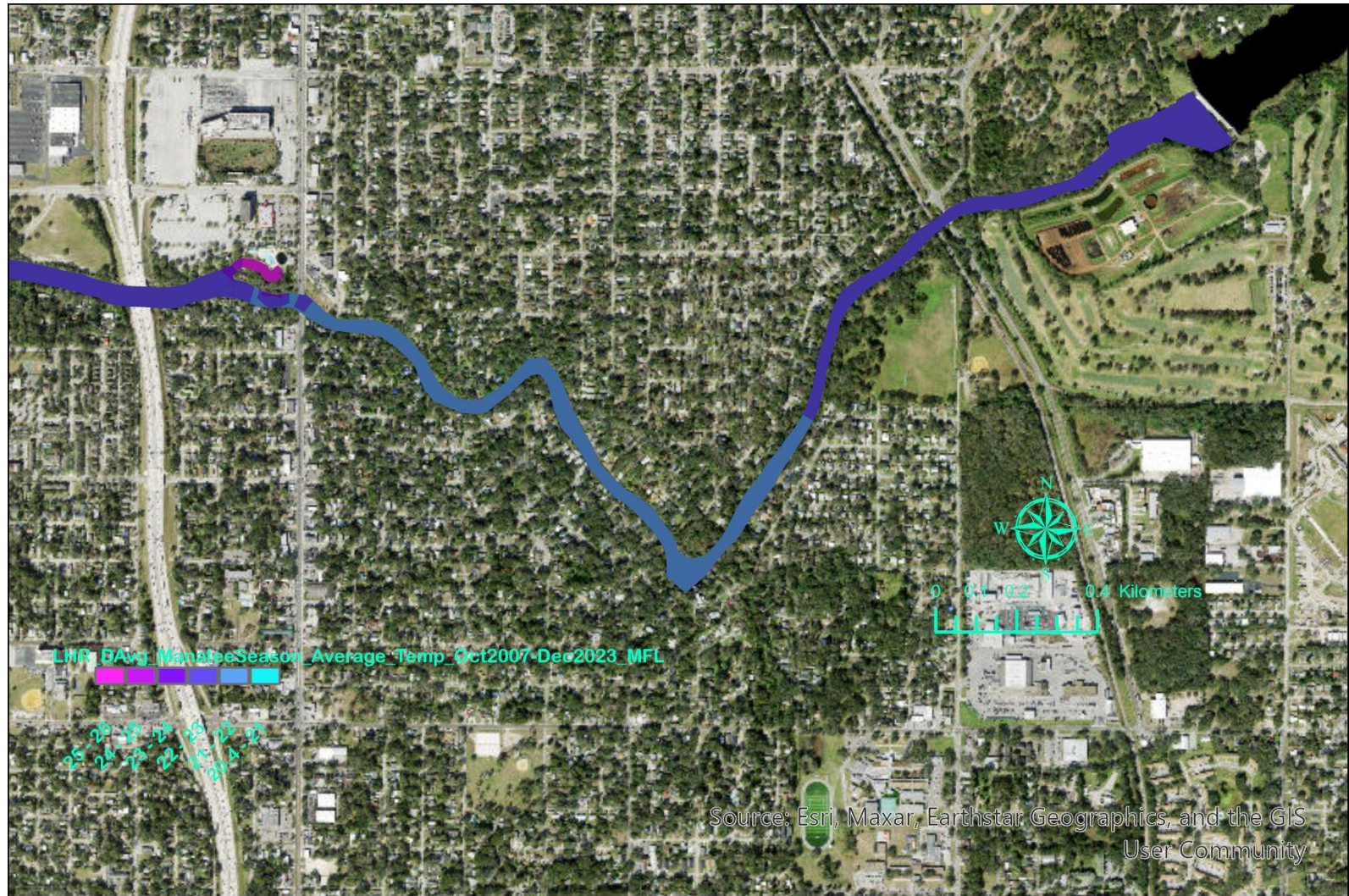
Figure C - 2.   Average top-layer temperature in the upstream reach of the LHR during manatee seasons of the 195-month simulation period from October 2007 to December 2023 for the MFL flow condition.
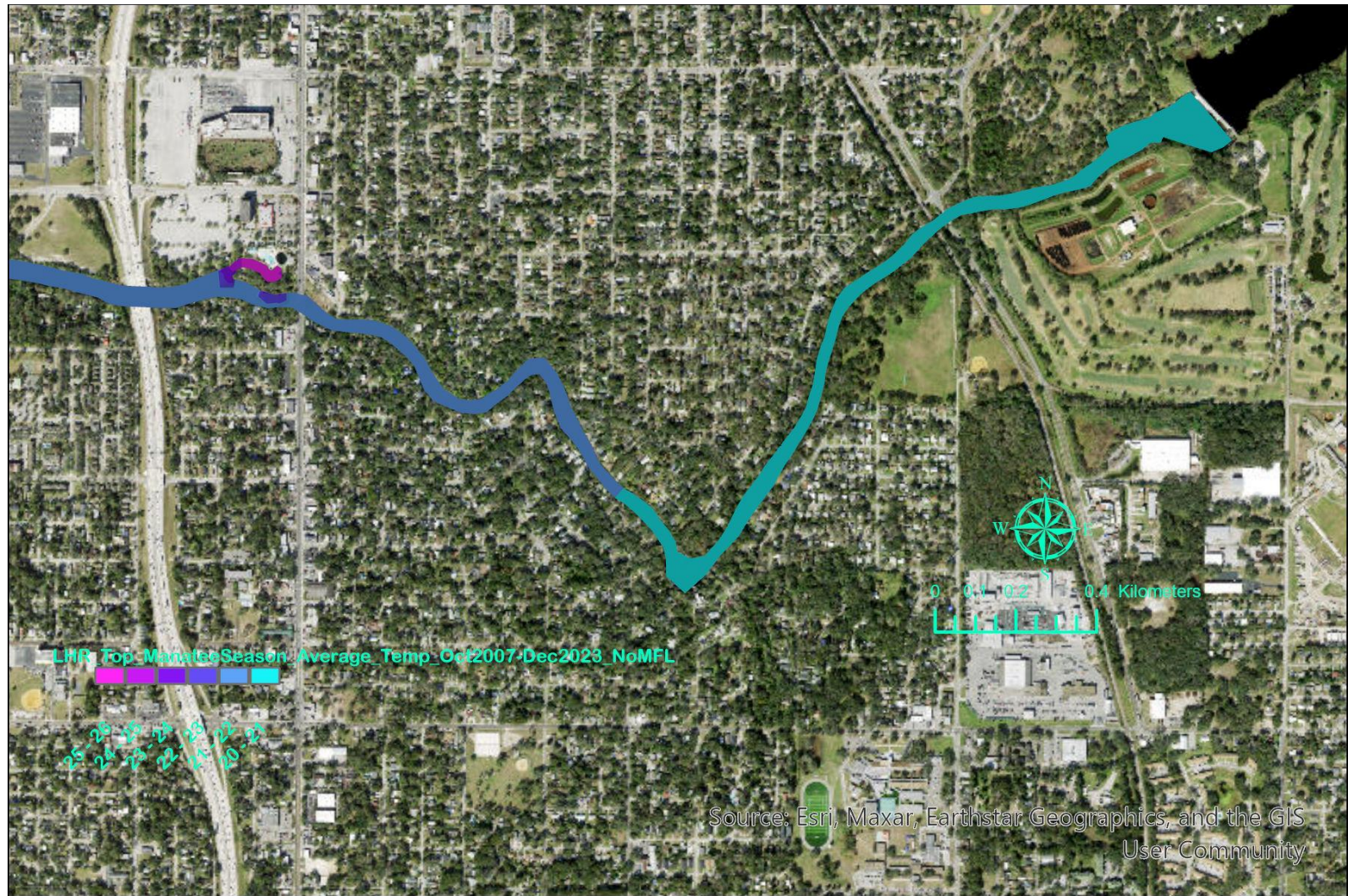
Figure C - 3. Average top-layer temperature in the upstream reach of the LHR during manatee seasons of the 195-month simulation period from October 2007 to December 2023 for the no MFL flow condition.
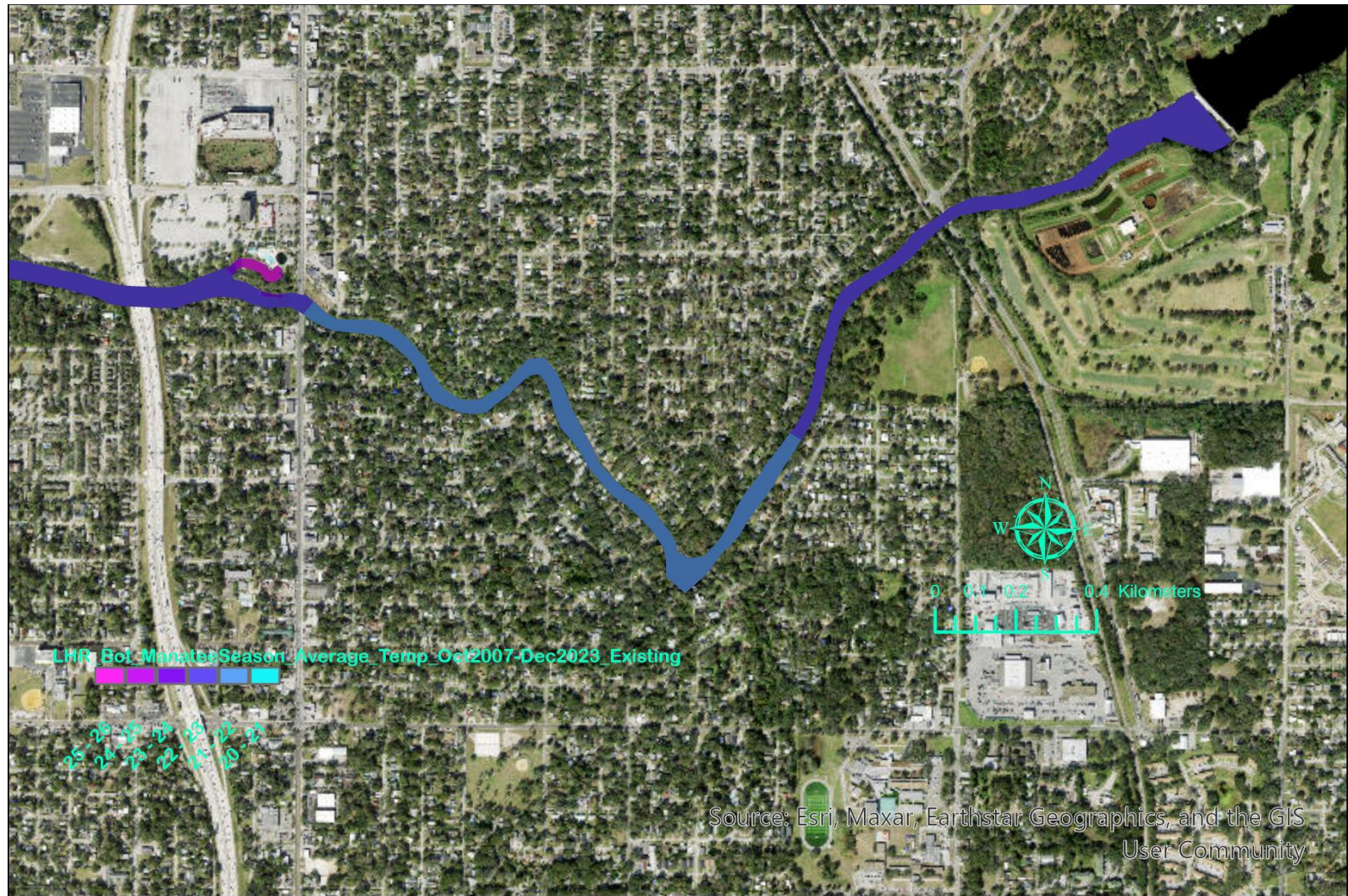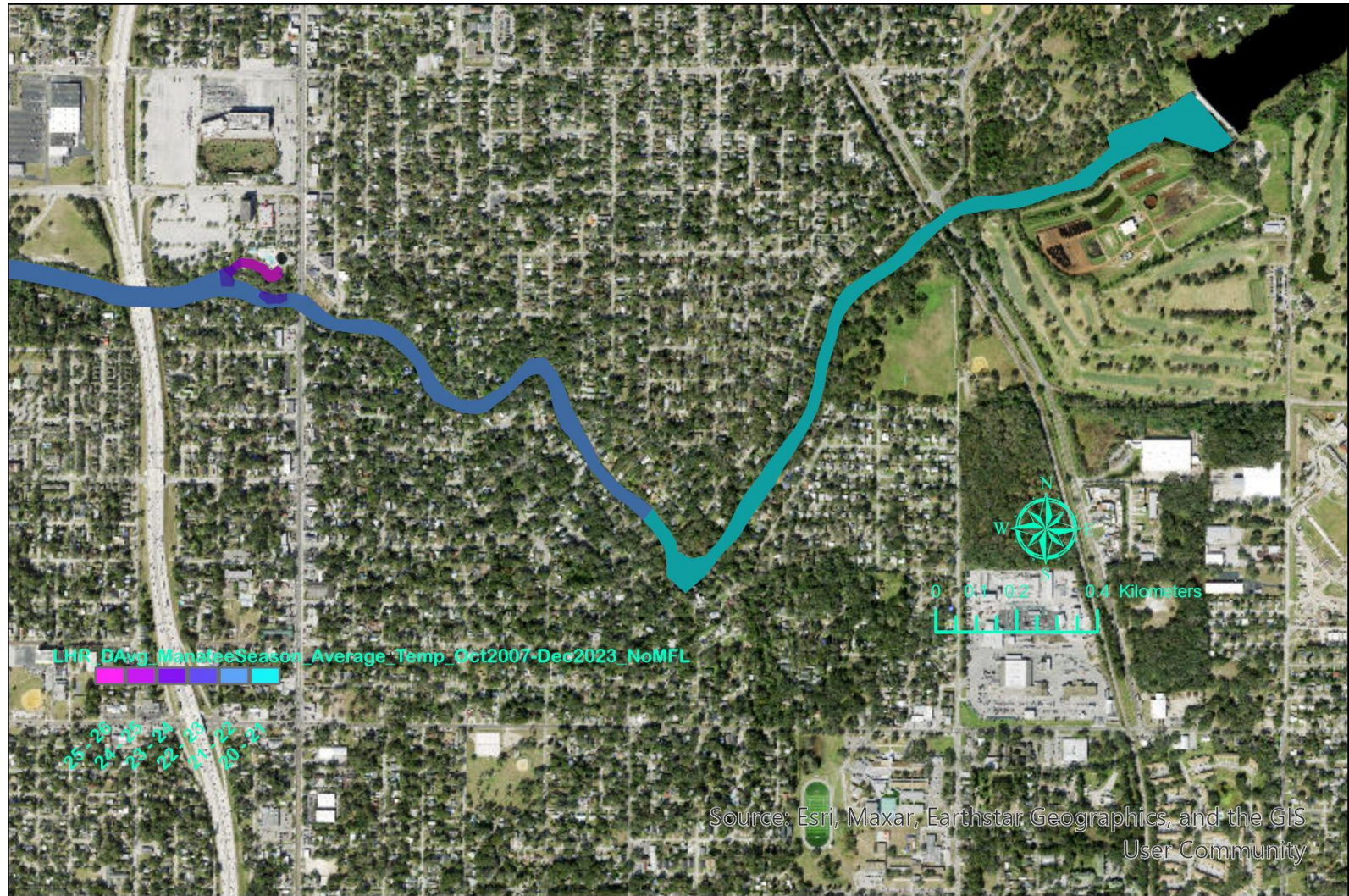
Figure C - 4. Average bottom-layer temperature in the upstream reach of the LHR during manatee seasons of the 195-month simulation period from October 2007 to December 2023 for the existing flow condition.
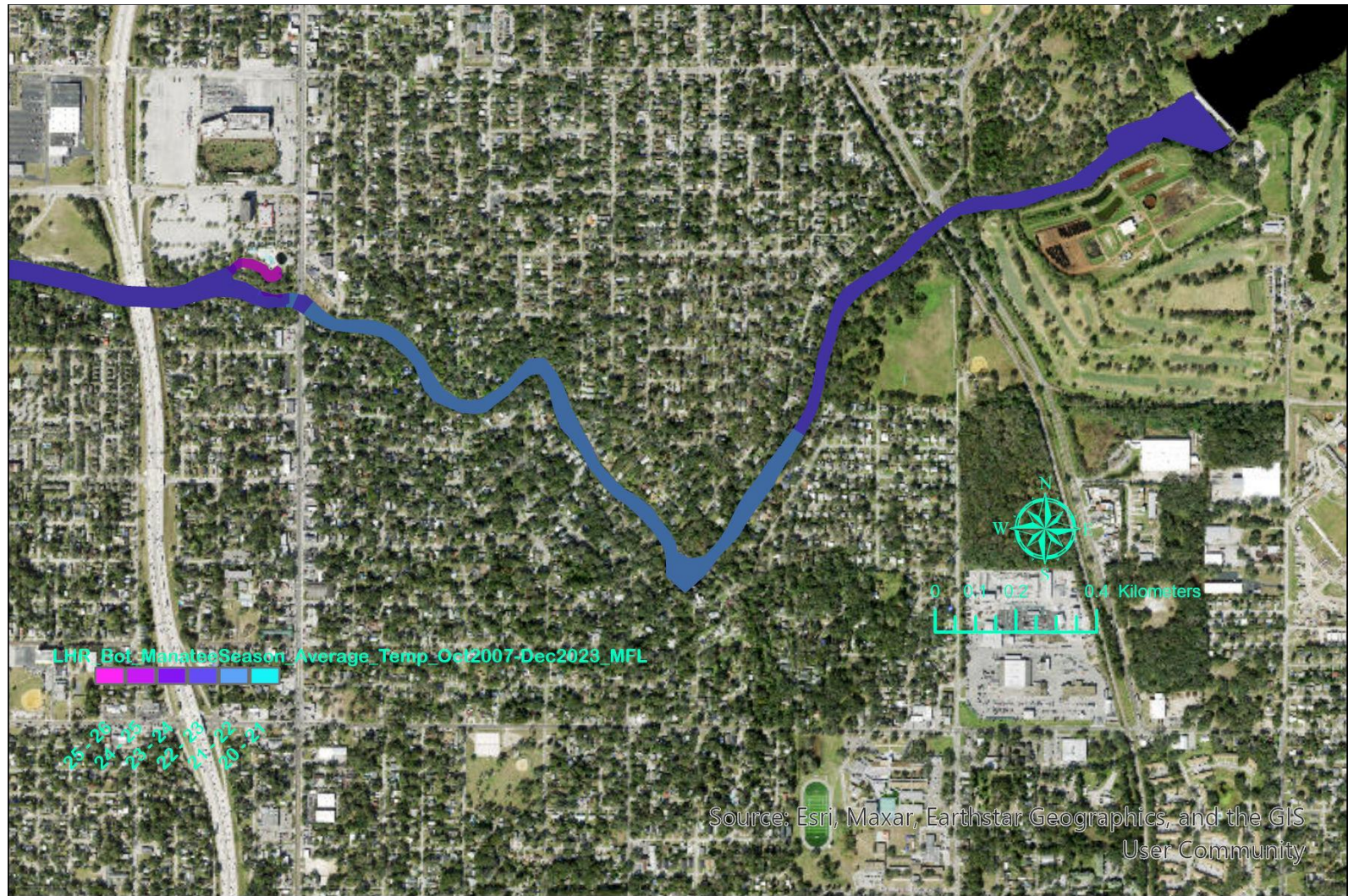
Figure C - 5. Average bottom-layer temperature in the upstream reach of the LHR during manatee seasons of the 195-month simulation period from October 2007 to December 2023 for the MFL flow condition.
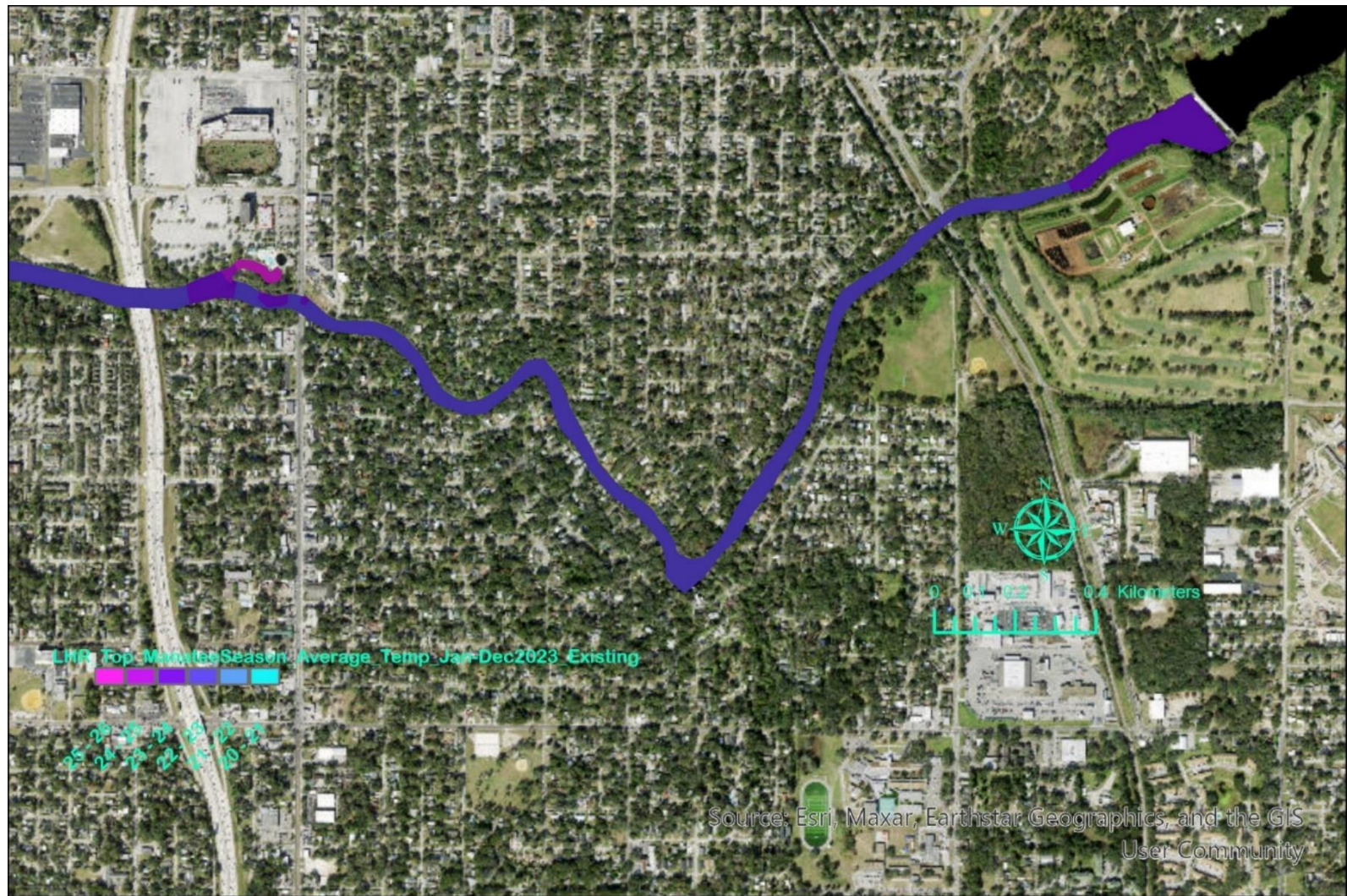
Figure C - 6. Average bottom-layer temperature in the upstream reach of the LHR during manatee seasons of the 195-month simulation period from October 2007 to December 2023 for the no MFL flow condition.

Figure C - 7. Average depth-averaged temperature in the upstream reach of the LHR during manatee seasons of the 195-month simulation period from October 2007 to December 2023 for the existing flow condition.

Figure C - 8. Average depth-averaged temperature in the upstream reach of the LHR during manatee seasons of the 195-month simulation period from October 2007 to December 2023 for the MFL flow condition.

Figure C - 9. Average depth-averaged temperature in the upstream reach of the LHR during manatee seasons of the 195-month simulation period from October 2007 to December 2023 for the no MFL flow condition.

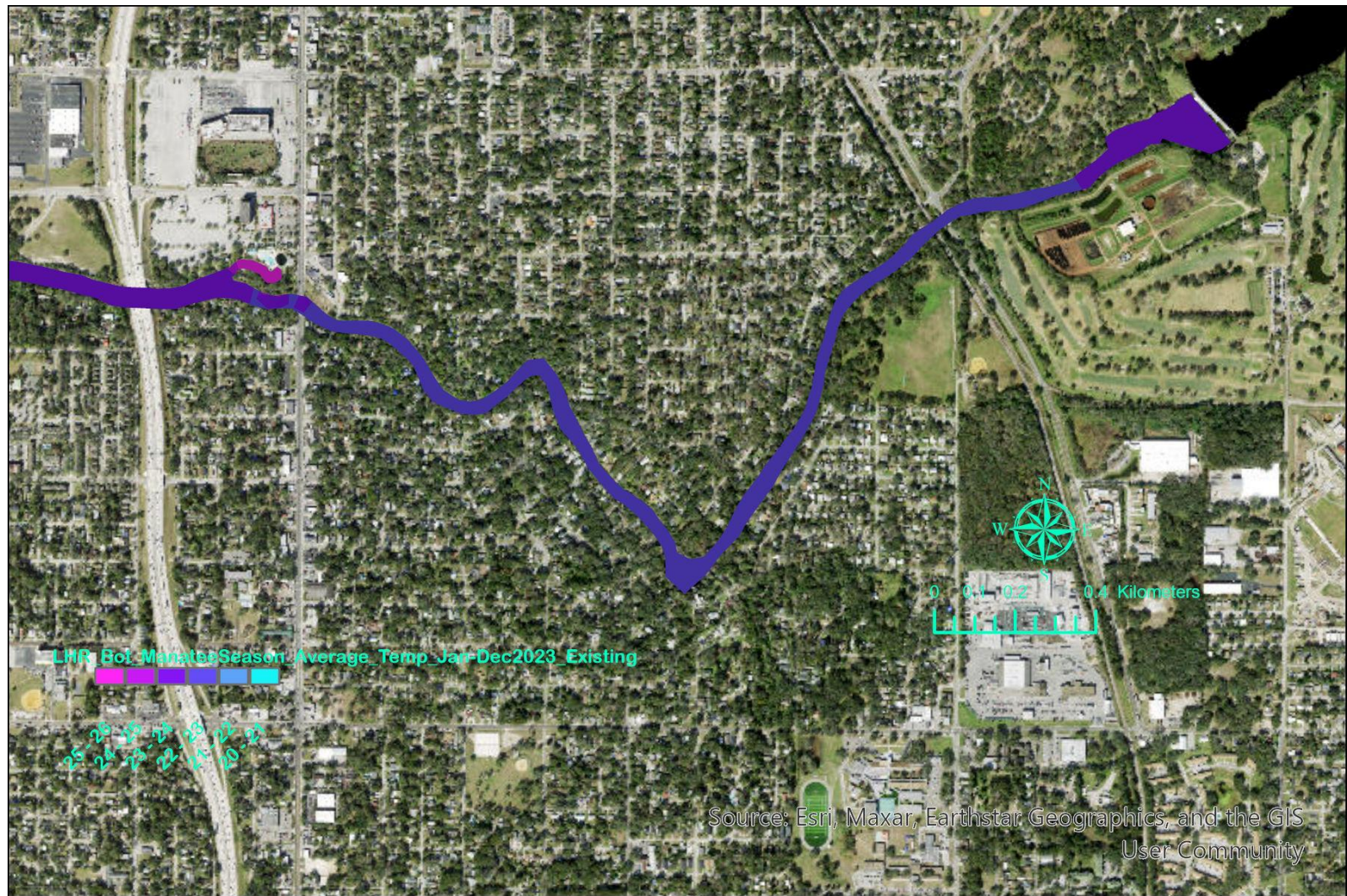Figure C - 10. Average top-layer temperature in the upstream reach of the LHR during the manatee season of 2023 for the existing flow condition.
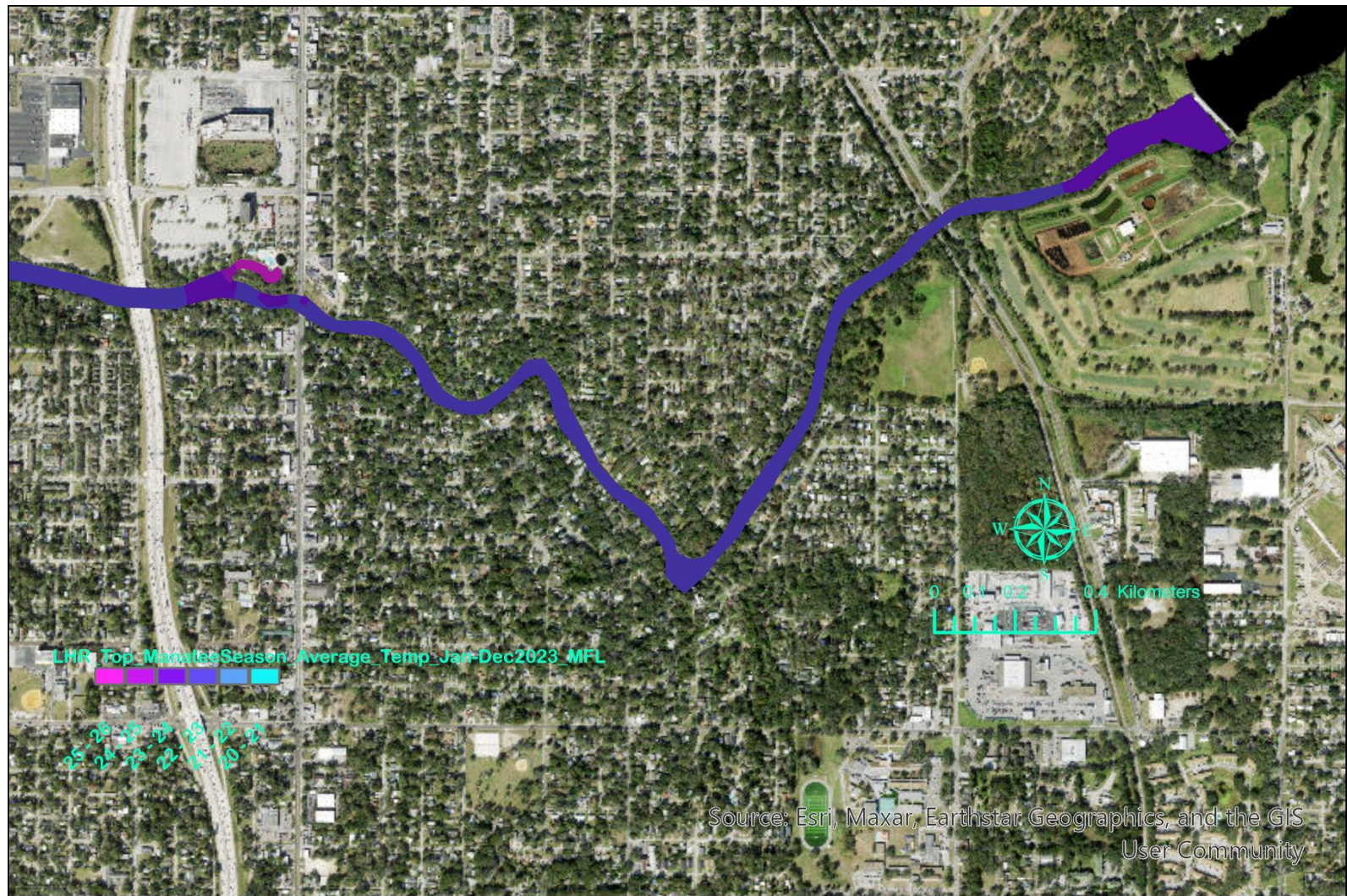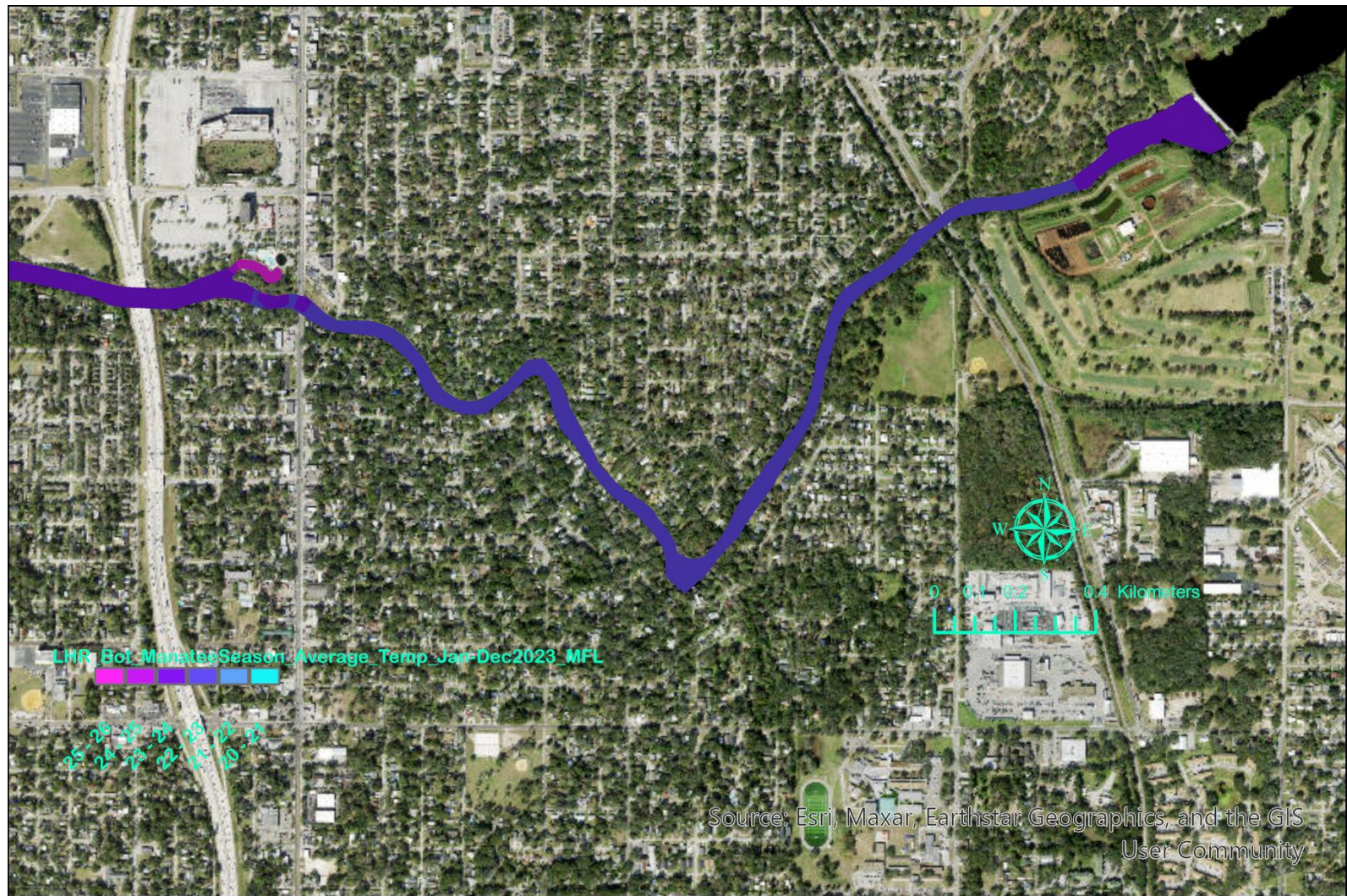
Figure C - 11. Average top-layer temperature in the upstream reach of the LHR during the manatee season of 2023 for the MFL flow condition.
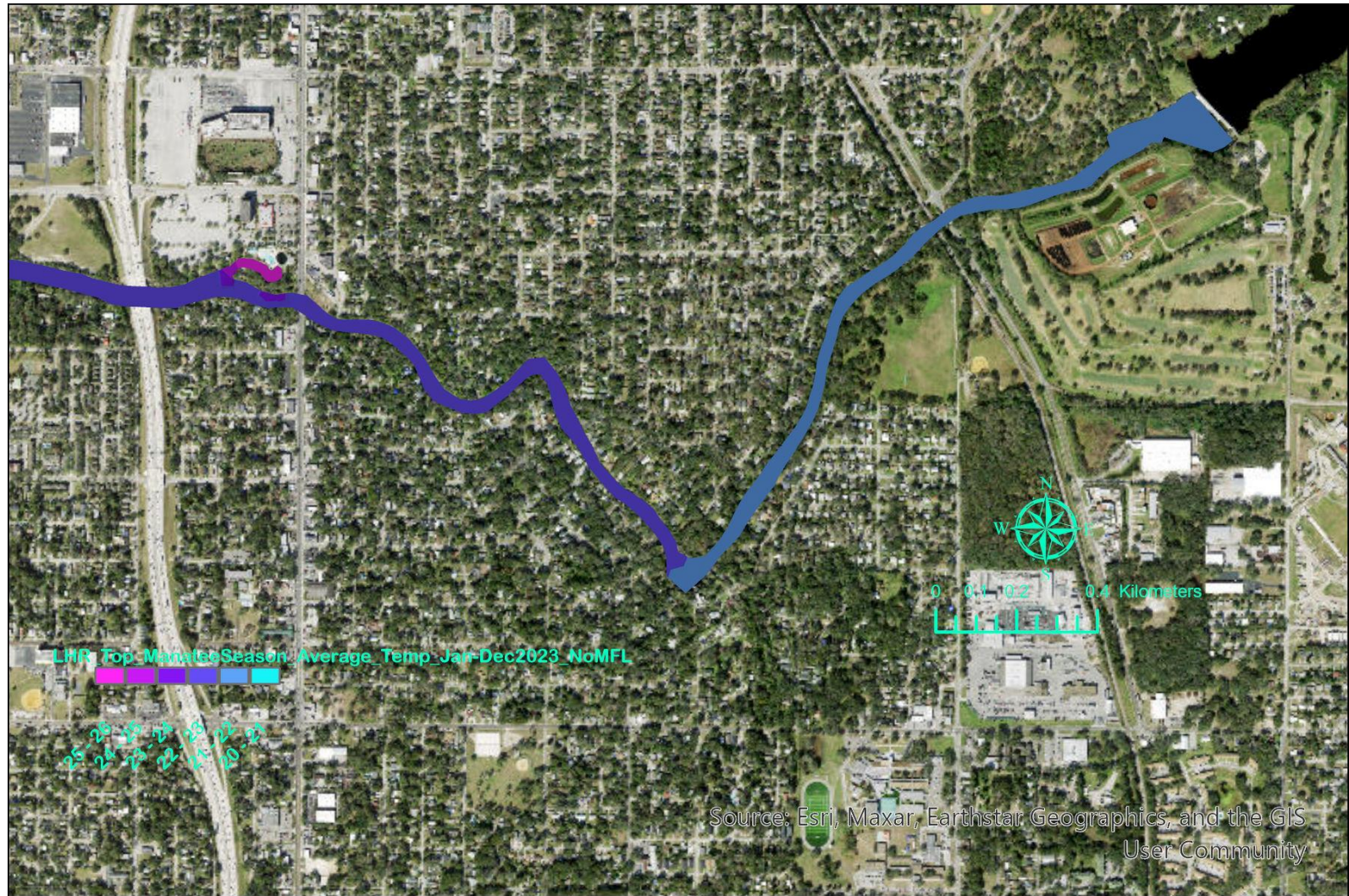
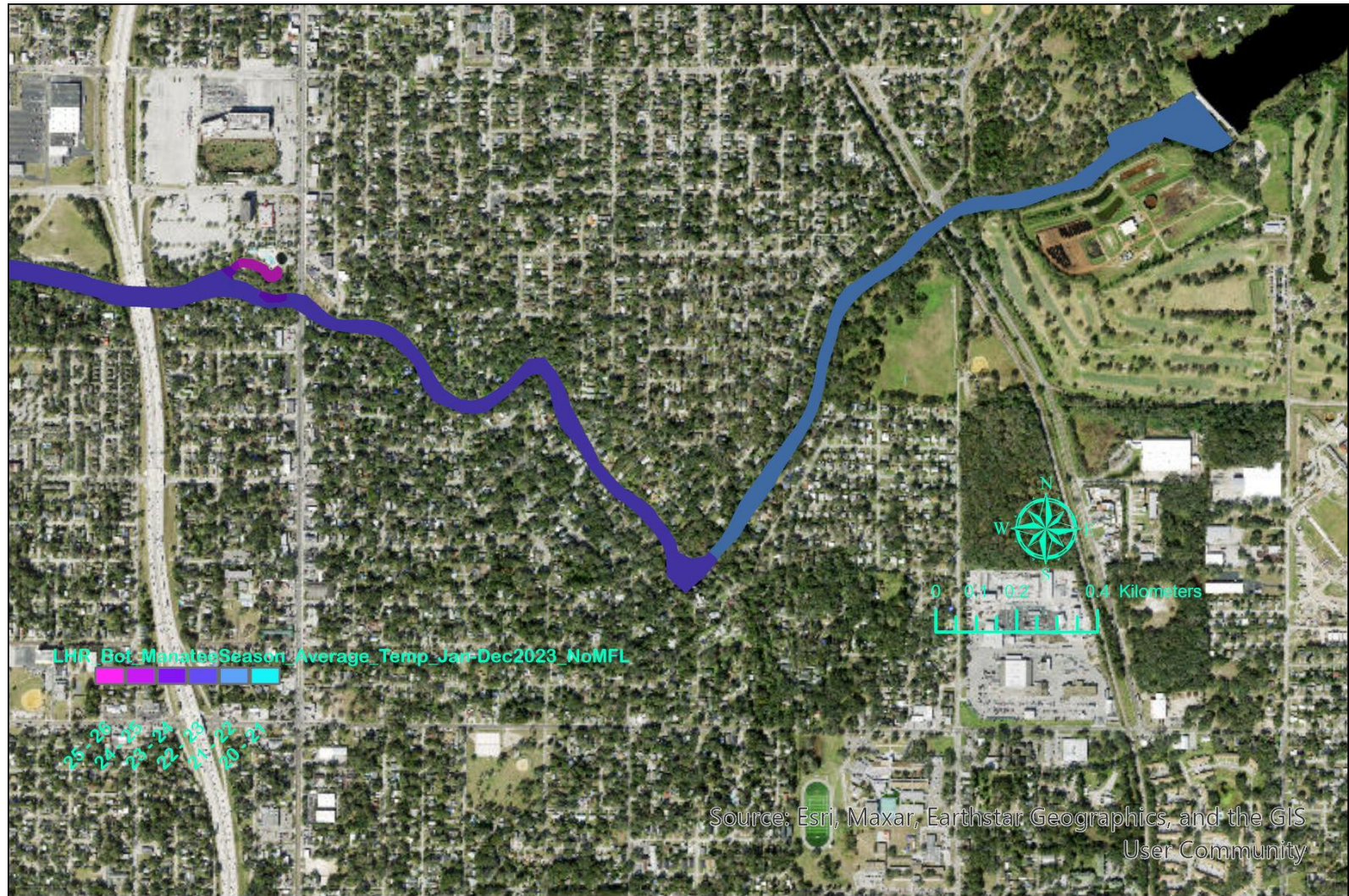Figure C - 12. Average top-layer temperature in the upstream reach of the LHR during the manatee season of 2023 for the no MFL flow condition.

Figure C - 13. Average bottom-layer temperature in the upstream reach of the LHR during the manatee season of 2023 for the existing flow condition.

Figure C - 14. Average bottom-layer temperature in the upstream reach of the LHR during the manatee season of 2023 for the MFL flow condition.
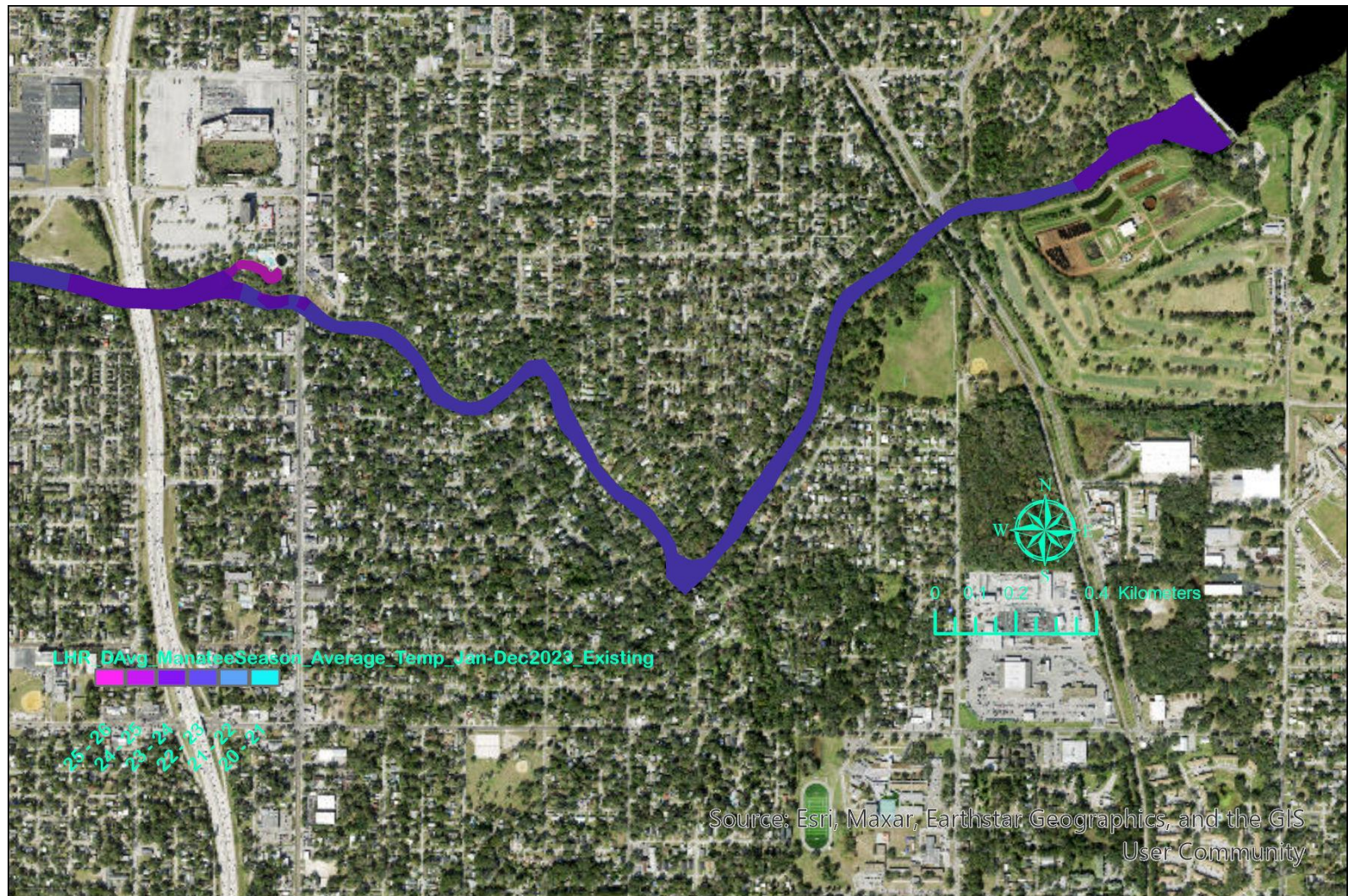
DRAFT

Figure C - 15. Average bottom-layer temperature in the upstream reach of the LHR during the manatee season of 2023 for the no MFL flow condition.

Figure C - 16. Average depth-averaged temperature in the upstream reach of the LHR during the manatee season of 2023 for the existing flow condition.
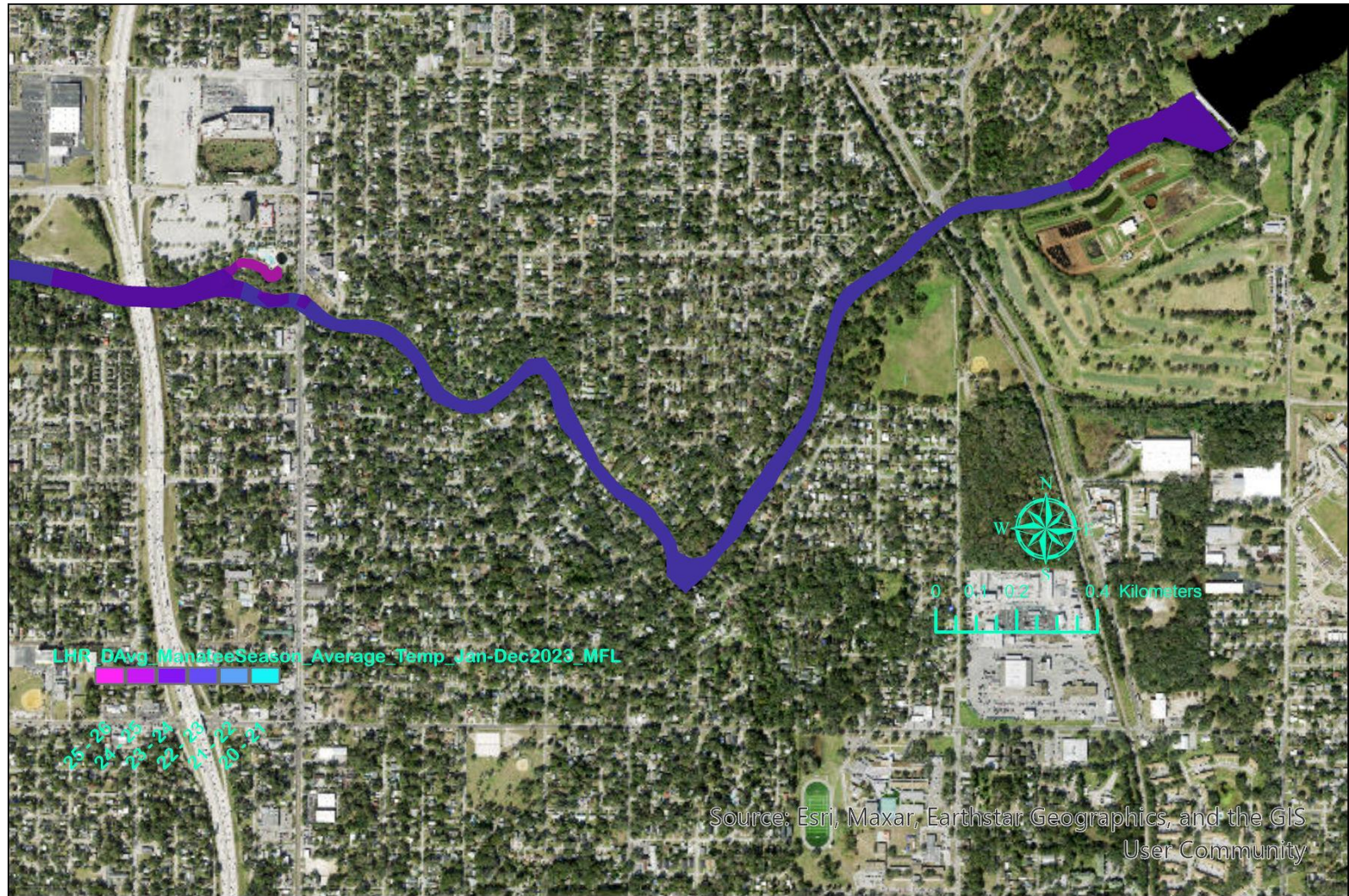
Figure C - 17. Average depth-averaged temperature in the upstream reach of the LHR during the manatee season of 2023 for the MFL flow condition.
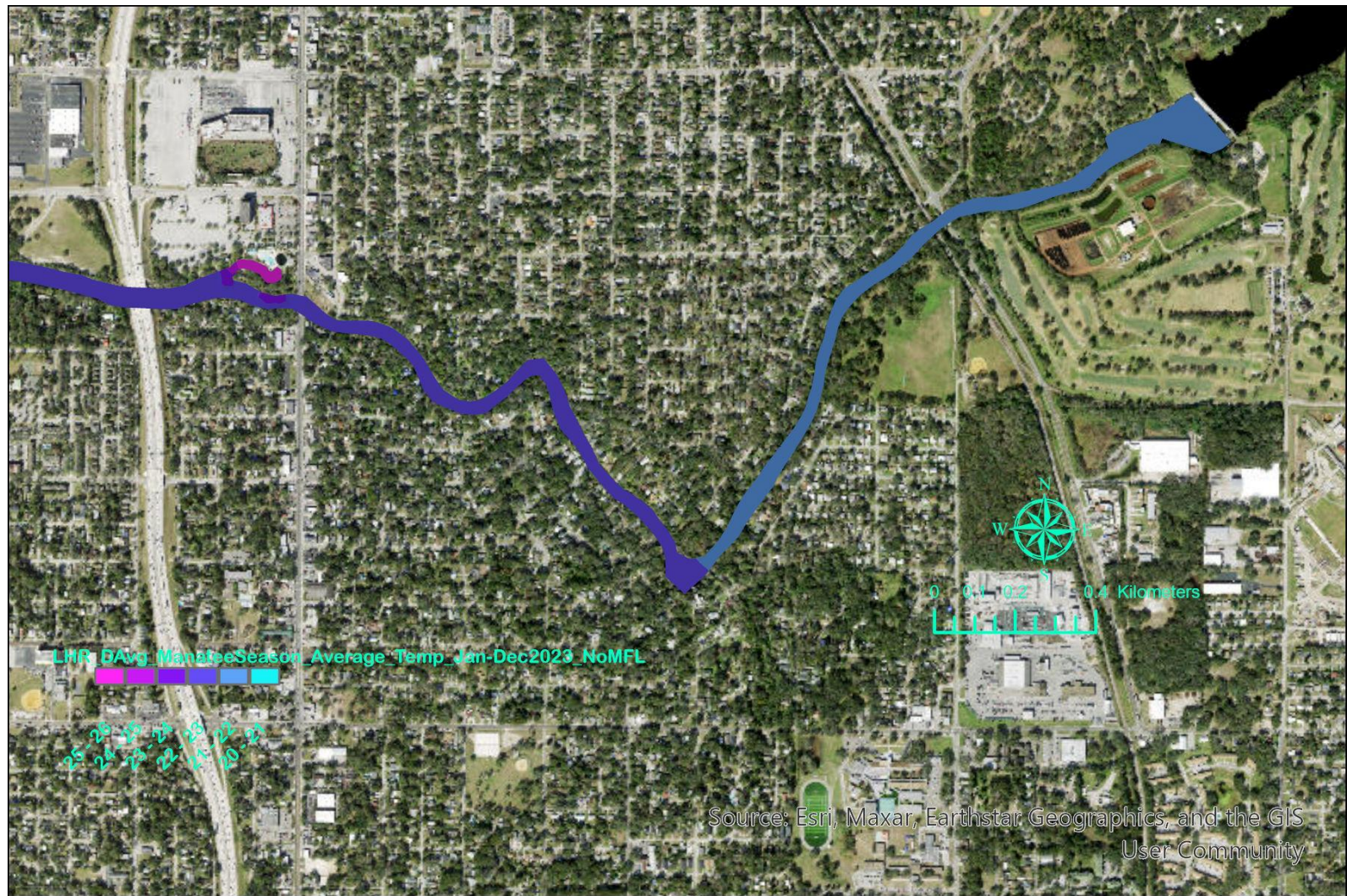
Figure C - 18. Average depth-averaged temperature in the upstream reach of the LHR during the manatee season of 2023 for the no MFL flow condition.